國立中山大學 電機工程學系

博士論文

程序設定快速啟動之螢光燈電子安定器

Electronic Ballasts for Fluorescent Lamps with Programmed Rapid-Start

研究生：陳威銘 撰

指導教授：莫清賢

中華民國九十三年六月

博碩士論文授權書

（國科會科學技術資料中心版本 92.2.17）

本授權書所授權之論文為本人在 國立中山 大學(~~學院~~) 電機工程 系所 電力 組 九十二 學年度第 二 學期取得 博 士學位之論文。

論文名稱： 程序設定快速啟動之螢光燈電子安定器

☑同意 □不同意 （政府機關重製上網）

本人具有著作財產權之論文全文資料，授予行政院國家科學委員會科學技術資料中心、國家圖書館及本人畢業學校圖書館，得不限地域、時間與次數以微縮、光碟或數位化等各種方式重製後散布發行或上載網路。

本論文為本人向經濟部智慧財產局申請專利(未申請者本條款請不予理會)的附件之一，申請文號為：____________，註明文號者請將全文資料延後半年再公開。

☑同意 □不同意 （圖書館影印）

本人具有著作財產權之論文全文資料，授予教育部指定送繳之圖書館及本人畢業學校圖書館，為學術研究之目的以各種方法重製，或為上述目的再授權他人以各種方法重製，不限地域與時間，惟每人以一份為限。

上述授權內容均無須訂立讓與及授權契約書。依本授權之發行權為非專屬性發行權利。依本授權所為之收錄、重製、發行及學術研發利用均為無償。上述同意與不同意之欄位若未鉤選，本人同意視同授權。

指導教授姓名：莫 清 賢

研究生簽名：陳 威 銘 學號:8931826

(親筆正楷) (務必填寫)

日期:民國 93 年 7 月 5 日

1. 本授權書（得自 http://sticnet.stic.gov.tw/sticweb/html/theses/authorize.html 下載或至 http://www.stic.gov.tw 首頁右下方下載）請以黑筆撰寫並影印裝訂於書名頁之次頁。
2. 授權第一項者，請確認學校是否代收，若無者，請個別再寄論文一本至台北市(106-36)和平東路二段 106 號 1702 室 國科會科學技術資料中心 王淑貞。(本授權書諮詢電話:02-27377746)
3. 本授權書於民國 85 年 4 月 10 日送請內政部著作權委員會(現為經濟部智慧財產局)修正定稿，89.11.21 部份修正。
4. 本案依據教育部國家圖書館 85.4.19 台(85)圖編字第 712 號函辦理。

國立中山大學研究生學位論文審定書

本校電機工程學系博士班

研究生 陳威銘 (學號：8931826) 所提論文

程序設定快速啟動之螢光燈電子安定器

經本委員會審查並舉行口試，符合博士學位論文標準。

學位考試委員簽章：

(召集人) 陳建富	莫清賢
林法正	梁從主
張永農	華志強
李嘉猷	李麗玲

指導教授 莫清賢

系主任 劉承宗

Electronic Ballasts for Fluorescent Lamps with Programmed Rapid-Start

by

Wei-Ming Chen

A Dissertation Submitted to the Graduate Division in Partial Fulfillment of the Reguirements for the Degree of Doctor of Philosophy

Department of Electrical Engineering of National Sun Yat-Sen University
Kaohsiung,Taiwan,Republic of China

(June 4 ,2004)

Chen, Tsann-Juh   Chin-Sien Moo

Pao-Jeng Lin   Tsorng-Juu Liang

Yong-Nong Chang   Chih-Chiang Hua

Jia-Yan Lee   Li-Ling Lee

Advisor : Chin-Sien Moo

Department Chairman : Ching-Tsy Lin

誌　謝

時間過的真快，一晃眼五年的碩博士求學生涯即將劃下句點，猶記得五年前我還是實驗室裡的小學弟，而如今已是個要被踢出實驗室的準博士了。非常慶幸能進入指導教授莫清賢老師的門下，五年多來，在老師專業領域與待人處世的指導下，使我在學業與生活上都獲益良多。如今博士論文得以順利完成，在此，要對恩師至上我最深的謝意。而亦非常感謝師母在生活上的關懷與照顧，使離家求學的我感受到無比的溫馨。同時，也感謝陳建富教授、林法正教授、華志強教授、李嘉猷教授、梁從主教授、張永農教授及李麗玲主任諸位口試委員對本論文的指導與指正，使本論文更臻完善。

其次要感謝耀慶學長、豪呈學長及再福學長對本論文提供許多寶貴意見及專業知識上的指導。也要感謝眾師兄弟—清然、宏良、明俊、東益、懷進、弘偉、憲坤、世宏、憲玟、易陞、沐恩、國興、戎傑、冠雄、俊凱、書平、志剛、聖億、正中、景元、建丞、文億、錀文、廣順、志成等在學業與生活上的互勉與關懷，讓我能渡過五年既充實又愉快的研究生活。

最後，特別感謝我的父母親以及家人多年來的辛苦栽培與全力支持，使我能無後顧之憂的專心於研究，讓我可以順利完成學業。而除了感謝之外，願以此成果與所有關心我、呵護我的人一同分享，並以此獻給我遠在另一方的父親。

學年度　　　　　：92
學期　　　　　　：2
校院　　　　　　：國立中山大學
系所　　　　　　：電機工程學系研究所
論文名稱（中）　：程序設定快速啟動之螢光燈電子安定器
論文名稱（英）　：Electronic Ballasts for Fluorescent Lamps with Programmed Rapid-Start
學位類別　　　　：博士
語文別　　　　　：eng
學號　　　　　　：8931826
提要開放使用　　：是
頁數　　　　　　：111
研究生（中）姓　：陳
研究生（中）名　：威銘
研究生（英）姓　：Chen
研究生（英）名　：Wei-Ming
指導教授（中）姓名：莫清賢
指導教授（英）姓名：Moo, Chin-Sien
關鍵字（中）　　：程序設定快速啟動、電子安定器、螢光燈、熾光放電。
關鍵字（英）　　：Programmed rapid-start, Electronic ballast, Fluorescent lamp, Glow discharge.

中文提要：

本文針對採用半橋串聯共振式換流器為主要電路架構之電子安定器提出三種程序設定快速啟動控制方式，分別為：(1)交流開關短路法、(2)具感應耦合式燈絲加熱電路之程序設定控制法、(3)串聯共振儲能槽諧振法，以改善快速啟動型螢光燈的啟動暫態特性。

首先提出的控制方式是藉由在傳統的串聯共振式電子安定器加入一固態交流開關來達成程序設定快速啟動。在預熱期間，安定器的固態交流開關將導通使燈管跨接零電壓，以消除此期間燈管的熾光電流。藉由調整安定器電路的操作頻率與主動切換開關的導通率，此安定器首先能產生適當大小的共振電流來加熱電極燈絲，並於交流開關截止時提供燈管足夠高的啟動電壓，最後於穩態操作時供應所需求之燈管功率。

第二種控制方式是在功因修正電路之儲能電感的鐵芯加繞兩組輔助線圈來作為燈絲加熱電路，並藉由控制安定器電路的主動切換開關，使功因修正電路在啟動後持續致動，以產生燈絲加熱電壓來加熱電極燈絲；並使共振式換流器電路在預熱階段不動作，避免燈管兩端產生跨壓，以消除燈管的熾光電流。當燈絲達到適當的電子發射溫度之後，隨即啟動串聯共振換流器來產生高壓以點亮燈管，然後穩定地操作燈管於所要求之功率。

最後所提出的控制方式是藉由在傳統的串聯共振式電子安定器的負載諧振網路加入一串聯共振儲能槽，並規劃從啟動到穩態各階段的操作頻率，以達到程序設定快速啟動。啟動後的預熱階段，電子安定器首先設定在串聯共振儲能槽的諧振頻率，以降低燈管電壓，確保不會發生熾光放電。經由電路參數設計，安定器能提供適當之燈絲預熱電流。當燈絲達到放射電子溫度後，接著調整安定器電路的操作頻率，以產生足夠高之燈管電壓來點燈，然後於穩態操作期間輸出所要求之燈管功率並提供適當的燈絲電流。

本文針對所提出之電子安定器電路，根據其開關導通情形建立電路的工作模式，分析電路工作原理。而為準確掌握燈絲操作特性，本文亦對燈絲電阻在預熱期間的變化詳加探討，並依據螢光燈之特性，將穩定工作時電弧視為純電阻，並加入燈絲電阻，建立螢光燈

於點亮前後的等效電路模型。此外，文中亦應用基本波近似法來簡化電路分析，並搭配燈管之等效電路模型，建立安定器之等效電路，並以此等效電路為基礎推導電路參數的設計方程式及設計流程。最後，本文以實驗證實理論分析之結果。

英文提要：

Three programmed rapid-start control schemes for the electronic ballasts with a half-bridge series-resonant inverter are proposed to improve the starting performance of the rapid-start fluorescent lamps. Included are: (1) programmed rapid-start control scheme with an ac switch, (2) programmed rapid-start control scheme with inductively coupled filament-heating circuit, and (3) programmed frequency control scheme with a series-resonant energy-tank.

The first control scheme is simply to add a solid-state ac switch onto the series-resonant electronic ballast to provide programmed rapid-start for the rapid-start fluorescent lamp. The ac switch is turned on to have a zero voltage across the lamp to eliminate the glow current during the preheating interval. By adjusting the operation frequency and the duty-ratio, the electronic ballast produces first an adequate resonant current for preheating the cathode filaments, then a sufficiently high lamp voltage for ignition, and finally a stable lamp arc of the required lamp power.

The second control scheme is accomplished by adding two auxiliary windings on the inductor of the power-factor-correction (PFC) circuit for the filament-heating circuits. During the preheating period, the PFC circuit is activated to provide the filament heating while the inverter remains idle to keep the lamp voltage at zero and hence to eliminate the glow current. After the filaments have been heated to the appropriate temperature, the inverter is initiated to ignite the lamp and then operate it at the required power.

The third control scheme is realized by programming the operation frequency of the electronic ballast with an additional series-resonant energy-tank on the load resonant network. During the preheating interval, the electronic ballast is programmed to operate at the resonance frequency of the series-resonant energy-tank to reduce the lamp voltage and hence to eliminate the glow discharge. With carefully designed circuit parameters, the electronic ballast is able to provide an adequate current for preheating. After the emission temperature has been reached, the operation frequency is adjusted to generate a high lamp voltage for ignition, and then is located at the steady-state frequency driving the lamp with the desired power and filament current.

In this dissertation, the mode operations of the proposed ballast circuits are analyzed in accordance with the conducting conditions of the power switches. The equivalent resistance model of fluorescent lamp is implemented to calculate the performances of the ballast-lamp circuit at steady-state. The design equations are derived and the computer analyses are performed with the fundamental approximation on the equivalent circuit models of fluorescent lamps. In addition, in order to accurately predict the operating characteristic of the preheating circuit, a mathematical model is developed to interpret the variations of the filament resistance during preheating. Finally, the laboratory electronic ballasts with the proposed control schemes are built and tested. Satisfactory performances are obtained from the experimental results.

摘　要

本文針對採用半橋串聯共振式換流器為主要電路架構之電子安定器提出三種程序設定快速啟動控制方式，分別為：(1)交流開關短路法、(2)具感應耦合式燈絲加熱電路之程序設定控制法、(3)串聯共振儲能槽諧振法，以改善快速啟動型螢光燈的啟動暫態特性。

首先提出的控制方式是藉由在傳統的串聯共振式電子安定器加入一固態交流開關來達成程序設定快速啟動。在預熱期間，安定器的固態交流開關將導通使燈管跨接零電壓，以消除此期間燈管的熾光電流。藉由調整安定器電路的操作頻率與主動切換開關的導通率，此安定器首先能產生適當大小的共振電流來加熱電極燈絲，並於交流開關截止時提供燈管足夠高的啟動電壓，最後於穩態操作時供應所需求之燈管功率。

第二種控制方式是在功因修正電路之儲能電感的鐵芯加繞兩組輔助線圈來作為燈絲加熱電路，並藉由控制安定器電路的主動切換開關，使功因修正電路在啟動後持續致動，以產生燈絲加熱電壓來加熱電極燈絲；並使共振式換流器電路在預熱階段不動作，避免燈管兩端產生跨壓，以消除燈管的熾光電流。當燈絲達到適當的電子發射溫度之後，隨即啟動串聯共振換流器來產生高壓以點亮燈管，然後穩定地操作燈管於所要求之功率。

最後所提出的控制方式是藉由在傳統的串聯共振式電子安定器的負載諧振網路加入一串聯共振儲能槽，並規劃從啟動到穩態各階段的操作頻率，以達到程序設定快速啟動。啟動後的預熱階段，電子安定器首先設定在串聯共振儲能槽的諧振頻率，以降低燈管電壓，確保不會發生熾光放電。經由電路參數設計，安定器能提供適當之燈絲預熱電流。當燈絲達到放射電子溫度後，接著調整安定器電路的操作頻率，以產生足夠高之燈管電壓來點燈，然後於穩態操作期間輸出所要求之燈管功率並提供適當的燈絲電流。

本文針對所提出之電子安定器電路，根據其開關導通情形建立電路的工作模式，分析電路工作原理。而為準確掌握燈絲操作特性，本文亦對燈絲電阻在預熱期間的變化詳加探討，並依據螢光燈之特性，將穩定工作時電弧視為純電阻，並加入燈絲電阻，建立螢光燈於點亮前後的等效電路模型。此外，

文中亦應用基本波近似法來簡化電路分析，並搭配燈管之等效電路模型，建立安定器之等效電路，並以此等效電路為基礎推導電路參數的設計方程式及設計流程。最後，本文以實驗證實理論分析之結果。

關鍵詞：程序設定快速啟動、電子安定器、螢光燈、熾光放電。

Abstract

Three programmed rapid-start control schemes for the electronic ballasts with a half-bridge series-resonant inverter are proposed to improve the starting performance of the rapid-start fluorescent lamps. Included are: (1) programmed rapid-start control scheme with an ac switch, (2) programmed rapid-start control scheme with inductively coupled filament-heating circuit, and (3) programmed frequency control scheme with a series-resonant energy-tank.

The first control scheme is simply to add a solid-state ac switch onto the series-resonant electronic ballast to provide programmed rapid-start for the rapid-start fluorescent lamp. The ac switch is turned on to have a zero voltage across the lamp to eliminate the glow current during the preheating interval. By adjusting the operation frequency and the duty-ratio, the electronic ballast produces first an adequate resonant current for preheating the cathode filaments, then a sufficiently high lamp voltage for ignition, and finally a stable lamp arc of the required lamp power.

The second control scheme is accomplished by adding two auxiliary windings on the inductor of the power-factor-correction (PFC) circuit for the filament-heating circuits. During the preheating period, the PFC circuit is activated to provide the filament heating while the inverter remains idle to keep the lamp voltage at zero and hence to eliminate the glow current. After the filaments have been heated to the appropriate temperature, the inverter is initiated to ignite the lamp and then operate it at the required power.

The third control scheme is realized by programming the operation frequency of the electronic ballast with an additional series-resonant energy-tank on the load resonant network. During the preheating interval, the electronic ballast is programmed to operate at the resonance frequency of the series-resonant energy-tank to reduce the lamp voltage and hence to eliminate the glow discharge. With carefully designed circuit parameters, the electronic ballast is able to provide an adequate current for preheating. After the emission temperature has been reached, the operation frequency is adjusted to generate a high lamp voltage for ignition, and then is located at the steady-state frequency driving the lamp with the desired power and filament current.

In this dissertation, the mode operations of the proposed ballast circuits are analyzed in accordance with the conducting conditions of the power switches. The equivalent resistance model of fluorescent lamp is implemented to calculate the performances of the ballast-lamp circuit at steady-state. The design equations are derived and the computer analyses are performed with the fundamental approximation on the equivalent circuit models of fluorescent lamps. In addition, in order to accurately predict the operating characteristic of the preheating circuit, a mathematical model is developed to interpret the variations of the filament resistance during preheating. Finally, the laboratory electronic ballasts with the proposed control schemes are built and tested. Satisfactory performances are obtained from the experimental results.

Keywords: Programmed rapid-start, Electronic ballast, Fluorescent lamp, Glow discharge.

List of Contents

List of Figures

List of Tables

List of Symbols

f_p	preheating frequency
f_s	steady-state frequency
$f_{r,pre}$	resonance frequency of resonant circuit during preheating
$f_{r,ign}$	resonance frequency of resonant circuit at ignition
$f_{r,std}$	resonance frequency of resonant circuit at steadt-state
f_o	operation frequency of inverter
T_o	operation period of inverter
d	duty-ratio
V_{lamp}	rms value of lamp voltage
I_{lamp}	rms value of lamp current
R_{lamp}	lamp resistance
P_{lamp}	lamp power
P_{arc}	arc power
P_f	filament power
r_f	filament resistance
r_{f_c}	resistance of cold filament
r_{f_h}	resistance of hot filament
T_c	temperature of cold filament
T_h	temperature of hot filament
V_p	rms value of preheating voltage
I_p	rms value of preheating current
t_p	preheating time
v_s	instantaneous value of line voltage
V_s	rms value of line voltage
V_m	amplitude of line voltage
f_L	frequency of line voltage
i_{in}	instantaneous value of input current

$i_{in,peak}$	peak value of unfiltered input current
$i_{in,avg}$	average value of unfiltered input current
P_{in}	input power
η	circuit efficiency
V_{dc}	dc-link voltage
r_{vo}	ripple factor of dc-link voltage
v_{ab}	output voltage of half-bridge inverter
V_1	rms value of fundamental component of v_{ab}
v_n	instantaneous value of n-th order harmonic component of v_{ab}
V_n	rms value of n-th order harmonic component of v_{ab}
V_{ign}	rms value of ignition voltage
V_f	effective value of filament voltage
I_f	rms value of filament current
N	turn-ratio of transformer
Q_L	loaded quality factor
Z_{in}	total impedance of resonant circuit

Chapter 1 Introduction

1-1 Research Background and Motivation

Fluorescent lamps have been widely used in industrial, commercial, and residential regions as one of the most important lighting devices. As compared with their counterparts, incandescent lamps, even though fluorescent lamps are bulky in size and heavy in weight and ballasts are essential to operate them properly, they inherently possess some advantages, such as higher luminous efficiency (lm/W), that is, higher energy conversion efficiency with the lamp, lower tube temperature and longer lamp life [1-5]. Therefore, fluorescent lamps provide a large percentage of today's lighting needs.

The fluorescent lamp is a low-pressure mercury electric discharge lighting source, in which light is produced predominantly by phosphors which are activated by ultraviolet energy generated by the mercury discharge. The fluorescent lamp is mainly composed of a glass tube filled with a mixture of argon gases and mercury vapors and two filament electrodes. The inner walls of the tube are coated with the phosphors and the cathode filaments of the lamp electrodes are coated with the emissive materials, which emit electrons. While a proper voltage (ignition voltage) is applied on the lamp, an electric discharge is produced between the electrodes. This discharge generates some visible radiation, but mostly invisible ultraviolet radiation. The phosphors absorb the invisible ultraviolet in turn to emit visible light [1].

Like most gas discharge lighting sources, the fluorescent lamp exhibits negative incremental resistance characteristics in the desired operation region. When operating the fluorescent lamp at a higher power, the lamp voltage is lower and the arc current is higher. On the other hand, as operating it at low power, the lamp voltage becomes high and current turns low, respectively. The negative incremental resistance characteristics may result in an unstable operation and bring about destruction if the lamp is directly connected to the voltage source. Thus, a current-limiting device is essential for limiting the current flowing through the lamp [1,6-8]. The current-limiting device is commonly called a ballast. In addition to current limitation, the ballast also provides a sufficiently high lamp voltage to ignite the lamp and then a proper lamp voltage to maintain gas discharge while running.

In practical applications, to operate the fluorescent lamp properly, a ballast is essential for regulating the discharge voltage and current. Conventionally, the electromagnetic ballast is mainly composed of a magnetic core inductor or a high-leakage transformer and a starter. Since its operation frequency is the same as the frequency of line source, the electromagnetic ballast will cause the noticeable lamp flicker resulted from gas ionization and deionization. In addition, this kind of ballast operating at such a low frequency is disadvantageous of a higher loss, audible hums, and bulky in size and heavy in weight.

In recent years, due to the rapid development of semiconductor components and power electronic technology for high frequency switching, the electronic ballast, instead of the electromagnetic ballast, is preferred to drive the fluorescent lamp at high frequency and high efficiency for improving the light quality. The high frequency electronic ballast has a lot of benefits as compared with the conventional electromagnetic ballast. When the fluorescent lamp is operated at high frequency, higher light output for the same electrical input at low frequency is obtained, i.e., the luminous efficiency is increased [1,4,5]. The ignition voltage of the lamp can be reduced with increasing frequency. The noticeable flicker becomes negligible due to the ionized gas does not have sufficient time to recombine as the line voltage passes through zero point. Therefore, the restriking voltage spikes disappear at high frequency operation. The audible noises heard from the conventional electromagnetic ballast can be eliminated completely since the operation frequency is above the acoustic frequency. Moreover, the elements of the ballast can be much lighter and more compact due to high frequency operation [7-14].

Both the mercury vapors and the phosphors in the fluorescent lamp tube are the harmful materials, which can pollute the environment. Once the failed fluorescent lamps are not handled properly, these harmful materials in the fluorescent tube will cause a serious impact upon the environment. Therefore, for the sake of environmental consideration, how to effectively prolong the lamp life for reducing the consumption of fluorescent lamps has become an important task in the electronic ballast design.

The starting operations of fluorescent lamps are commonly classified into preheating-start, rapid-start and instant-start [1]. For the different starting operations, the different types of fluorescent lamps must be used. Among various types of fluorescent lamps, the fluorescent lamp designed for rapid-start is conventionally recommended for lighting applications requiring frequent switching to preserve long lamp life cycles. A long operation life of the fluorescent lamp can be retained by properly starting and operating the lamp. Before ignition, the ballast should provide a proper preheating voltage or current to heat the cathode filament until an appropriate temperature for electron emission. If the lamp is ignited before the cathode filaments are properly heated, this might cause the cathode filaments sputtering acutely. On the other hand, if the cathode filaments are heated to a too high temperature before ignition, the coating materials on the electrodes might be over evaporated. Both inappropriate preheating conditions will increase the depletion of the coating materials on the cathode filaments and blacken the lamp ends, shortening the lamp life [15-24]. After the lamp is successfully ignited, the ballast should supply a proper filament voltage or current to maintain the cathode filament at the emission temperature. This is helpful for retaining a long lamp life but can increase the energy consumption at the steady-state operation [18,22].

In addition, the glow discharge should be prevented. The results of recent research have shown that the glow discharge is a very important factor affecting the operation life of the fluorescent lamp. By eliminating the glow discharge in the fluorescent lamps, the damage to the cathode filaments during starting can be reduced [25-29]. Glow discharge is an indication of cathode filament sputtering before stable arc current flows through the lamp. That is, glow current is the irregular current caused by the cathode filament sputtering. There are two paths for glow discharge. One is directly from one end of the lamp to another end. The other is from the cathode filament to the fluorescent coating on the inner walls of the tube [9]. In general, the glow current is very small and thus it is not easily detected. However, it will cause the filaments to wear out.

The glow discharge may occur when the cathode filaments are being preheated and especially when a voltage appears across the fluorescent lamp. Therefore, it is essential for a ballast design to limit the lamp voltage during the preheating interval. For this purpose, many electronic ballasts with programmed rapid-start have been developed [24,29-41]. Nevertheless, most of them are able to reduce but not get rid of the glow current. To completely eliminate the glow discharge, an additional filament-heating circuit with transformer may be used [29]. However, this solution requires a more complicated power circuit with a more sophisticated control leading to a higher cost and larger volume, and is not applicable for the electronic ballasts with a half-bridge series-resonant inverter.

Electronic ballasts with a half-bridge resonant inverter have been widely adopted in commercial products due to their simple configurations and high efficiency [42-51]. At present, many control ICs designed for the electronic ballasts with half-bridge resonant inverters have also been developed [31-34,52-54]. Figure 1-1 shows the conventional electronic ballast with a quasi half-bridge series-resonant inverter. The load resonant circuit presents series-resonant parallel-loaded and thus the fluorescent lamp is in parallel with a starting-aid capacitor, C_f. This starting-aid capacitor has two functions. One is to provide an appropriate preheating current during the preheating interval and a compensated filament current to maintain the emission temperature at steady-state operation. The other is to generate a sufficiently high ignition voltage by taking part in the resonance of the load circuit. Such a design can simplify the circuit configuration but will also cause the glow discharge. At the preheating stage, the lamp is regarded as an open circuit and thus the resonant current, i_r, is the filament current, i_f. While the resonant current flows though the starting-aid capacitor and the cathode filaments for preheating, a voltage is simultaneously produced on the lamp causing a glow discharge inevitably, as shown in Figure 1-2.

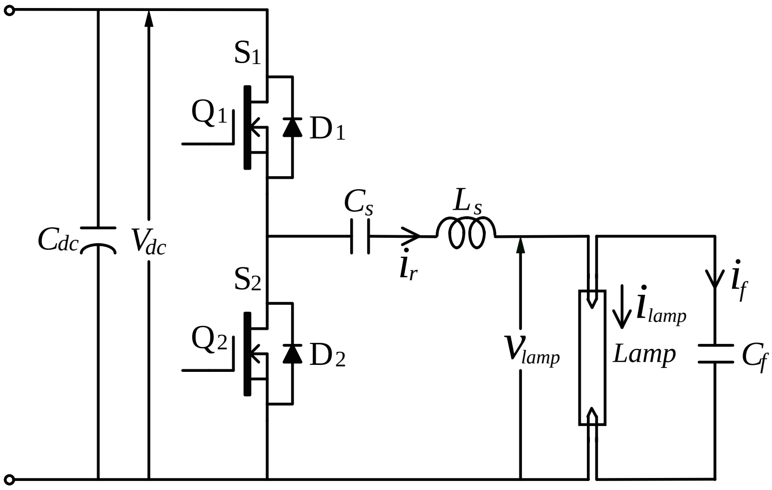

Figure 1-1 Half-bridge series-resonant parallel-loaded inverter

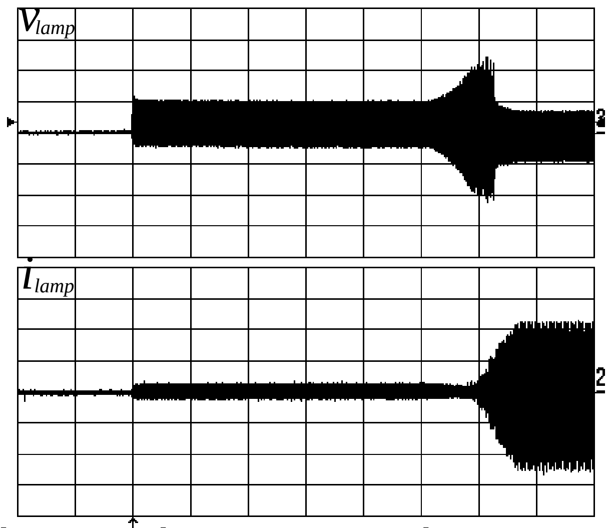

Figure 1-2 Starting transient waveforms

To get rid of the glow discharge in the rapid-start fluorescent lamps driven by half-bridge series-resonant electronic ballasts, three programmed rapid-start control schemes are proposed in this dissertation. The control schemes are: (1)

programmed rapid-start control scheme with an ac switch, (2) programmed rapid-start control scheme with inductively coupled filament-heating circuit, and (3) programmed frequency control scheme with a series-resonant energy-tank. The first control scheme is simply to add a shunt switch on the lamp. During the preheating stage, the lamp voltage can be maintained at zero to eliminate the glow current by turning on the switch. Once the filament temperature has reached the adequate emission temperature, the shunt switch is turned off. Then, an ignition voltage is applied to start the lamp. The second control scheme is accomplished by adding two auxiliary windings on the inductor of the power-factor-correction (PFC) circuit for the filament-heating circuits and remaining the load resonant inverter at idle state until the cathode filaments have been heated to the appropriate temperature. This ensures that no voltage across the lamp while applying the preheating voltage on the cathode filaments. Thus, this control scheme can effectively eliminate the glow current. The third control scheme is simply to add a series-resonant energy-tank as the starting-aid circuit. With the starting-aid circuit, the lamp can be started in a sophisticated manner. During the preheating stage, the lamp voltage can be greatly reduced to a very low level by deliberately operating the inverter at the resonance frequency of the starting-aid circuit. After the cathode filaments have been preheated to an appropriate emission temperature, the inverter frequency is adjusted to generate the required high ignition voltage for starting the lamp. Thus, with these proposed control schemes, the lamp can be started up without the adverse effects on the lamp life.

In this dissertation, the equivalent resistance model of fluorescent lamp is implemented to calculate the performances of the ballast-lamp circuit at steady-state. In order to accurately predict the operation characteristic of the preheating circuit, the variations of the filament resistance during preheating are investigated and its mathematical model is developed. In addition, for the presented programmed rapid-start electronic ballasts, the design equations are derived and the circuit analyses are performed with the fundamental approximation on the equivalent circuit models of fluorescent lamps. Accordingly, the design guidelines for determining circuit parameters are provided.

1-2 Programmed Rapid-Start

The programmed rapid-start is a newer starting method developed for the rapid-start fluorescent lamps. This starting method can reduce damage to the cathode filaments during starting and thus can prolong the lamp life [29]. The operation of programmed rapid-start of an electronic ballast is described by three stages: preheating, ignition, and steady-state. At first, the ballast can provide a proper preheating current or voltage for heating the cathode filaments. The preheating time of the rapid-start electronic ballasts is typically between 0.5 and 1 second. While the cathode filaments have been preheated up to a proper emission temperature, the ballast is able to generate a sufficiently high voltage across the lamp for ignition. Finally, at steady-state operation, the ballast provides the required lamp power.

At present, some control ICs designed for the electronic ballasts with half-bridge resonant inverter have already been built with the function of programmed rapid-start [31-34]. Figure 1-3 shows the starting scenario of the conventional programmed rapid-start for half-bridge series-resonant electronic ballast. When the ballast is powered on, the half-bridge series-resonant inverter is operated at a higher initial operation frequency. The initial operation frequency of the inverter is much higher than the resonance frequency of the load resonant circuit, thus the load resonant circuit presents high inductive, resulting in very small resonant current. In general, the resonant current is the preheating current. Then, the operation frequency decreases to increase the preheating current. When the preheating current reaches the preset level, the operation frequency is remained at a constant to provide a constant preheating current so as to heat the cathode filaments. After the preheating stage, the operation frequency decreases again. At this stage, the operation frequency is changed from the preheating frequency, f_p, toward the resonance frequency, $f_{r,ign}$, to generate a sufficiently high lamp voltage for ignition. Once the lamp is successfully ignited, the operation frequency is set to the steady-state frequency, f_s, to output the desired lamp power.

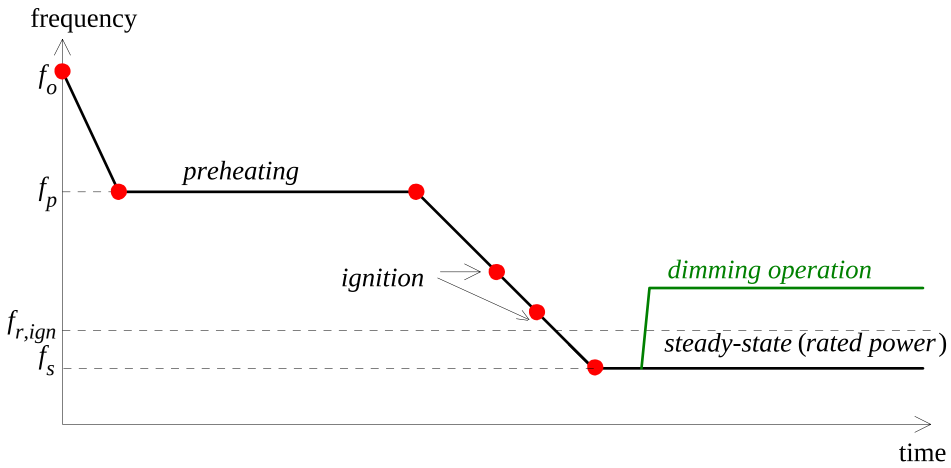

Figure 1-3 Starting scenario of the conventional programmed rapid-start

Inevitably, such a control scheme can cause a glow discharge at the preheating stage. By increasing the preheating frequency, the lamp voltage during preheating can be reduced and thus the glow current can be reduced, but cannot be eliminated. Therefore, how to effectively eliminate the glow current during starting has become an important task in the programmed rapid-start electronic ballast design nowadays.

1-3 Content Arrangement

The content of this dissertation is divided into 6 chapters.

Chapter 1 introduces the characteristics of fluorescent lamp and the ballast and expounds the research motivation of this dissertation.

Chapter 2 presents the operation principle of half-bridge resonant inverters and develops an equivalent circuit model for fluorescent lamps.

Chapter 3 shows the proposed programmed rapid-start electronic ballast with an ac switch which is introduced as the starting-aid circuit of the lamp. The circuit configuration, operation, analysis, starting scenario and experimental results are shown here.

Chapter 4 shows the proposed programmed rapid-start electronic ballast with inductively coupled filament-heating circuits. The details of this circuit are shown in this chapter.

Chapter 5 shows the proposed programmed rapid-start electronic ballast with a series-resonant energy-tank which is introduced as the starting-aid circuit of the lamp. The details of this circuit are shown in this chapter.

Chapter 6 gives some conclusions on this dissertation, and gives some discussions on the future development on this topic.

Chapter 2 Half-Bridge Resonant Inverter and Fluorescent Lamp

In this chapter, the operation principle of the half-bridge resonant inverter is presented and the circuit characteristics at different operation modes are analyzed. In order to accurately predict the operation characteristic of the preheating circuit, the variations of the filament resistance during preheating are investigated and its mathematical model is developed. Furthermore, the equivalent resistance model of fluorescent lamp at steady-state is presented.

2-1 Half-Bridge Resonant Inverter

The half-bridge resonant inverters were invented in 1959 by Baxandall, and have been widely used in various applications [55-64]. The electronic ballast with the half-bridge resonant inverter has also been widely adopted in commercial products due to its simple configuration and high efficiency. The half-bridge resonant inverters can be classified into quasi half-bridge resonant inverters and standard half-bridge resonant inverters, as shown in Figure 2-1. The half-bridge resonant inverter mainly includes two bi-directional active power switches, S_1 and S_2, and a load resonant circuit. Each power switch S_1(S_2) is composed of an active switch Q_1(Q_2) and its intrinsic anti-parallel diode D_1(D_2). According to the combination form of the reactive components and the load, the load resonant circuits can commonly be classified into series resonant circuit, parallel resonant circuit, and series-parallel resonant circuit. Among them, the series-parallel resonant circuit is more suitable to be used for driving the fluorescent lamps since it can easily provide filament current for lamps.

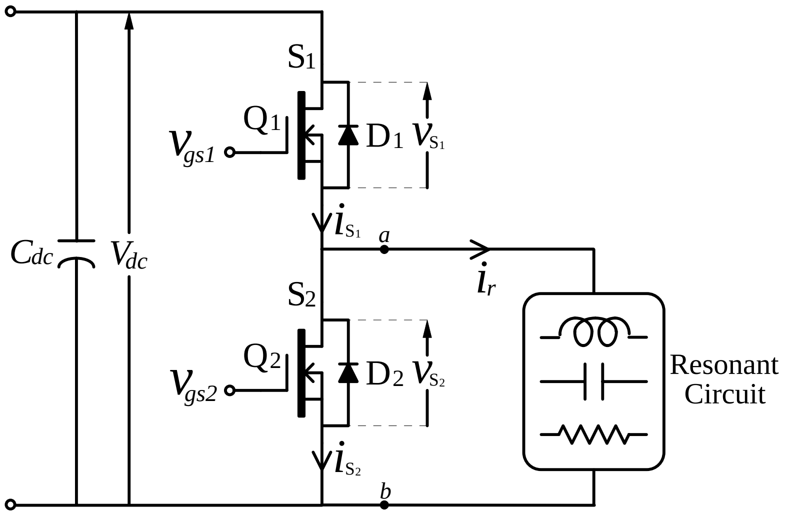

(a) Quasi half-bridge

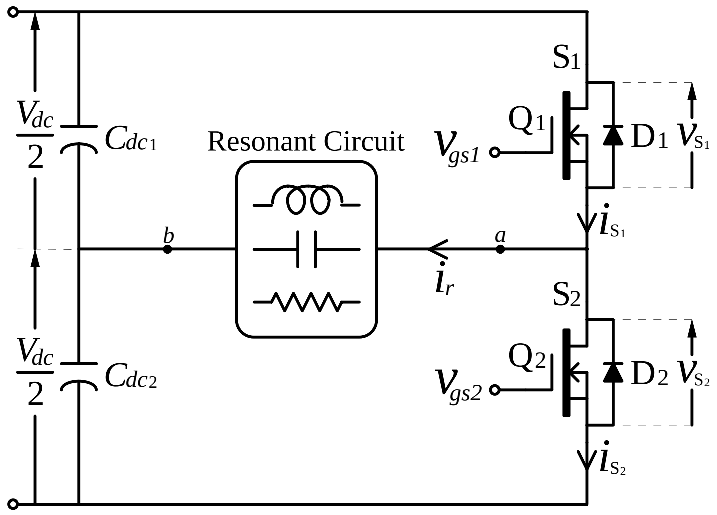

(b) Standard half-bridge

Figure 2-1 Half-bridge resonant inverters

The active switches, Q_1 and Q_2, of the half-bridge inverter are gated by two complementary signals, v_{gs1} and v_{gs2}, respectively. To prevent cross condition, the waveforms of v_{gs1} and v_{gs2} should be nonoverlapping and have a short dead time. By symmetrically driving two active switches, the output of the quasi half-bridge resonant inverter is a square-wave voltage with a dc term of $V_{dc}/2$ on the load resonant circuit. Therefore, a dc-blocking capacitor must be used for blocking the dc term of the square-wave. Due to the dc term of the square-wave, before ignition, the voltage across lamp can include a dc component and thus a higher ignition voltage can be obtained. However, this dc component may increase the glow current during the preheating interval. On the other hand, the standard half-bridge resonant inverter outputs a square-wave voltage without any dc term on the load resonant circuit. Therefore, there is no dc component across the lamp to increase the glow current during preheating and dc-blocking capacitor is not necessary. However, the standard half-bridge resonant inverter requires two identical dc-link voltage sources and hence two identical dc-link capacitors.

With a high load quality factor of the load resonant circuit, almost all the harmonic contents will be filtered out by the load resonant circuit. Only the fundamental current at the switching frequency will be present in the load resonant inverter. Therefore, the circuit can be analyzed using the fundamental component approximation [42-44,65]. The operation of the half-bridge resonant inverter can be divided into three cases according to the relationship between the resonance frequency and the switching frequency. The circuit operation is described as follows:

Case I. Switching frequency equals resonance frequency ($f_s = f_r$)

At $f_s = f_r$, the load resonant circuit presents resistive. The resonant current i_r is in phase with the fundamental voltage V_1 and the phase angle ψ between i_r and V_1 is zero. Figure 2-2 illustrates the theoretical waveforms of the half-bridge resonant inverter. While i_r is equal to zero, Q_1 is turned on. i_r rises from zero and flows through Q_1. Once i_r reaches zero again, Q_1 is turned off and Q_2 is turned on. At this time, i_r becomes negative. The negative resonant current flows through Q_2. The conduction sequence of the semiconductor devices is Q_1-Q_2-Q_1. The active power switches are turned on and off at zero current, resulting in zero switching losses and high efficiency. However, in many applications, the output power of the resonant circuit is often controlled by varying the switching frequency or duty-ratio of the half-bridge inverter. The zero current switching-on or switching-off will not exist due to the variation of switching frequency or duty-ratio. Therefore, in practical application, this case is not often adopted.

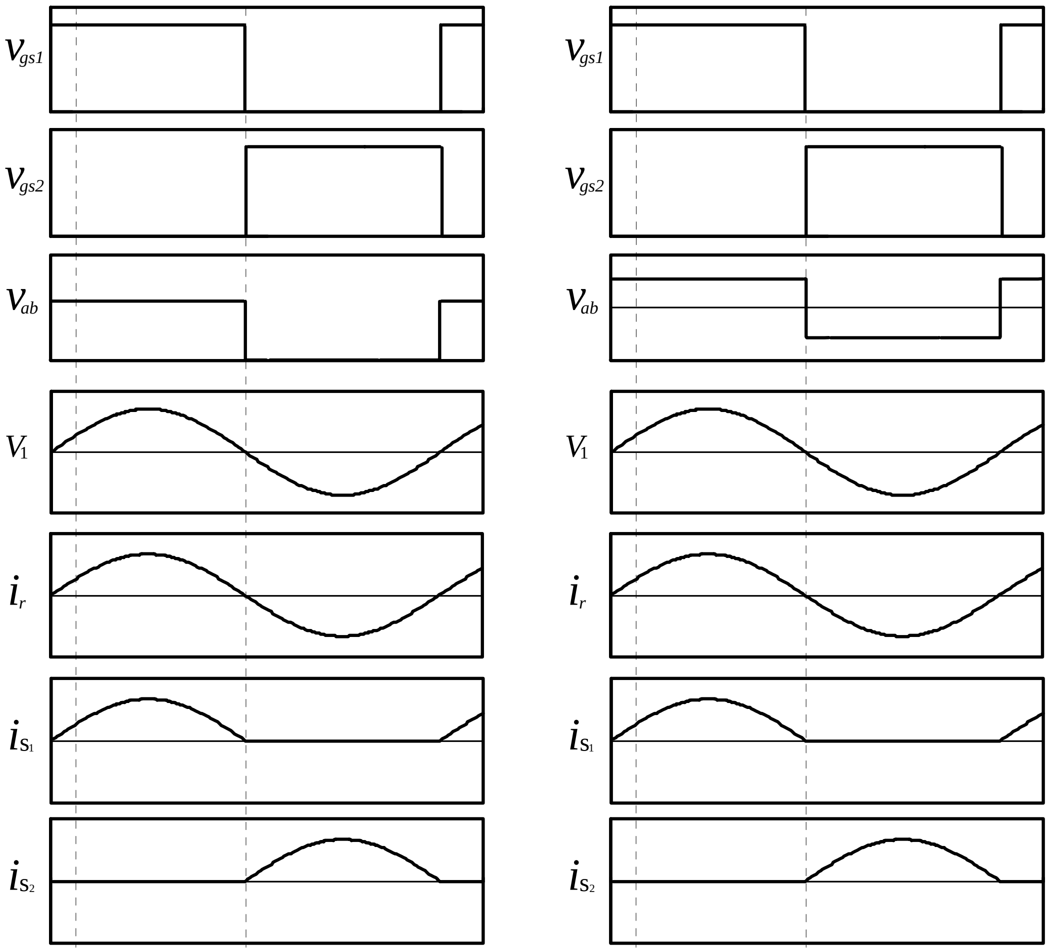

(a) Quasi half-bridge (b) Standard half-bridge

Figure 2-2 Waveforms of the half-bridge resonant inverters ($f_s = f_r$)

Case II. Switching frequency above resonance frequency ($f_s > f_r$)

For $f_s > f_r$, the load resonant circuit presents inductive. i_r lags behind V_1 by the phase angle ψ, where $\psi > 0$. The conduction sequence of the semiconductor devices is D_1-Q_1-D_2-Q_2-D_1. Figure 2-3 shows the theoretical waveforms of the half-bridge resonant inverter. While v_{gs2} varies from high to low, Q_2 is turned off. At the instant, i_r is negative and transferred from Q_2 to D_1. After the short period of the dead time, v_{gs1} varies from low to high. However, Q_1 is not turned on instantly. Until i_r resonates to zero, D_1 turns off naturally and Q_1 is then turned on to carry i_r. When D_1 is conductive, the voltage across S_1 is equal to the conduction voltage (-0.7V) of D_1. Therefore, Q_1 is turned on at zero voltage. When v_{gs1} varies from high to low, Q_1 is turned off. At this time, i_r is transferred from Q_1 to S_2 and thus

v_{s1} increases, causing v_{s2} to decrease. As v_{s2} reaches -0.7V, D_2 is turned on to carry i_r. Thus, the turn-off transition of the active power switch is forced by the gate-signal, while the turn-on transition is caused by the turn-off transition of the opposite active power switch, not by the gate-signal.

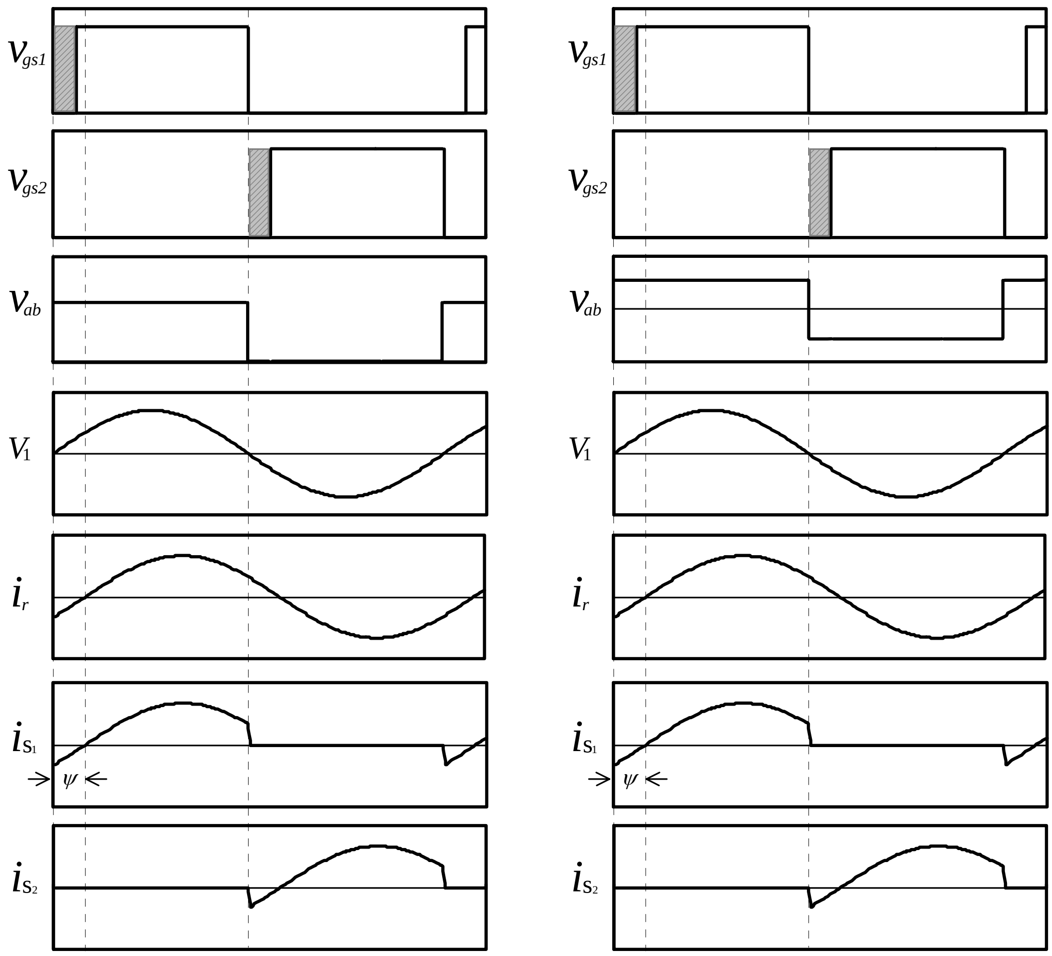

(a) Quasi half-bridge (b) Standard half-bridge

Figure 2-3 Waveforms of the half-bridge resonant inverters ($f_s > f_r$)

The active power switches have the merit of zero voltage switching-on (ZVS). Therefore, the switching-on losses of the active power switches are near zero, Miller's effect is absent, input capacitance of the active power switch is not increased by Miller's effect, the gate drive power is low, and the turn-on switching speed is high. The diodes are just turned off naturally when the resonant current changes direction at a very low *di*/*dt*. Therefore, a slow anti-parallel diode is enough. Usually, MOSFET's body-drain diode can be used as the anti-parallel diode.

For $f_s > f_r$, the switching-on losses of the active power switches are zero, however, that is not the same for the active power switches to be switched off. Both the switching voltage and current waveforms overlap during switching-off, causing the switching-off losses. Also, Miller's effect is considerable, increasing the input capacitance of the active power switch, the gate drive requirements, and reducing the turn-off speed. However, the switching-off losses can be reduced by adding a shunt capacitor to one of the active power switches. Hence, in order to achieve high efficiency, the resonance frequency of the load resonant circuit is usually set below the switching frequency.

Case III. Switching frequency below resonance frequency ($f_s < f_r$)

For $f_s < f_r$, the load resonant circuit presents capacitive. i_r leads V_1 by the phase angle $|\psi|$, where $\psi < 0$. The conduction sequence of the semiconductor devices is Q_1-D_1-Q_2-D_2-Q_1. Figure 2-4 shows the theoretical waveforms of the half-bridge resonant inverter. While v_{gs1} varies from low to high, Q_1 is turned on. At the instant, i_r is positive and transferred from D_2 to Q_1. Since i_r leads V_1, i_r resonates to zero before v_{gs1} varies from high to low. As i_r becomes negative, Q_1 turns off naturally and i_r is transferred from Q_1 to D_1. The voltage across S_1 varies from 1V to -0.7V approximately and the voltage across S_2 remains at about V_{dc}. Therefore; Q_1 is turned off at zero voltage, resulting in no switching-off loss. While v_{gs2} varies from low to high, Q_2 is turned on. At this time, i_r is transferred from D_1 to Q_2 and the voltage across S_2 reduces from V_{dc} to zero. Q_2 is turned on at a high voltage, equal to V_{dc}, and thus the switching-on loss of the active power switch is not zero. Once the switching current of S_2 becomes negative, D_2 is turned on and Q_2 turns off naturally. From the above analyses, it is well known that the turn-on transition of the active power switch is forced by the gate-signal, while the turn-off transition is caused by the turn-on transition of the opposite active power switch, not by the gate-signal.

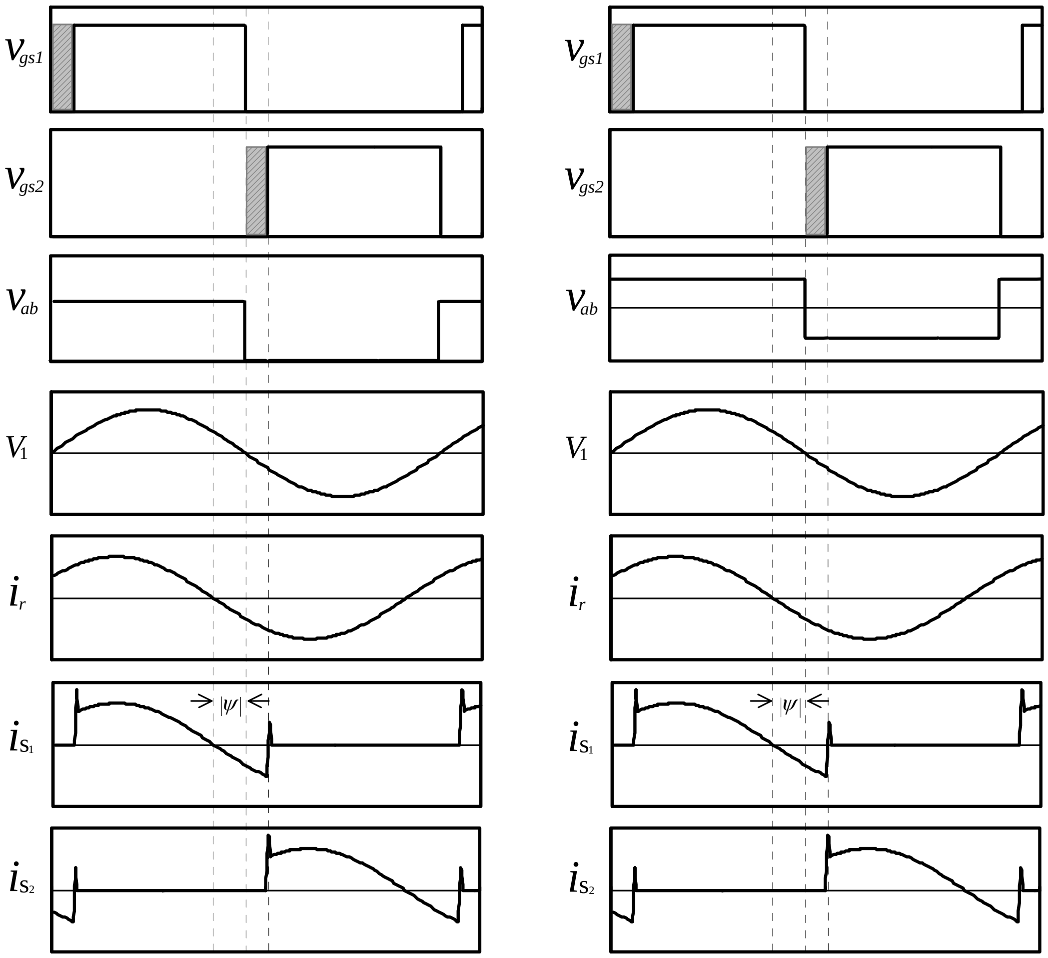

(a) Quasi half-bridge (b) Standard half-bridge

Figure 2-4 Waveforms of the half-bridge resonant inverters ($f_s < f_r$)

Once the ZVS operation for the active power switches cannot be achieved, some detrimental effects will be presented:

1). As the anti-parallel diode is turned off, the voltage across it rises from -0.7V to V_{dc}. The diode turns off at a very large *dv/dt* and thus at a very large *di/dt*, generating a high reverse-recovery current spike. Therefore, the diode reverse-recovery stress is very large. The spike flows through the other active power switch because it cannot flow through the resonant circuit. High current spikes may destroy the active power switches and always cause a considerable increase in switching losses and noise.

2). In general, each active power switch owns its output capacitor. Before the active power switch is turned on, its output capacitor is charged to V_{dc}.

Therefore, when the active power switch is turned on, its output capacitor is discharge, causing a switching loss of $CV_{dc}^{2}/2$.

3). Since the voltage of gate-signal increases and the voltage of active power switch decreases during the turn-on transition, Miller's effect is significant, increasing the input capacitance of the active power switch and the gate drive charge and power requirements, and reducing the turn-on switching speed.

2-2 Modeling Fluorescent Lamp

Being the load of the half-bridge resonant inverter, the fluorescent lamp plays a key role in the operation of the ballast-lamp circuit. Therefore, building the equivalent circuit model of the fluorescent lamp is very useful for analyzing and designing high frequency electronic ballasts. Figure 2-5 shows the basic structure of the fluorescent lamp and the conceptual diagram of its discharge characteristics [66,67]. The fluorescent lamp can be divided into two parts: cathode filaments and arc. The cathode filament can emit the electrons to the oppositional cathode filament to form the arc current. Thus, the coating material on the cathode filament emitting the electrons will be consumed. The structures of two ends of the fluorescent lamp present symmetrical. Each terminal can be either the positive electrode or the negative electrode. Therefore, the fluorescent lamp must be driven by a symmetrical ac source. Otherwise, the lamp life may be shortened.

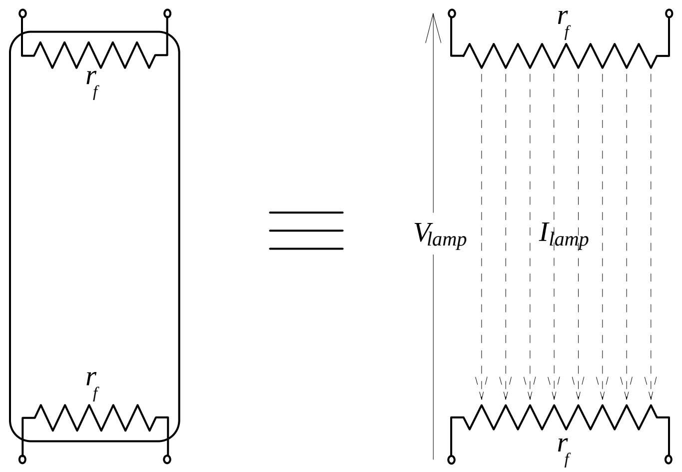

Figure 2-5 Basic structure of fluorescent lamp

2-2-1 Preheating Characteristics of Cathode Filament

In order to prolong the operation life of the fluorescent lamps, for preheating-start and rapid-start fluorescent lamps, the ballast circuit should provide a filament current or voltage to preheat the cathode filaments at the initial stage of lighting lamps. The preheating current or voltage cannot be too large; otherwise, the glow discharge may take place on two ends of the fluorescent lamp before ignition. This phenomenon can cause the coating material on the filaments over-evaporated. On the other hand, if the preheating current or voltage is too small, the cathode filaments may not be preheated to the proper emission temperature before ignition. Igniting a lamp at a low filament temperature requires a relatively high ignition voltage, resulting in extremely sputtering on the cathode filaments. This increases the loss rate of the emissive coating on the cathode filaments. The lamp ends become blackened due to the combination of the coating material with the fluorescent powders on the inner walls of tube and the gases in the lamp. Hence, both improper preheating conditions will shorten the lamp life.

With different structures of the fluorescent lamps, the filament resistances are not the same. Furthermore, the filament resistance varies with the filament temperature. As the filament temperature increasing, its resistance becomes high. The relation between the temperature and the resistance of the cathode filament can be expressed as [23-25,29]:

$$\frac{T_h}{T_c} = \left[\frac{r_{f\_h}}{r_{f\_c}}\right]^{0.814} \tag{2-1}$$

where T_c and T_h are the cold temperature before preheating and the hot temperature during preheating, both are in Kelvin thermometric scale; r_{f_c} and r_{f_h} are the resistances of the cold filament and the hot filament, respectively. In general, the appropriate emission temperature of the cathode filaments is about 1000K (920~1280K). Therefore, while the ratio of the hot resistance of the cathode filament to its cold resistance reaches about 4.5, the cathode filament will be heated up to a proper emission temperature. In general, the ratio is suggested to be from 4 to 6 [23-25,30].

Both of the constant-voltage preheating and the constant-current preheating can be used to preheat the cathode filament. As the filament temperature rises, the filament resistance increases, too. Thus, the variations in filament resistances of the two preheating methods are not the same. Figures 2-6~2-9 show the variations of the filament resistances of T8-36W, T8-32W, T12-40W and T12-20W fluorescent lamps under both filament-heating methods. The dashed lines of r_{f_UB} and r_{f_LB} represent the upper and lower bound of hot filament resistance, respectively. The minimum preheating time, t_{min}, for rapid-start operation defined by the America National Standards Institute (ANSI) is 0.5 second [21,28].

Figures 2-6(a), 2-7(a), 2-8(a) and 2-9(a) are the variations of the filament resistances at different preheating voltages. Initially, the filament power is higher due to the lower filament resistance. The filament temperature rises rapidly and thus the filament resistance increases rapidly. As the filament resistance increasing, the filament power decreases gradually and the increasing rate of the filament temperature becomes slow. The filament resistance stops increasing until the cathode filament reaches the thermal equilibrium. As for the case of constant current preheating, Figures 2-6(b), 2-7(b), 2-8(b) and 2-9(b) show the variations of the filament resistances at different preheating currents. At first, the filament resistance is low and thus the filament power is low. The filament temperature rises slowly at the initial stage. However, as the filament resistance increases, the filament power becomes higher gradually and the increasing rate of the filament temperature becomes rapider, resulting in the variation of the filament resistance intensified gradually. The filament resistance stops increasing until eventually reaches the thermal equilibrium.

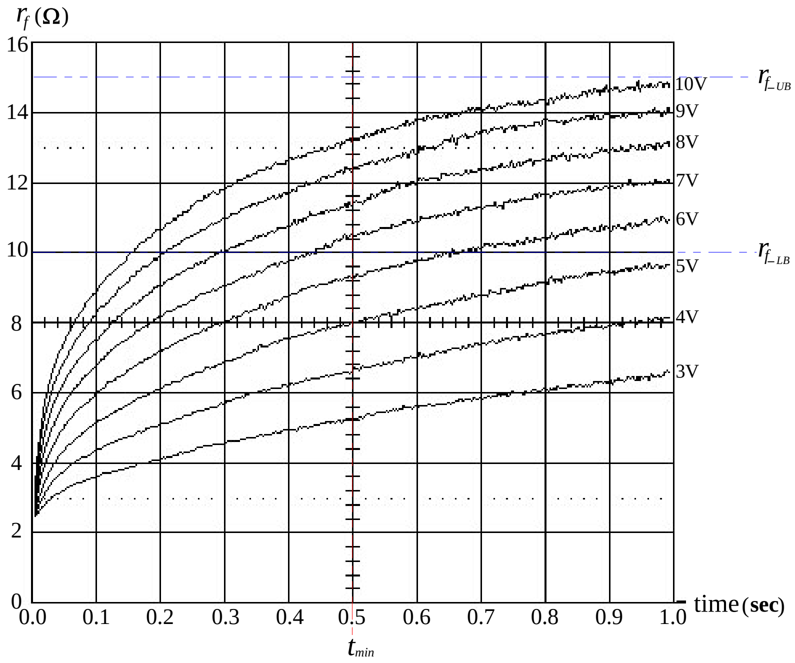

(a) Constant-voltage preheating

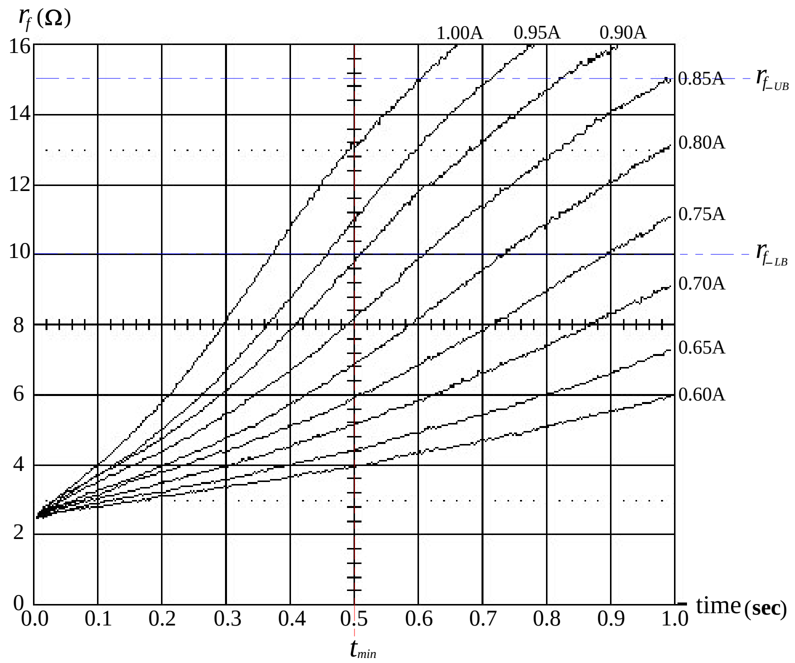

(b) Constant-current preheating

Figure 2-6 Variations of filament resistance (Experimental results for T8-36W)

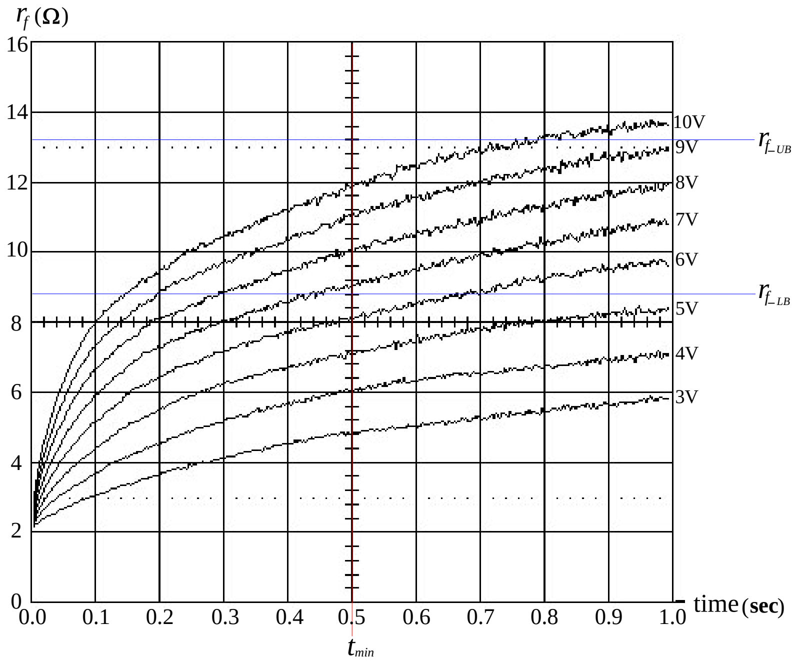

(a) Constant-voltage preheating

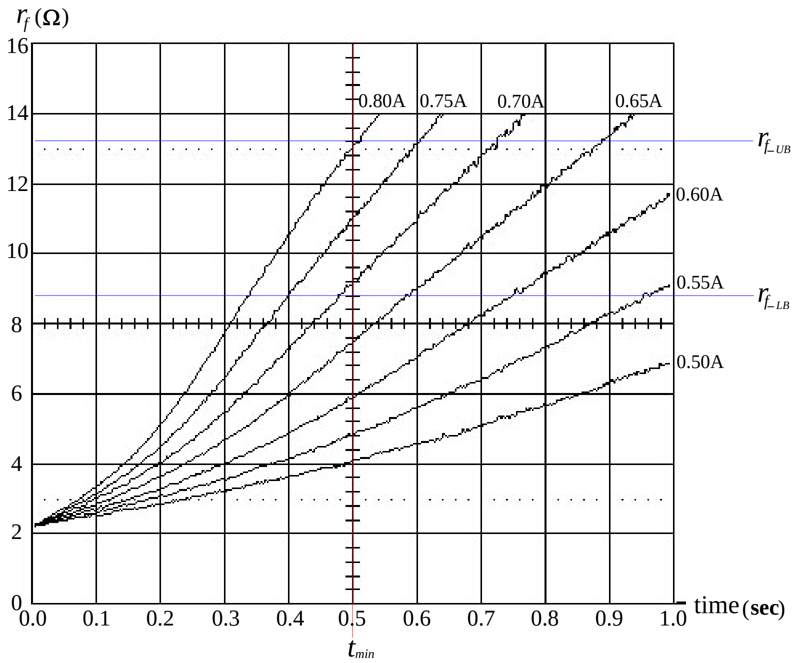

(b) Constant-current preheating

Figure 2-7 Variations of filament resistance (Experimental results for T8-32W)

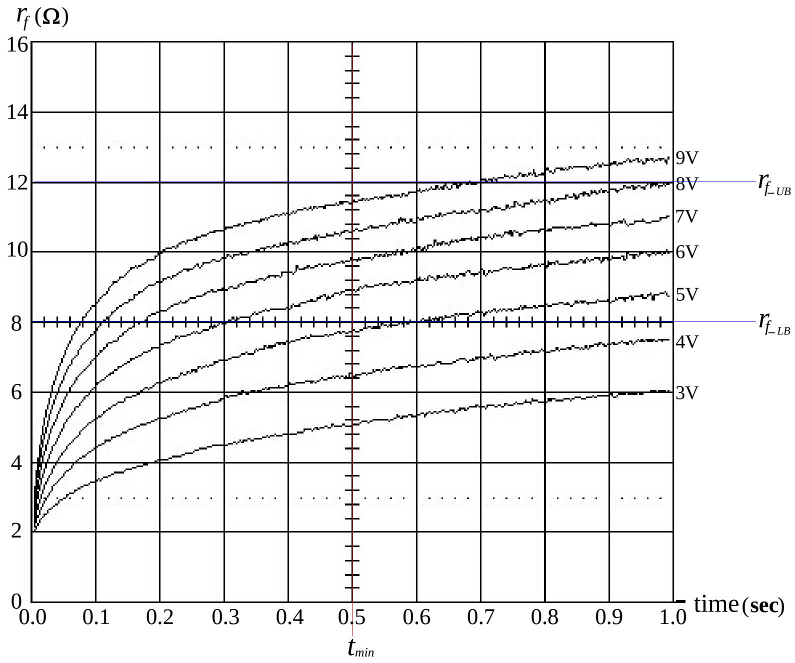

(a) Constant-voltage preheating

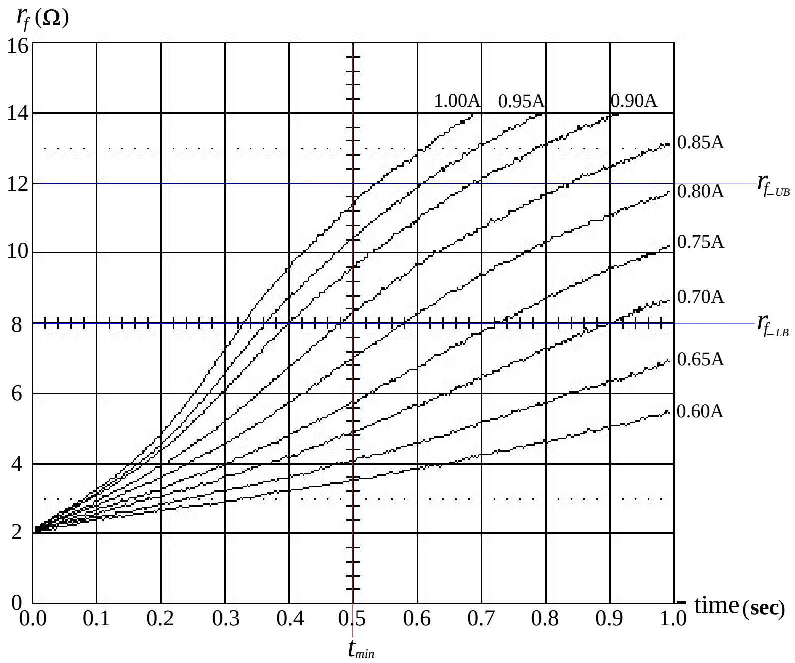

(b) Constant-current preheating

Figure 2-8 Variations of filament resistance (Experimental results for T12-40W)

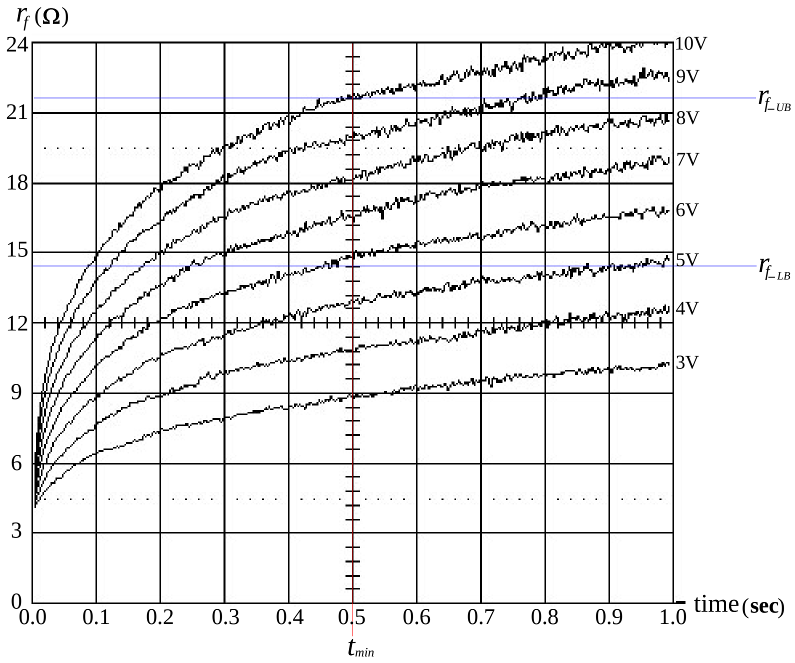

(a) Constant-voltage preheating

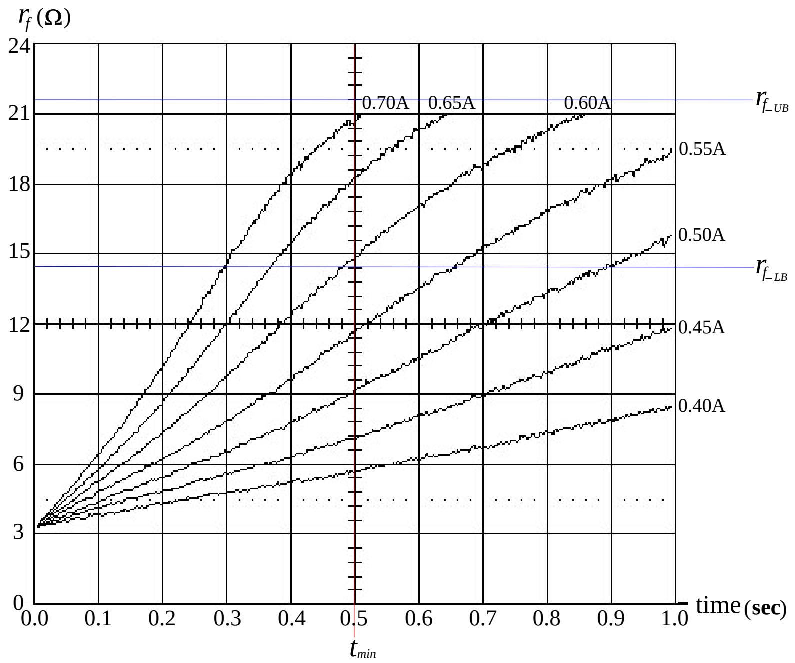

(b) Constant-current preheating

Figure 2-9 Variations of filament resistance (Experimental results for T12-20W)

From the above discussions, it can be found that if applying an adequate constant-voltage for preheating, the preheating results, i.e. T_h/T_c, are acceptable (4~6) for different fluorescent lamps at the same preheating time. However, the optimal filament temperature (1000K) cannot be assured to achieve. On the other hand, if applying a constant-current for preheating, the preheating results may be very different for different fluorescent lamps at the same preheating time. However, the optimal filament temperature can always be achieved in some preheating period. Therefore, if the preheating procedure must be finished in a preset period, the constant-voltage preheating is a better choice. On the contrary, as adopting the constant-current preheating, the optimal preheating result can be achieved by monitoring the filament temperature or filament resistance.

2-2-2 Mathematical Model of Filament Resistance

The filament resistance is dependent upon its temperature. At steady-state operation, the filament temperature should be maintained at a proper emission temperature. Too high or too low filament temperature will shorten the lamp life. The filament resistance exhibits positive temperature coefficient characteristic and the variation of the filament resistance at the emission temperature is small. Therefore, at steady-state, treating the filament resistance as a constant will not cause any influential error for circuit analyses. However, when the cold lamp is started up, the temperature of the cathode filament varies from low to high and so does its resistance. The filament resistance cannot be treated as a constant as calculating the preheating voltage, current and power.

From the measured curves of Figures 2-6~2-9, it is well known that the variation of the filament resistance during preheating is significantly affected by the preheating voltage V_p or current I_p. Therefore, the curves for the filament preheated by a constant-voltage controllable source can be represented by a resistance equation as a function of preheating time t_p with preheating-voltage-dependent coefficients shown in (2-2).

$$r_f(t_p, V_p) = A_V(V_p) - B_V(V_p) \cdot \exp\left(\frac{-t_p}{\tau_{VB}(V_p)}\right) - C_V(V_p) \cdot \exp\left(\frac{-t_p}{\tau_{VC}(V_p)}\right) \qquad (2\text{-}2)$$

On the other hand, the curves for the filament preheated by a constant-current controllable source can be represented by a resistance equation as a function of preheating time t_p with preheating-current-dependent coefficients shown in (2-3).

$$r_f(t_p, I_p) = \frac{1}{A_I(I_p) + \left(B_I(I_p) - A_I(I_p)\right) \cdot \exp\left(\dfrac{-t_p}{\tau_I(I_p)}\right)} \tag{2-3}$$

By using the regression analysis, the constant coefficients in (2-4)~(2-8) and in (2-9)~(2-11) can be derived, respectively. Table 2-1 shows the derived coefficients for two given fluorescent lamps. Then, from (2-2) and (2-3) with the derived coefficients, the variations of the filament resistance with respect to the preheating time and the preheating voltage or current can be depicted in Figures 2-10 and 2-11. Comparing Figures 2-6 and 2-8 with Figures 2-10 and 2-11, it can be found that, for both examples, well agreement is found between the measured results and the calculations by using (2-2) and (2-3). Hence, (2-2) and (2-3) can be used to describe the variations of the filament resistances during preheating.

$$A_V(V_p) = A_{V2}V_p^2 + A_{V1}V_p + A_{V0} \tag{2-4}$$

$$B_V(V_p) = B_{V2}V_p^2 + B_{V1}V_p + B_{V0} \tag{2-5}$$

$$C_V(V_p) = C_{V2}V_p^2 + C_{V1}V_p + C_{V0} \tag{2-6}$$

$$\tau_{VB}(V_p) = \tau_{VB2}V_p^2 + \tau_{VB1}V_p + \tau_{VB0} \tag{2-7}$$

$$\tau_{VC}(V_p) = \tau_{VC2}V_p^2 + \tau_{VC1}V_p + \tau_{VC0} \tag{2-8}$$

$$A_I(I_p) = A_{I2}I_p^2 + A_{I1}I_p + A_{I0} \tag{2-9}$$

$$B_I(I_p) = B_{I0} \tag{2-10}$$

$$\tau_I(I_p) = \tau_{I0} + \tau_{I1} \cdot \exp\left(-\frac{I_p}{\tau_{I2}}\right) \tag{2-11}$$

Table 2-1 Constant coefficients for filament model

(a) Constant-voltage preheating

		T8-36W	T12-40W
$A_V(V_p)$	A_{V2}	-0.0569	-0.0275
	A_{V1}	1.7427	1.5101
	A_{V0}	3.4544	2.5655
$B_V(V_p)$	B_{V2}	-0.0504	-0.0537
	B_{V1}	1.0847	0.8686
	B_{V0}	2.3196	1.5426
$C_V(V_p)$	C_{V2}	-0.0130	0.0108
	C_{V1}	0.6354	0.6251
	C_{V0}	-1.0421	-0.8144
$\tau_{VB}(V_p)$	τ_{VB2}	0.0123	0.0195
	τ_{VB1}	-0.2315	-0.2213
	τ_{VB0}	1.4518	1.1509
$\tau_{VC}(V_p)$	τ_{VC2}	-0.0002	0.0004
	τ_{VC1}	0.0015	-0.0057
	τ_{VC0}	0.0276	0.0705

(b) Constant-current preheating

		T8-36W	T12-40W
$A_I(I_p)$	A_{I2}	-0.1146	0.1209
	A_{I1}	0.2204	-0.2412
	A_{I0}	-0.0545	0.1867
$B_I(I_p)$	B_{I0}	0.4000	0.4850
$\tau_I(I_p)$	τ_{I2}	0.1721	0.1621
	τ_{I1}	29.255	23.789
	τ_{I0}	0.1094	0.1166

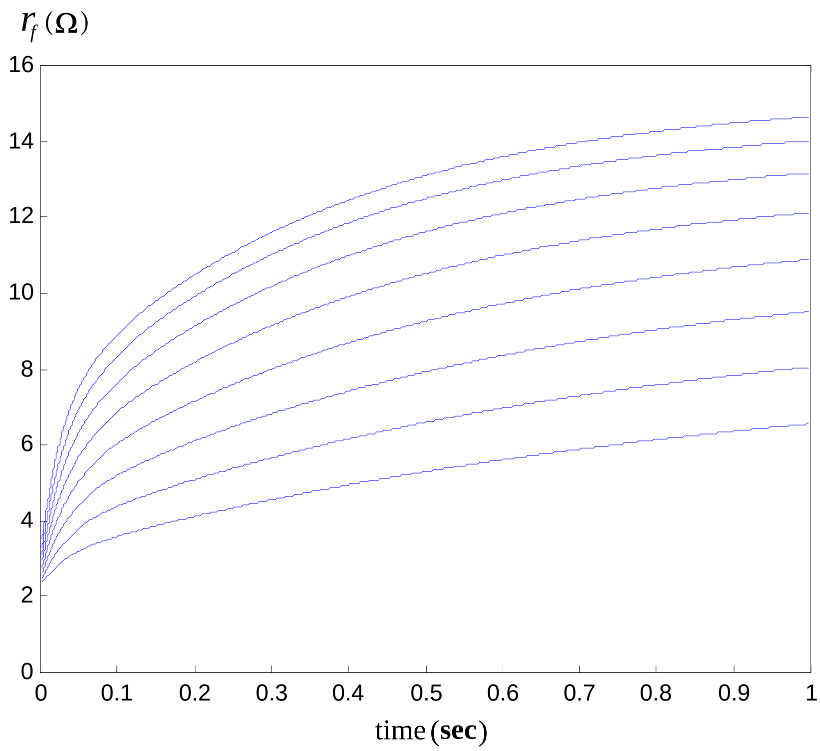

(a) Constant-voltage preheating

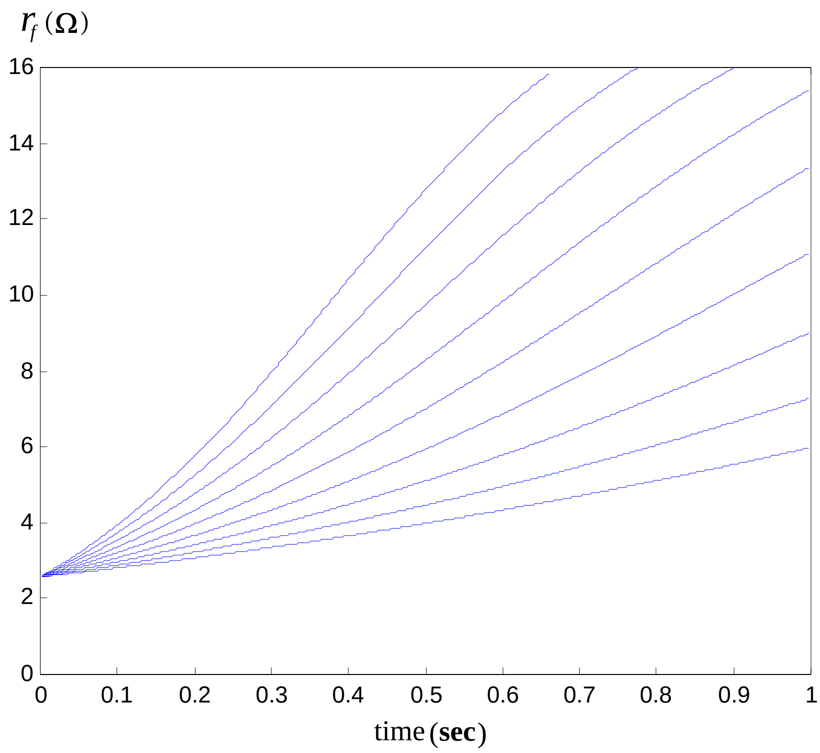

(b) Constant-current preheating

Figure 2-10 Variations of filament resistance (Calculated results for T8-36W)

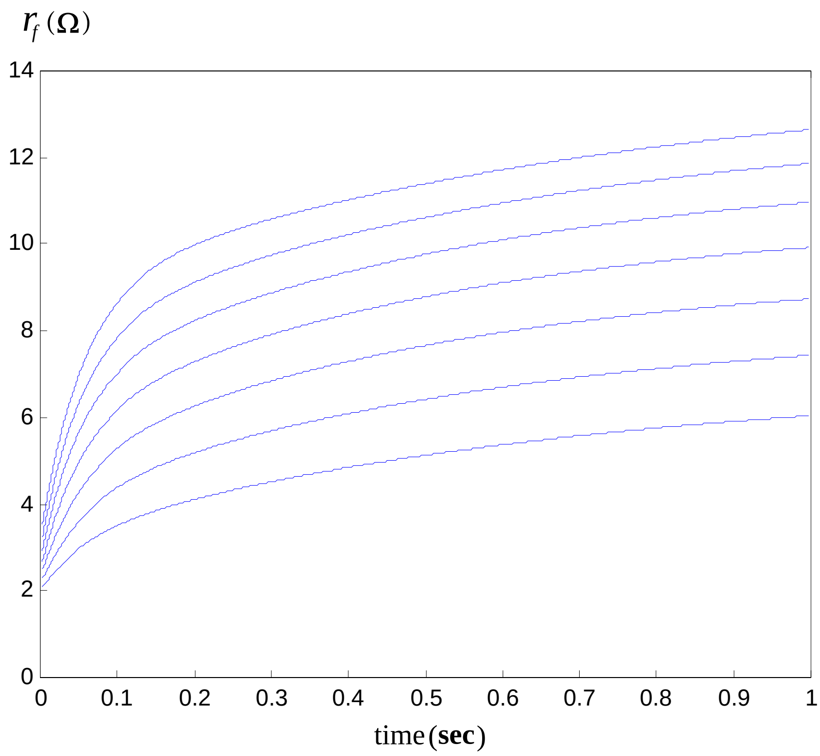

(a) Constant-voltage preheating

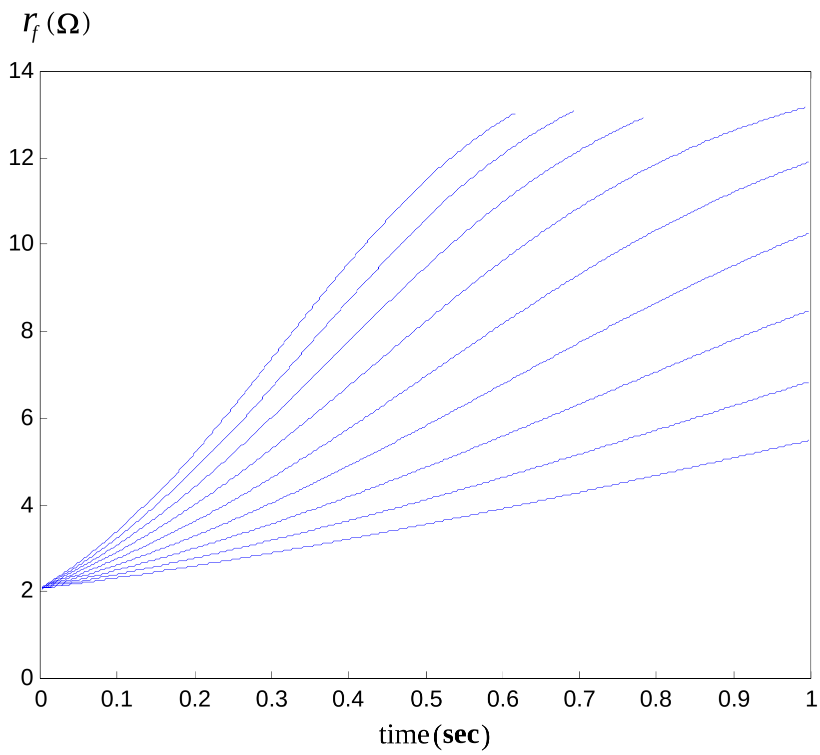

(b) Constant-current preheating

Figure 2-11 Variations of filament resistance (Calculated results for T12-40W)

2-2-3 Equivalent Circuit Model of Fluorescent Lamp

Although the structure of the fluorescent lamp looks simple, its discharge mechanism is very complicated. Fortunately, the fluorescent lamp, when operated at a high frequency, has been demonstrated to be approximately resistive and the lamp characteristic is not sensitive to the operation frequency when the frequency lies between 10kHz and 200kHz. Therefore, the operation characteristics of the high-frequency electronic ballast can be calculated by using the lamp resistance model.

In practice, the resistance of the filaments distributes from one end to the other and each part of the filament can emit the electrons to form the arc current, as shown in Figure 2-5. Therefore, the accurate circuit analyses can be realized when a distributed circuit model of the filament resistance is used. However, this will increase the complexity of the circuit analyses. In general, in order to simplify the analyses, each cathode filament can be represented by a lumped resistance, r_f.

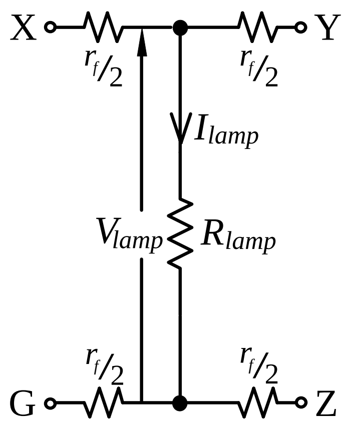

Figure 2-12 Equivalent resistance model of fluorescent lamp

Figure 2-12 shows the adopted lamp model, which is represented by a power-dependent resistance of the lamp arc R_{lamp} and a filament resistance for each cathode filament [67-69]. The equivalent lamp arc resistance is connected between the midpoints of two cathode filaments for more precise calculations. In general, the rated lamp voltage and current, V_{lamp} and I_{lamp}, can be obtained from the manufacturer. While the fluorescent lamp is operated at the rated power, the equivalent lamp arc resistance R_{lamp} can be derived simply by :

$$R_{lamp} = \frac{V_{lamp}}{I_{lamp}} \tag{2-12}$$

Chapter 3 Programmed Rapid-Start Electronic Ballast with An AC Switch

In order to get rid of the glow discharge in the rapid-start fluorescent lamp driven by the half-bridge series-resonant electronic ballast, a programmed rapid-start control scheme is proposed in this chapter. In the proposed control scheme, an ac switch is introduced as the starting-aid circuit of the lamp. With the starting-aid circuit, the lamp voltage at the preheating stage can be maintained at zero by turning on the ac switch. This will ensure that no glow discharge may occur during the preheating interval.

3-1 Circuit Configuration

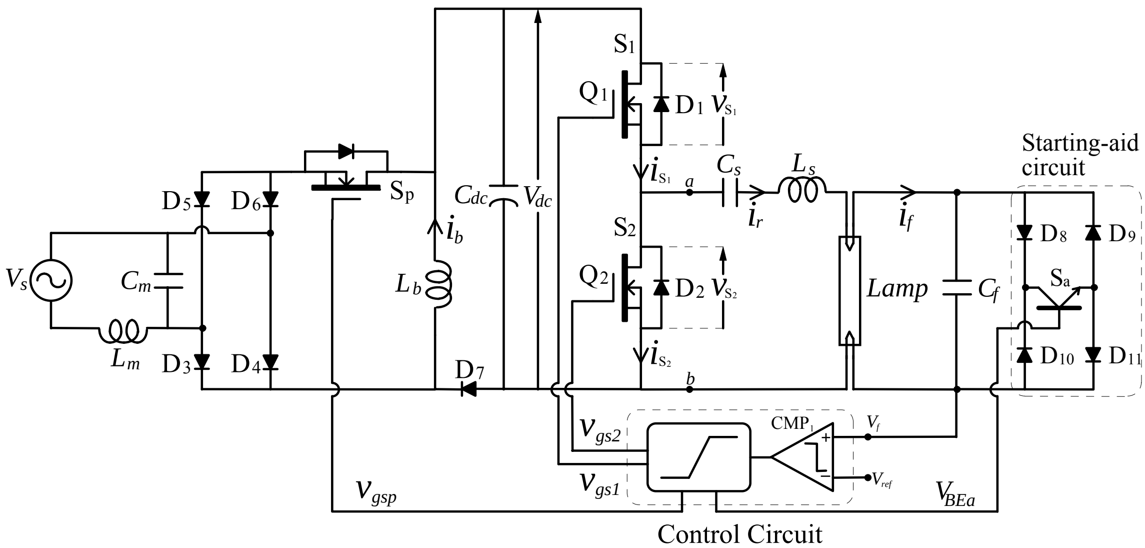

Figure 3-1 Circuit configuration of the two-stage electronic ballast

Figure 3-1 shows the circuit configuration of the proposed two-stage high-power-factor electronic ballast with programmed rapid-start. It mainly consists of a diode-bridge rectifier, a buck-boost converter with a dc-link capacitor, C_{dc}, and a quasi half-bridge series-resonant parallel-loaded inverter with the starting-aid circuit. Two power MOSFETs, S_1 and S_2, are adopted as the power switches of the half-bridge inverter for high-frequency switching. Each power switch is composed of an active switch and its intrinsic anti-parallel diode. The load resonant circuit of the inverter is formed by the fluorescent lamp and the reactive components C_s, L_s and C_f. The starting-aid circuit, which is added on the load resonant circuit in parallel with C_f and the fluorescent lamp, is composed of a diode-bridge rectifier and a transistor, S_a. The buck-boost converter, which operates as a PFC stage, consists of an inductor, L_b, a freewheeling diode, D_7, and an active power switch, S_p. A small low-pass filter, L_m and C_m, is used to remove the high frequency current harmonics at the input line.

However, the two-stage topology requires two control circuits, which are used to control the buck-boost converter and the quasi half-bridge resonant inverter, respectively, and three active power switches, resulting in higher cost and lower efficiency. In order to solve this problem, the buck-boost converter can be integrated into the quasi half-bridge resonant inverter to form the single-stage high-power-factor electronic ballast, as shown in Figure 3-2. The diode, D_8, is added to provide a path for the resonant current i_r when Q_2 is turned on and to block inductor current i_b from flowing through the input line when Q_2 is turned off. The diode, D_9, is used for freewheeling i_r. By sharing the active power switch and the control circuit, the component count can be effectively reduced [70-73].

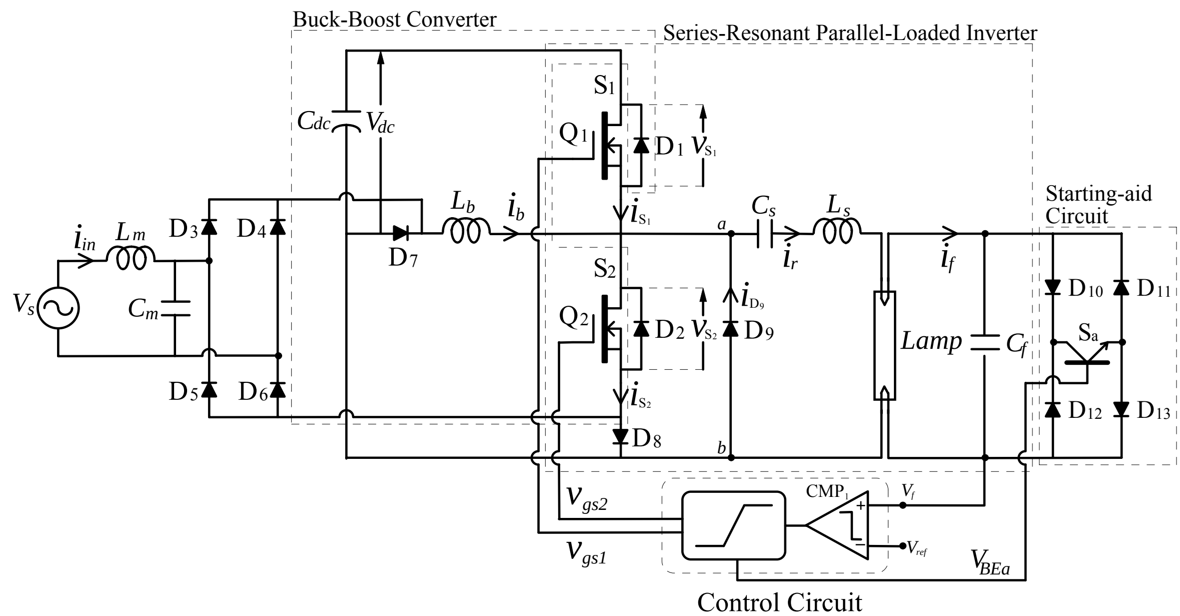

Figure 3-2 Circuit configuration of the single-stage electronic ballast

3-2 Circuit Operation

The active switches, Q_1 and Q_2, of the ballast circuit are gated by two complementary signals, v_{gs1} and v_{gs2}, respectively, with a short dead time to output a square-wave voltage on the load resonant circuit. Neglecting the dead time, the duty-ratio of v_{gs1} is (1-d) when that of v_{gs2} is d. By regulating the operation frequency and duty-ratio of the active switches and controlling the transistor S_a, the ballast can provide an appropriate preheating current during the preheating interval and a compensated filament current to maintain the emission temperature at steady-state operation. In addition, it can generate a sufficiently high voltage to ignite the lamp.

The operation of the ballast-lamp circuit is described by three stages: preheating, ignition, and steady-state. During the preheating stage, the transistor S_a is at “on” state and the ballast provides a current flowing through the cathode filament for preheating. Since the ac switch is turned on, the lamp voltage can be maintained at zero to ensure that no glow current will occur. When the filament temperature reaches the emission temperature, S_a is turned off and the operation frequency of the active switches is changed toward the resonance frequency, $f_{r,ign}$, to generate a very high ignition voltage. Once the lamp has been successfully ignited, the operation frequency and the duty-ratio are regulated to produce the required lamp power. S_a is kept at its “off” state during the steady-state operation.

The operation of the electronic ballast can be subdivided into six modes within one high-frequency switching cycle according to the conducting conditions of the power switches, as shown in Figure 3-3. The input filter is omitted for simplicity. Figure 3-4 illustrates the theoretical waveforms for each mode. To achieve a high power factor, the buck-boost converter is operated in discontinuous conduction mode (DCM). The operation frequency of the inverter is greater than the resonance frequency of the load resonant circuit to ensure ZVS at the switching-on of the active switch Q_1. The circuit operation is described as follows:

Mode I ($t_0<t<t_1$):

Prior to Mode I, the positive load resonant current, i_r, flows through D_9. At the beginning of Mode I, Q_2 is switched on. The rectified line voltage is imposed on the inductor, L_b. With DCM operation, the inductor current i_b of the buck-boost converter increases linearly from zero. The slope of i_b is proportional to the rectified line voltage. When i_r resonates to zero, D_9 turns off and Mode II is entered.

Mode II ($t_1<t<t_2$):

During this mode, Q_2 is kept at on state and carries both the inductor current and the load resonant current. The load resonant current goes through D_8 and the inductor current flows back through the rectifier to the line source. The rectified line voltage is applied on L_b and i_b increases continuously.

Mode III ($t_2<t<t_3$):

At the beginning of Mode III, i_b reaches its peak and Q_2 is switched off. Both i_b and i_r are transferred from Q_2 to D_1 to charge the dc-link capacitor, C_{dc}. i_b decreases linearly and i_r resonates from negative to positive.

Since the peak of i_b is proportional to the rectified input voltage, the duration for i_b declining to zero is not constant but varies with the rectified line voltage. Thus, there are two possible modes following Mode III, depending on which of the current i_b and i_r reaches zero first.

Mode IV-a ($t_3<t<t_4$):

When the line voltage is high, i_r declines to zero before i_b does. Mode III ends at the time when the sum of i_b and i_r becomes zero, and then, the circuit enters mode IV-a. At this instant, D_1 turns off naturally and Q_1 is then turned on to carry the sum of i_b and i_r with ZVS. In this mode, i_b decreases continuously. This mode ends when i_b decreases to zero.

Mode IV-b ($t_3<t<t_4$):

At low line voltage, the peak of i_b is small and declines to zero faster. In case that i_b decreases to zero earlier than i_r does, Mode IV-b instead of Mode IV-a, follows Mode III. In this mode, i_r flows through D_1 continuously. This mode ends at the time when i_r resonates to zero. Then, Q_1 is turned on to carry i_r with ZVS.

Mode V ($t_4<t<t_5$):

During this mode, the positive i_r flows through Q_1. C_{dc} supplies energy to the load resonant circuit.

Mode VI ($t_5<t<t_6$):

Mode VI represents the short period of the dead time. At the beginning of this mode, Q_1 is switched off. At the instant, i_r is positive and freewheels through D_9. When Q_2 is switched on, the mode ends and the operation returns to Mode I of the next cycle.

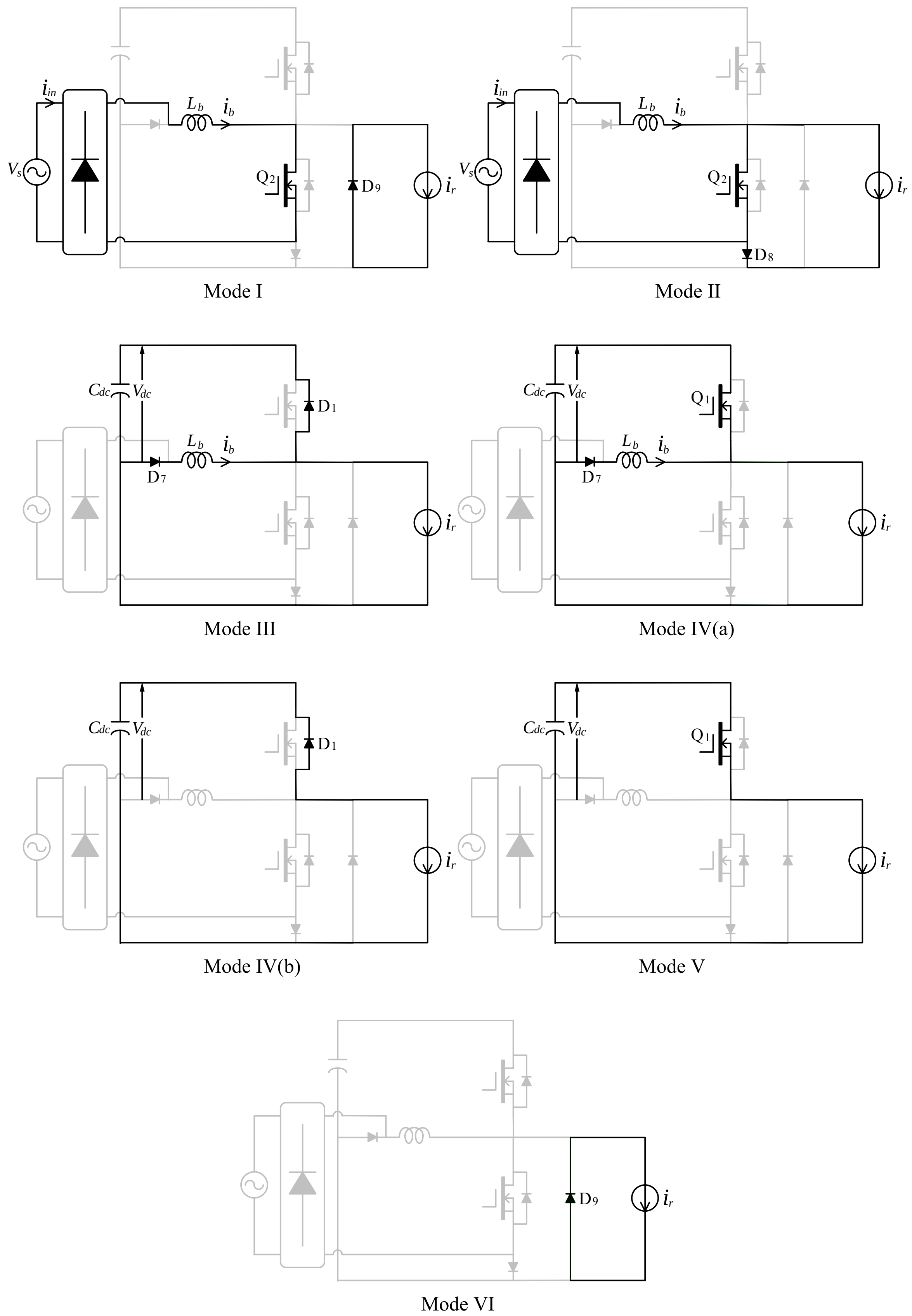

Figure 3-3 Operation modes

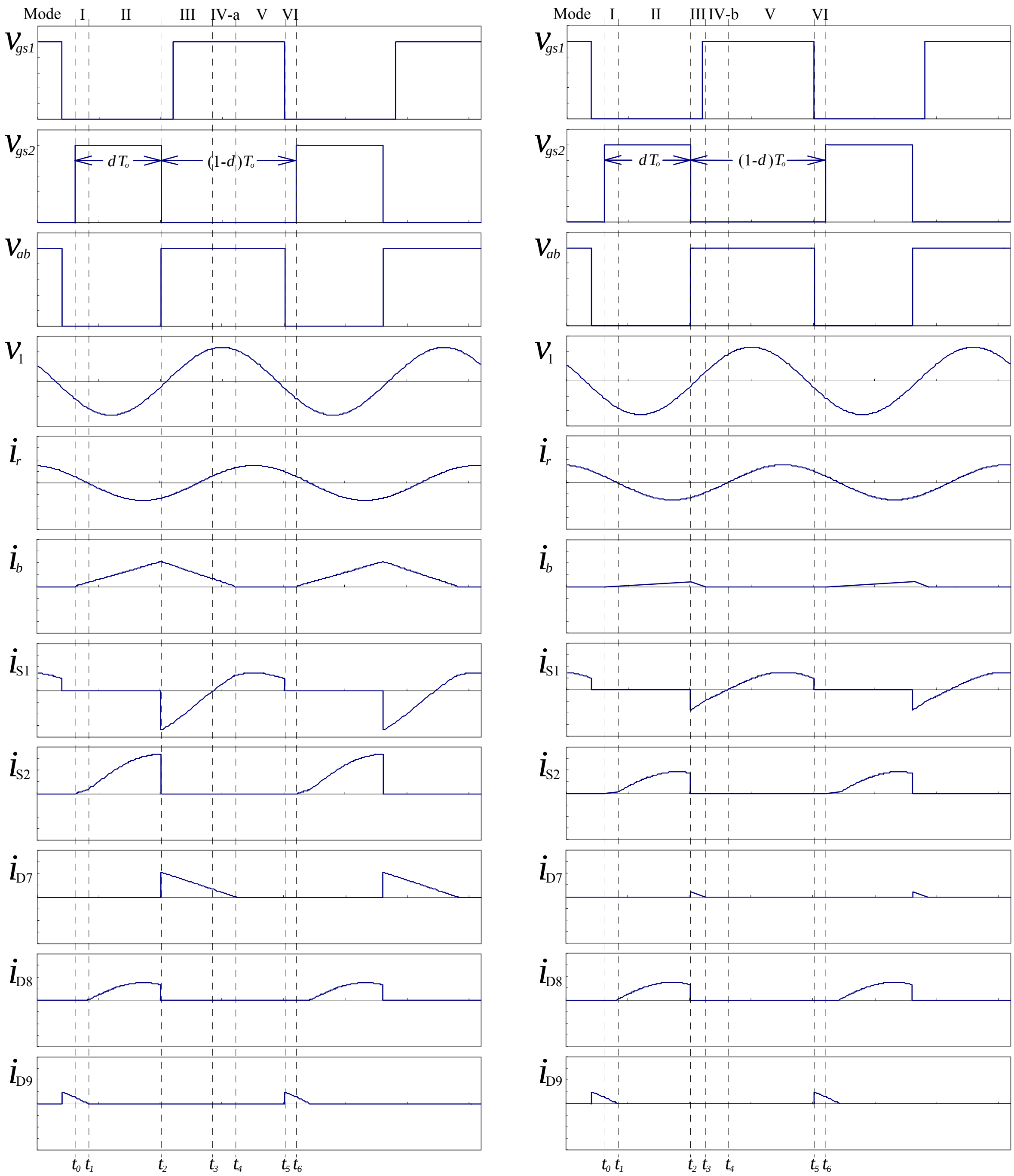

(a) Near line peak voltage (b) Near zero crossing

Figure 3-4 Theoretical waveforms

3-3 Circuit Analysis

For simplifying the analysis, the following assumptions are made:

1) All the circuit components are ideal.
2) The load quality factor of the load resonant circuit is high enough so that the

load resonant current is sinusoidal.

3) The capacitance of C_{dc} is large enough, thus the dc-link voltage V_{dc} can be approximated as a voltage source at steady-state.
4) The lamp is regarded as an open circuit before ignition, and a resistance at the steady-state operation.

From the operation modes described above, it can be well known that the input power is first delivered to the dc-link capacitor through the buck-boost converter and then delivered to the lamp through the load resonant inverter, that is, no the interaction of the energy delivery between the two power converters. Thus, the electronic ballast can be treated as two independent stages, the buck-boost power factor corrector and the load resonant inverter. However, as undertaking the analysis of the variation of the dc-link voltage, the interaction between two power converters must be considered.

3-3-1 Buck-Boost Power Factor Corrector

The electronic ballast is supplied from the ac line voltage source.

$$v_s(t) = V_m \sin(2\pi f_L t) \tag{3-1}$$

where f_L and V_m are the frequency and amplitude of the line voltage source, respectively. In practice, f_L is much lower than the inverter operation frequency, f_o. Under such an assumption, the rectified line voltage can be considered as a constant over a high frequency cycle of the inverter. During the Modes I and II, the line source supplies current to the buck-boost converter and the unfiltered input current, i_{in}, is equal to i_b. Since the buck-boost converter is operated at DCM over an entire line frequency cycle, i_b rises from zero at the beginning of Mode I and reaches its peak at the end of Mode II. Then, it declines to zero before the end of Mode IV. The waveform of i_{in} is conceptually shown in Figure 3-5. Its peaks follow a sinusoidal envelope and can be expressed as:

$$i_{in,peak}(t) = \frac{V_m \sin(2\pi f_L t)}{L_b} dT_o \tag{3-2}$$

where T_o is the high-frequency operation period. The average input current in every switching period can be expressed as:

$$i_{in,avg}(t)=\frac{V_m \sin(2\pi f_L t)}{2L_b}d^2 T_o \tag{3-3}$$

This equation reveals that the average input current is proportional to the ac line voltage and in phase with it if the operation frequency and duty-ratio retain constant over a line cycle. As a result, a high power factor can be achieved by using a small filter at the input line terminal to remove the high-frequency contents.

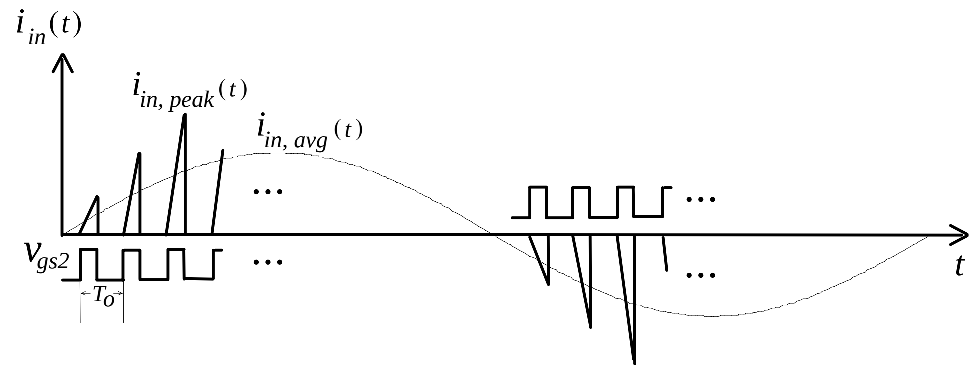

Figure 3-5 Conceptual waveform of i_{in}

The input power can be obtained by taking average of the instantaneous line power over one line frequency cycle.

$$P_{in}=\frac{1}{2\pi}\int_0^{2\pi} v_s(t)\cdot i_{in,avg}(t)d(2\pi f_L t)=\frac{V_m^2 d^2 T_o}{4L_b} \tag{3-4}$$

For a circuit efficiency of η, the lamp power P_{lamp} can be obtained as:

$$P_{lamp}=P_{in}\cdot\eta=\frac{V_m^2 d^2 T_o}{4L_b}\cdot\eta \tag{3-5}$$

In order to operate the buck-boost converter at DCM, the following equation should be satisfied.

$$V_m\left|\sin(2\pi f_L t)\right|\cdot dT_o - V_{dc}\cdot(1-d)T_o \le 0 \tag{3-6}$$

This equation indicates that if the DCM operation of the buck-boost power factor corrector at the line peak voltage can be achieved, it will always be operated at DCM over one line frequency cycle. Therefore, the dc-link voltage V_{dc} should be high enough and satisfy the following equation.

$$V_{dc} \geq \frac{d}{1-d} V_m \tag{3-7}$$

3-3-2 Series-Resonant Parallel-Loaded Inverter

The square-wave voltage, v_{ab}, applied to the load resonant circuit can be represented by the Fourier series:

$$v_{ab} = (1-d)V_{dc} + \sum_n \left[\frac{\sqrt{2}V_{dc}}{n\pi} \sqrt{(1-\cos(2n\pi d))} \sin(n\omega_o t + \pi + \theta_n) \right] \tag{3-8}$$

where $\omega_o = 2\pi f_o$ and,

$$\theta_n = \tan^{-1}\left(\frac{\sin(2n\pi d)}{1-\cos(2n\pi d)} \right) \tag{3-9}$$

With a high load quality factor of the load resonant circuit, almost all the harmonic contents, as well as the dc term, will be filtered out by the load resonant circuit. Only the fundamental current at the switching frequency will be present in the load resonant inverter. Therefore, the circuit can be analyzed using the fundamental component approximation. The rms value of the fundamental component of v_{ab} is:

$$V_1 = \frac{\sqrt{2}V_{dc} \sin(\pi d)}{\pi} \tag{3-10}$$

The operation of the ballast-lamp circuit is divided into three stages: preheating, ignition, and steady-state. For the different stages, the equivalent circuits of the load resonant inverter are not the same. Hence, the load resonant inverter must be executed a complete analysis for each stage.

● *Preheating*

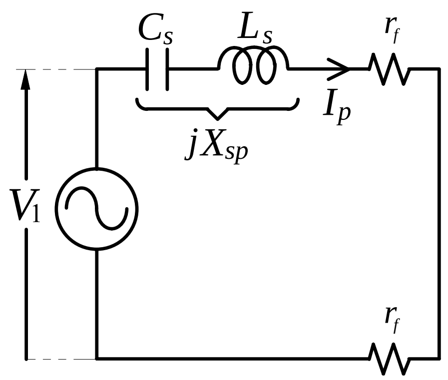

Figure 3-6 Equivalent circuit of the resonant inverter during preheating

During the preheating interval, the resonant inverter is operated at the preheating frequency, f_p, and the starting-aid circuit is short-circuited. Therefore, there is no voltage across the lamp. This ensures that no glow current will occur at the preheating stage. The equivalent circuit of the half-bridge series-resonant parallel-loaded inverter is shown in Figure 3-6 and the natural resonance frequency of the circuit is:

$$f_{r,pre} = \frac{1}{2\pi\sqrt{L_s C_s}} \tag{3-11}$$

From the equivalent circuit, the relation between the preheating current I_p and the fundamental voltage V_1 can be expressed as:

$$I_p = \frac{V_1}{\sqrt{4r_f^2 + X_{sp}^2}} \tag{3-12}$$

where r_f is the resistance on each cathode filament and,

$$X_{sp} = 2\pi f_p L_s - \frac{1}{2\pi f_p C_s} \tag{3-13}$$

This equation indicates that while f_p is closer to $f_{r,pre}$, the ballast circuit can provide enough preheating current to preheat the filaments up to a proper temperature at a lower V_1 and hence lower V_{dc}. To start the lamp rapidly, the preheating current may be chosen as high as possible but should be limited by the rated filament current.

At the preheating stage, it is noted that only the cathode filaments in the load resonant circuit consume the input power. However, with such an integrated ballast circuit, the buck-boost power factor corrector draws power continually from the input line source. The residual input power, which is not consumed by the cathode filaments, is accumulated in C_{dc} leading to the increase in V_{dc}. The increasing energy in C_{dc} during the preheating interval can be expressed as:

$$\frac{1}{2}C_{dc}\left\{\left[V_{dc}(t+\Delta t)\right]^2-\left[V_{dc}(t)\right]^2\right\}=\left[\eta P_{in}-2r_f I_p^2\right]\cdot\Delta t$$
$$=\left[\frac{\eta d^2 V_m^2}{4L_b f_p}-\frac{4r_f V_{dc}^2(t)\left[\sin(\pi d)\right]^2}{\pi^2\left[4r_f^2+X_{sp}^2\right]}\right]\cdot\Delta t \tag{3-14}$$

A higher V_{dc} can result in a higher ignition voltage but also impose high stress on the switching devices. From (3-14), it can be observed that the variation of V_{dc} during the preheating interval can be controlled by adjusting the duty-ratio of the ballast circuit. By decreasing the duty-ratio, the input power can be reduced leading to a lower V_{dc}. Therefore, in order to reduce V_{dc} and hence the component stresses, the duty-ratio during preheating, d_p, is set much smaller than the duty-ratio at steady-state, d_s.

- *Ignition*

After the cathode filaments have been preheated to an appropriate emission temperature, the starting-aid circuit is open-circuited. At this stage, the equivalent circuit of the load resonant inverter is shown in Figure 3-7 and the natural resonance frequency of the circuit becomes higher.

$$f_{r,ign}=\frac{1}{2\pi\sqrt{L_s\left(\dfrac{C_s\times C_f}{C_s+C_f}\right)}} \tag{3-15}$$

The rms value of the lamp voltage for ignition can be expressed as:

$$V_{ign} = \frac{C_s\left[\left(r_f\omega_o C_f\right)^2+1\right]^{\frac{1}{2}}}{\left\{\left(2r_f\omega_o C_s C_f\right)^2+\left[\omega_o^2 L_s C_s C_f-\left(C_s+C_f\right)\right]^2\right\}^{\frac{1}{2}}}V_1 \tag{3-16}$$

This equation indicates that the lamp voltage will become extremely high if the inverter is operated at the resonance frequency of the load resonant circuit. For conventional control, the resonance frequency is designed to lie between the preheating frequency and the steady-state frequency. This ensures that the operation will pass through the ignition stage when the inverter frequency is adjusted from the preheating frequency to the steady-state frequency.

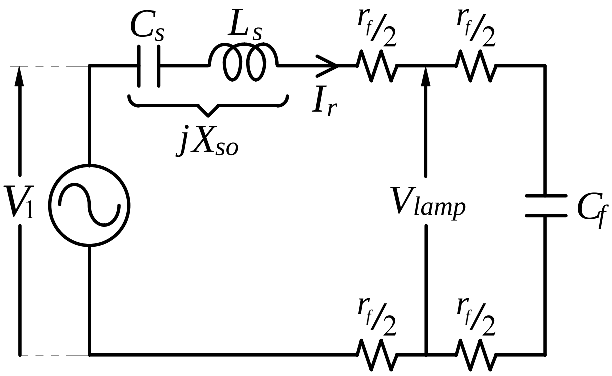

Figure 3-7 Equivalent circuit of the resonant inverter at the ignition stage

● *Steady-State*

At steady-state, the starting-aid circuit is remained open-circuited. The ballast circuit is operated at the steady-state operation frequency f_s and the rated duty-ratio d_s to output the required lamp power. The equivalent circuit of the load resonant inverter is shown in Figure 3-8, in which the fluorescent lamp is represented by a power-dependent resistance model. From the equivalent circuit, the compensated filament current for maintaining the emission temperature at steady-state operation can be expressed as:

$$I_f = \frac{2\pi f_s C_f V_{lamp}}{\left(1+4r_f^2\pi^2 f_s^2 C_f^2\right)^{\frac{1}{2}}} \tag{3-17}$$

The relationship between V_1 and the lamp voltage can be calculated as:

$$V_{lamp} = \left[\left(1 - 2\pi f_s C_f X_{ss}\right)^2 + \left(\frac{X_{ss}}{R_{lamp}}\right)^2 \right]^{-1/2} \cdot V_1 \tag{3-18}$$

where

$$X_{ss} = 2\pi f_s L_s - \frac{1}{2\pi f_s C_s} \tag{3-19}$$

The filament resistances are neglected in the equation since they are very small as compared with the equivalent resistance of the lamp arc and the impedance of the load resonant circuit at the steady-state frequency.

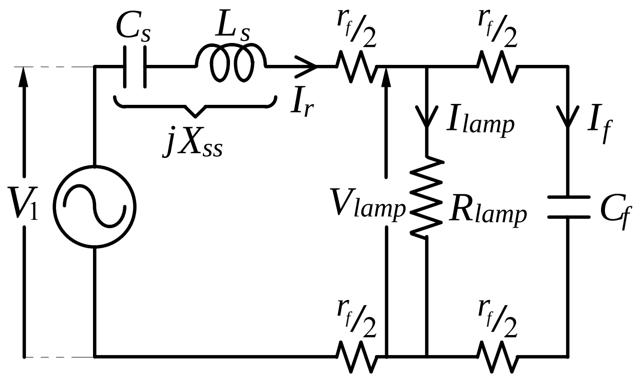

Figure 3-8 Equivalent circuit of the resonant inverter at steady-state

3-4 Design Example

An electronic ballast for an Osram T8-36W rapid-start fluorescent lamp is illustrated as a design example. The circuit specifications are listed in Table 3-1. The rated lamp power, P_{lamp}, is 36W consisting of an arc power of 33W and a filament power of 3W. The circuit parameters are designed to operate the buck-boost power factor corrector at DCM and to turn on the active switch Q_1 with ZVS so that a high power factor and high circuit efficiency can be achieved. The design procedure is outlined as follows.

Table 3-1 Circuit specifications (Osram T8-36W)

<table>
<tr><td colspan="2">Input voltage, V_s</td><td>110V, 60Hz</td></tr>
<tr><td colspan="2">Dc-link voltage at steady-state, V_{dc}</td><td>250V</td></tr>
<tr><td rowspan="2">Rated lamp power, P_{lamp}</td><td>Arc power, P_{arc}</td><td>33W</td></tr>
<tr><td>Filament power, P_f</td><td>3W</td></tr>
<tr><td colspan="2">Rated lamp voltage, V_{lamp}</td><td>94.5V</td></tr>
<tr><td colspan="2">Rated lamp current, I_{lamp}</td><td>0.35A</td></tr>
<tr><td colspan="2">Equivalent lamp resistance, R_{lamp}</td><td>270Ω</td></tr>
<tr><td colspan="2">Filament resistance (25°C), r_f</td><td>2.5Ω</td></tr>
<tr><td colspan="2">Filament current, I_f</td><td>0.3A</td></tr>
<tr><td colspan="2">Preheating frequency, f_p</td><td>24kHz</td></tr>
<tr><td colspan="2">Duty-ratio during preheating, d_p</td><td>0.25</td></tr>
<tr><td colspan="2">Steady-state operation frequency, f_s</td><td>32kHz</td></tr>
<tr><td colspan="2">Duty-ratio at steady-state, d_s</td><td>0.5</td></tr>
</table>

Step 1. Determine the buck-boost converter inductor

Assuming a circuit efficiency of 85% at steady-state and substituting it into (3-5), L_b is then calculated to be 1.1mH.

Step 2. Determine C_f

C_f can be obtained from the following equation.

$$C_f = \frac{1}{2\pi f_s\left[\left(\frac{V_{lamp}}{I_f}\right)^2 - r_f^2\right]^{1/2}} \tag{3-20}$$

C_f = 15.8 nF.

Step 3. Determine C_{dc}

The lamp current crest factor (CF) is highly dependent to the magnitude of the dc-link voltage ripple. Therefore, in order to remain a long lamp life, the ripple of the dc-link voltage should be as small as possible to keep lamp current CF be far below 1.7 [9]. However, a smaller ripple of the dc-link voltage requires a larger dc-link capacitance C_{dc}, resulting in higher cost. In this design, the ripple factor r_{vo} of the dc-link voltage at steady-state is set to be below 2%. Then, C_{dc} can be obtained from the following equation.

$$C_{dc} \geq \frac{P_{in}}{2\pi f_L V_{dc}^2 r_{vo}} \tag{3-21}$$

$C_{dc} \geq 90$ μF.

In this design example, C_{dc} is chosen as 100μF.

Step 4. Determine L_s and C_s

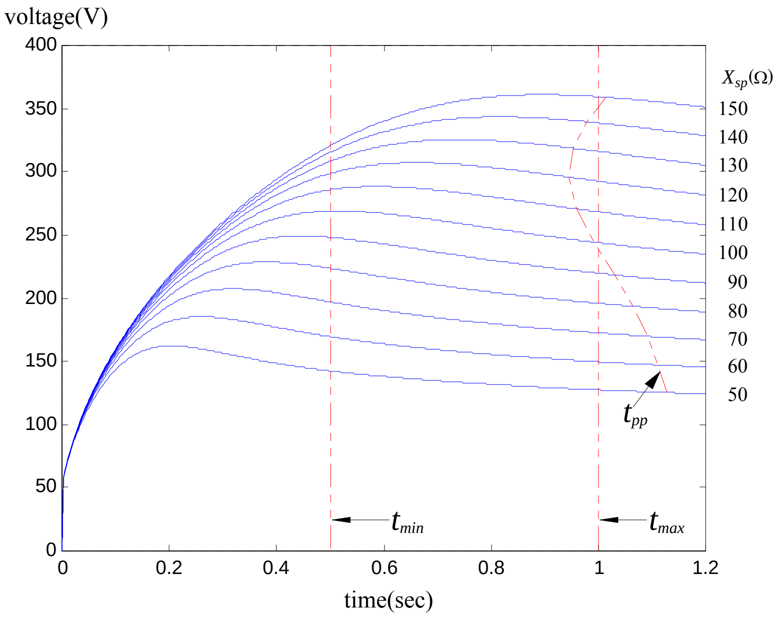

Figure 3-9 Variation of the dc-link voltage during preheating

By using the filament model derived in the previous chapter, the variation of the dc-link voltage during preheating for some X_{sp} values can be depicted in Figure 3-9. The dashed line of t_{pp} represents the proper preheating time. At this time, the appropriate hot filament resistance approximately 4.5 times the cold filament resistance. The dashed lines of t_{min} and t_{max} are the acceptable minimum and maximum preheating time for rapid-start operation, respectively. As indicated in this figure, a smaller X_{sp} can reduce the dc-link voltage during preheating and hence the voltage stress on circuit components. However, it requires a longer preheating time to heat the cathode filament to a proper emission temperature. In addition, a smaller X_{sp} may lead to a larger preheating current, resulting in higher current stress on the circuit components. In this design, X_{sp} is chosen to be 100Ω to keep the dc-link voltage during preheating is below 280V and the preheating time is shorter than 1 second.

From (3-18), there are two solutions for X_{ss}:

$$X_{ss} = \frac{R_{lamp}^2 2\pi f_s C_f \pm R_{lamp}\sqrt{\left(1 + R_{lamp}^2 4\pi^2 f_s^2 C_f^2\right)\left(\frac{V_1}{V_{lamp}}\right)^2 - 1}}{\left(1 + R_{lamp}^2 4\pi^2 f_s^2 C_f^2\right)} \tag{3-22}$$

Although there are two solutions for X_{ss}, the smaller one, however, will make the load resonant circuit of the inverter present capacitive. In order to reduce the switching-on loss of the active switch Q_1, the load resonant circuit is preferred to be inductive. Therefore, only the larger solution is a valid candidate. For the illustrative example, X_{ss} is 321.5Ω. Then, L_s and C_s can be obtained from the following equations:

$$L_s = \frac{f_s X_{ss} - f_p X_{sp}}{2\pi\left(f_s^2 - f_p^2\right)} \tag{3-23}$$

$$C_s = \frac{f_s^2 - f_p^2}{2\pi f_s f_p\left(f_p X_{ss} - f_s X_{sp}\right)} \tag{3-24}$$

The calculated results are L_s = 2.8mH and C_s = 20.6nF.

3-5 Simulation Results

From the circuit parameters obtained from the above section, an IsSpice model of the proposed electronic ballast is built to simulate. Figure 3-10 shows the main voltage and current waveforms of the ballast circuit during the preheating interval. Figure 3-11 is the key voltage and current waveforms of the ballast circuit at steady-state operation. Figure 3-12 shows the simulation waveforms of the input voltage and current and the inductor current i_b of the buck-boost PFC circuit. The simulation results are the same as the theoretical predictions.

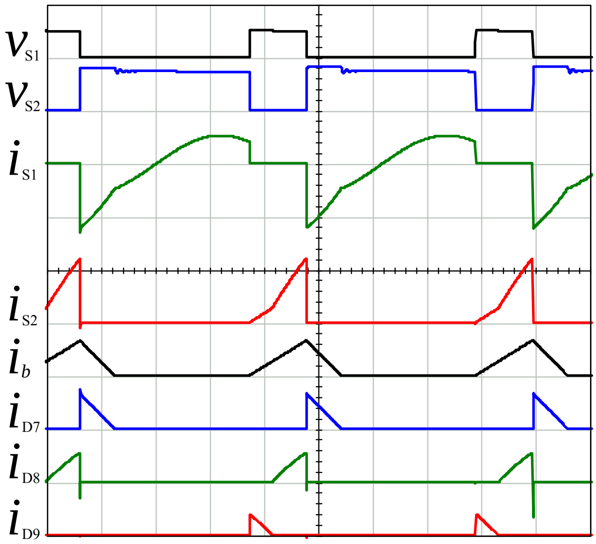

voltage:500V/div; current:2A/div; time:10μs/div

(a) Near line peak voltage

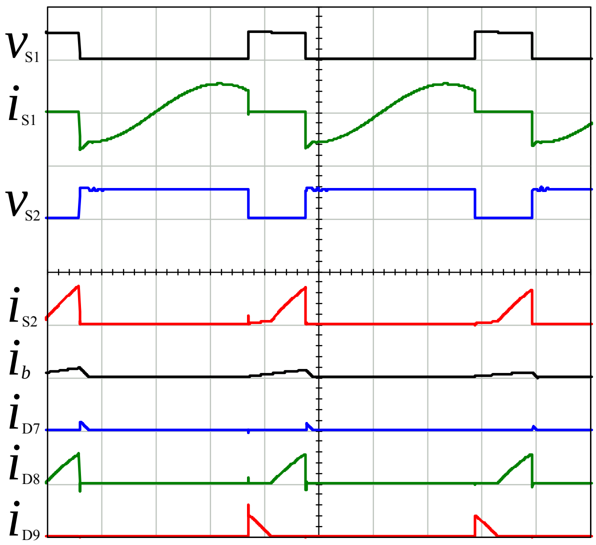

voltage:500V/div; current:2A/div; time:10μs/div

(b) Near zero crossing

Figure 3-10 Waveforms of v_{S1}, v_{S2}, i_{S1}, i_{S2}, i_b, i_{D7}, i_{D8} and i_{D9} during preheating

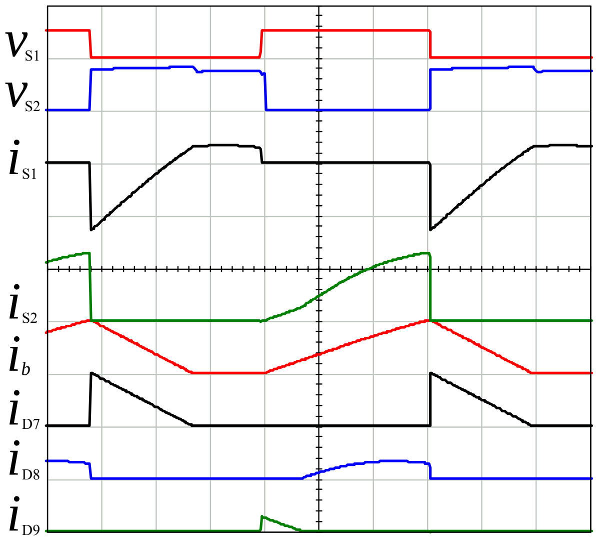

voltage:500V/div; current:2A/div; time:5μs/div

(a) Near line peak voltage

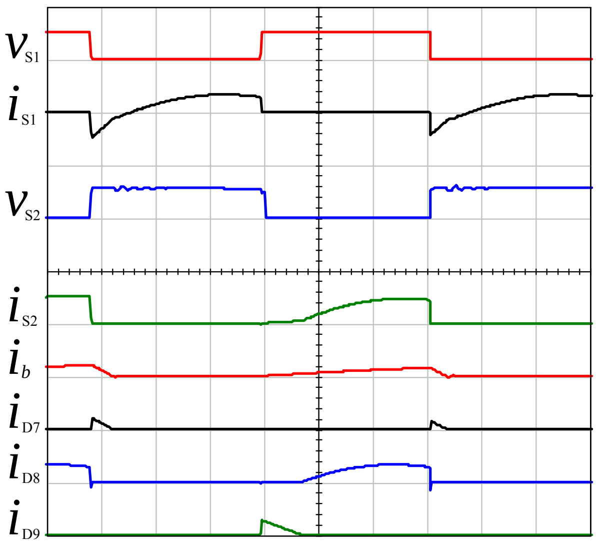

voltage:500V/div; current:2A/div; time:5μs/div

(b) Near zero crossing

Figure 3-11 Waveforms of v_{S1}, v_{S2}, i_{S1}, i_{S2}, i_b, i_{D7}, i_{D8} and i_{D9} at steady-state

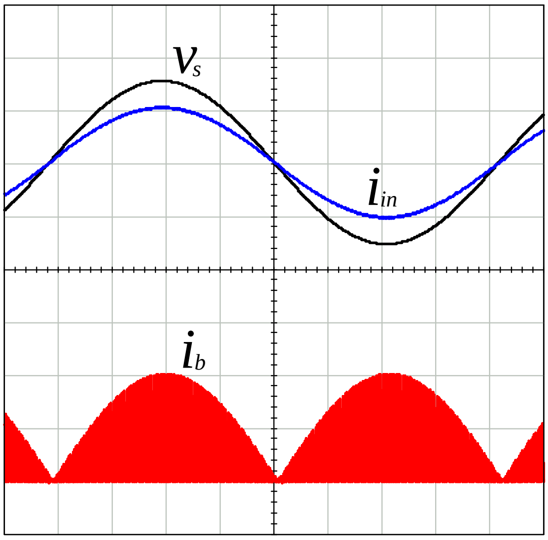

v_s:100V/div; i_{in}:0.5A/div; i_b:1A/div; time:2ms/div

Figure 3-12 Waveforms of v_s, i_{in} and i_b at steady-state

3-6 Experimental Results

Table 3-2 Circuit parameters

Steady-state operation frequency, f_s	32kHz
Preheating frequency, f_p	24kHz
Resonance frequency of resonant circuit, $f_{r,ign}$	31.8kHz
Inductance of buck-boost converter, L_b	1.1mH
Dc-link capacitance, C_{dc}	100μF
Resonant inductance, L_s	2.80mH
Resonant capacitance, C_s	20.6nF
Parallel capacitance, C_f	15.8nF
Filtering inductance, L_m	2.0mH
Filtering capacitance, C_m	270nF

A prototype of the proposed electronic ballast for a rapid-start fluorescent lamp of Osram T8-36W was built and tested to verify the theoretical predictions. The circuit parameters are listed in Table 3-2. The resonance frequency of the series-resonant energy-tank is designed at 21kHz. During the ignition transient, the resonance frequency of the load resonant circuit is 31.8kHz, which lies between the preheating frequency and the steady-state frequency. At steady-state, the resonance frequency of the load resonant circuit including the lamp becomes 24.8kHz. Figure 3-13 illustrates the variations of the operation frequency of the electronic ballast, lamp voltage and resonance frequency of the load resonant circuit. As the ballast is started, the operation frequency begins from the preheating frequency and then goes through the ignition frequency, and finally rises to the steady-state frequency.

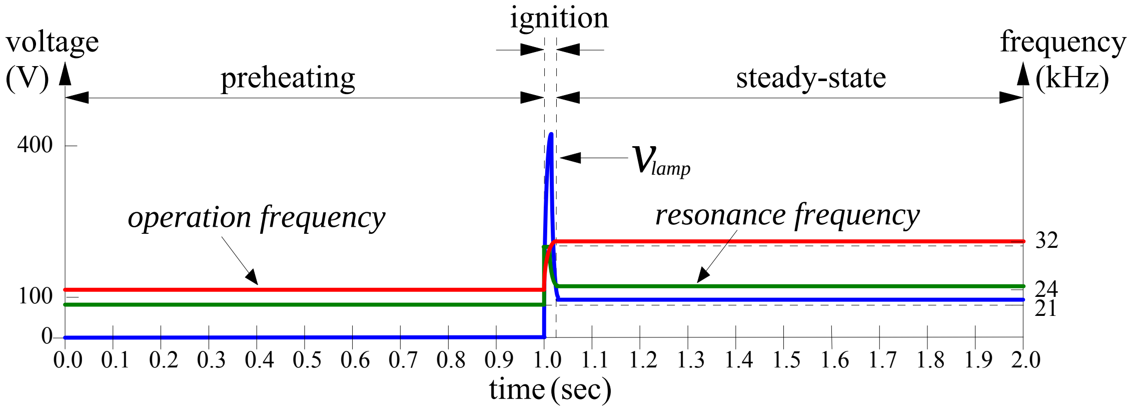

Figure 3-13 Variations of the operation frequency, lamp voltage and resonance frequency

Figure 3-14 shows the experimental results during the starting period. When switched on, the electronic ballast draws power from the line source. The preheating interval lasts for 1 second. During this interval, almost only the cathode filaments consume the input power. The dc-link voltage rises first rapidly up to 270V and then gradually reduces to 240V. The filament current varies accordingly. At the end of the preheating interval, the peak of filament current reduces to 1.0A and the peak of filament voltage increases up to 11V. This indicates that the ratio of the hot filament resistance to the cold resistance has already reached the value of about 4.5 at this point. Since the starting-aid circuit is short-circuited, neither lamp voltage nor glow current is found during preheating time. When the cathode filaments have reached the appropriate emission temperature, the starting-aid circuit is open-circuited and the operation frequency is increased rapidly toward the resonance frequency of the load resonant circuit. As the operation frequency increases, the lamp voltage is increased up for ignition. After being ignited, the lamp arc current flows and eventually reaches the thermal equilibrium.

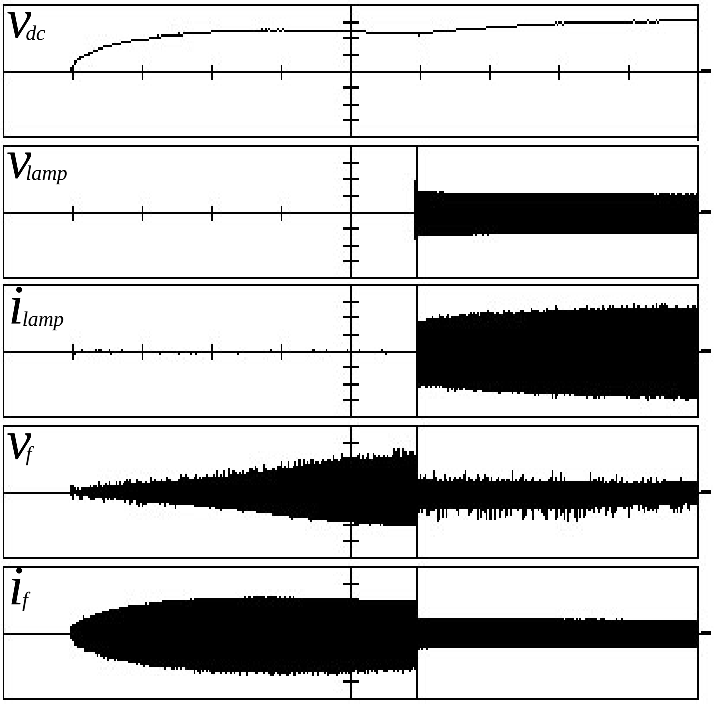

v_{dc}, v_{lamp}:100V/div; i_{lamp}:0.2A/div; v_f:5V/div; i_f:0.5A/div; time:0.2s/div

Figure 3-14 Starting transient waveforms

Figure 3-15 shows the waveforms of the input voltage and current and the inductor current i_b of the buck-boost PFC circuit. The input current is sinusoidal and in phase with the input voltage. The power factor is 0.99 and the total current harmonic distortion (THD) is 8%. The circuit efficiency is 86% when the lamp is operated at the rated power. The buck-boost power factor corrector is operated at DCM over the entire cycle of the line source. Figures 3-16 and 3-17 show the voltage and current waveforms of the active power switches during the preheating interval and at the steady-state operation. These waveforms indicate that the ZVS operation for the active switch Q_1 of the ballast circuit can always be retained. Figure 3-18 shows the measured lamp voltage and current waveforms at the steady-state operation. The lamp current is nearly sinusoidal with a crest factor below 1.55.

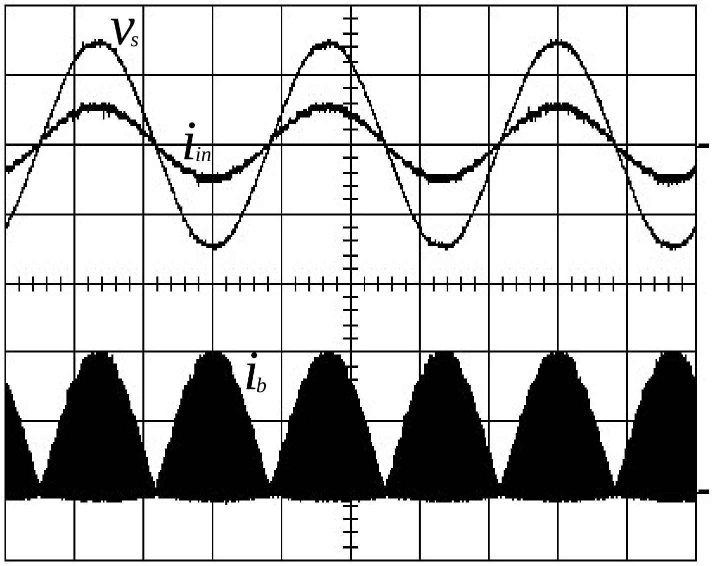

voltage:100V/div; current:1A/div; time:5ms/div

Figure 3-15 Waveforms of v_s, i_{in} and i_b

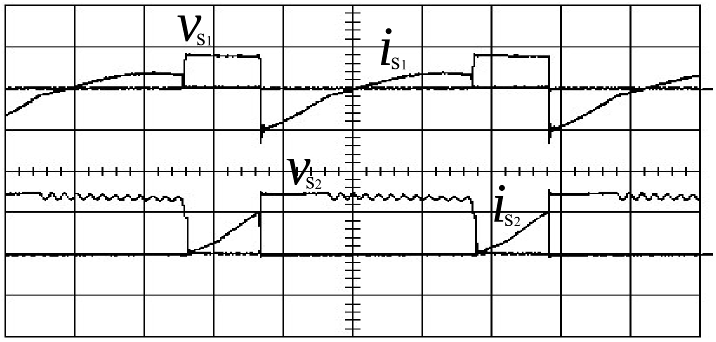

voltage:200V/div; current:2A/div; time:10μs/div

(a) Near line peak voltage

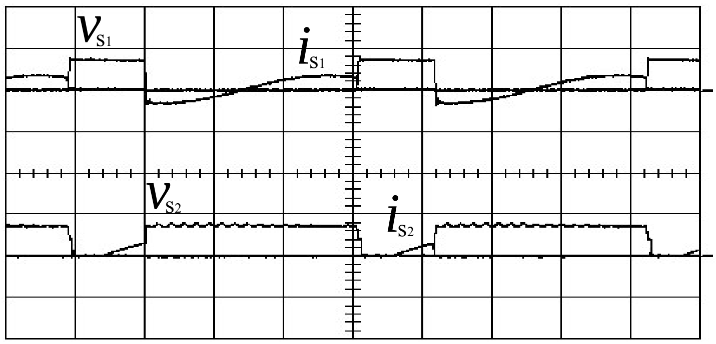

voltage:200V/div; current:2A/div; time:10μs/div

(b) Near zero crossing

Figure 3-16 Switching voltage and current waveforms during preheating

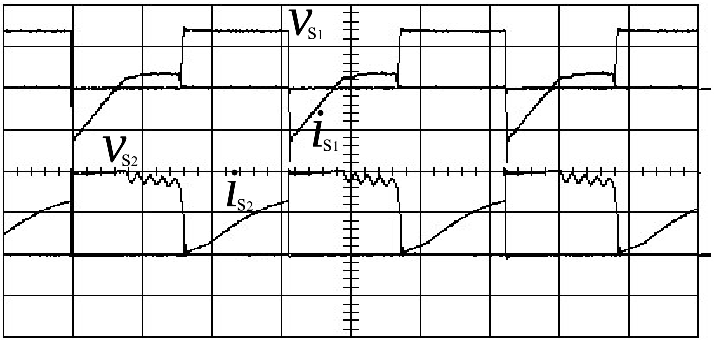

voltage:200V/div; current:2A/div; time:10μs/div

(a) Near line peak voltage

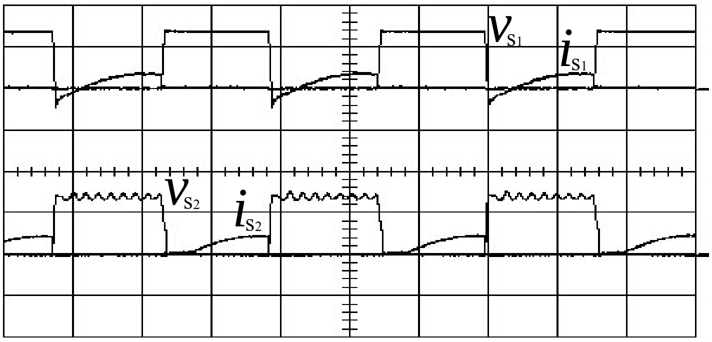

voltage:200V/div; current:2A/div; time:10μs/div

(b) Near zero crossing

Figure 3-17 Switching voltage and current waveforms at steady-state

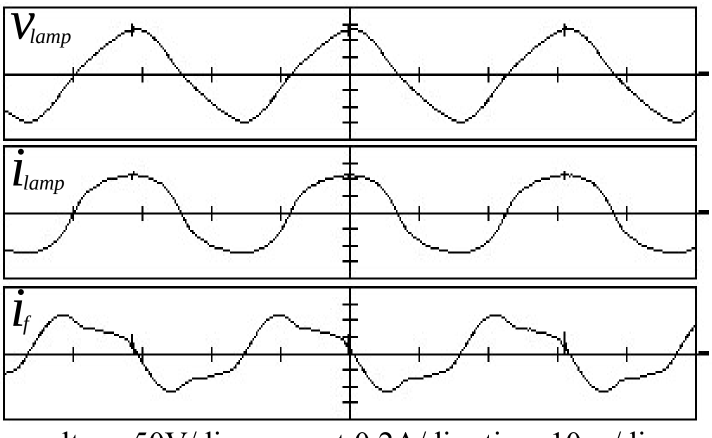

voltage:50V/div; current:0.2A/div; time:10μs/div

Figure 3-18 Lamp voltage and current waveforms at steady-state

Chapter 4 Programmed Rapid-Start Electronic Ballast with Inductively Coupled Filament-Heating Circuits

From Figure 1-1, it can be found that the filament-heating current provided by the half-bridge resonant inverter flows through the shunted capacitor for preheating is the reason of causing a voltage across the lamp during the preheating period. Therefore, if the filament-heating voltage or current can be provided by another additional circuit but not by the half-bridge resonant inverter and the voltage on the load resonant circuit is remained at zero during the preheating period, the lamp voltage during preheating can be kept at zero certainly.

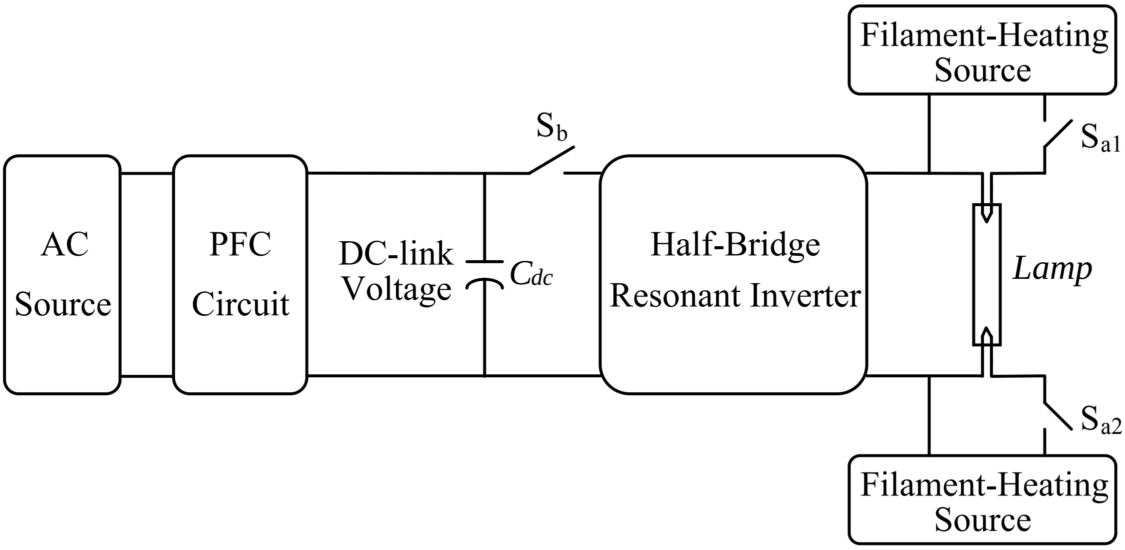

Figure 4-1 Block diagram of the proposed electronic ballast

Figure 4-1 is the block diagram of the proposed electronic ballast for starting the fluorescent lamp with zero glow current. During the preheating interval, the active switches, S_{a1} and S_{a2}, are turned on, so that the filament-heating source provides a proper filament voltage (or current) to preheat the cathode filaments. At this time, the active switch, S_b, is remained at “off” state. Therefore, the half-bridge resonant inverter will produce no voltage on the lamp and hence no glow current. After the cathode filaments have been preheated to an appropriate emission temperature, S_b is turned on and the inverter is operated to generate the required high lamp voltage for ignition. However, such a circuit topology requires an additional filament-heating source and another active switches, resulting in higher cost and more complicated circuit configuration. In order to simplify the circuit configuration and reduce the cost, the switches S_{a1}, S_{a2} and the filament-heating circuit can be integrated with the PFC circuit; while the switch S_b is merged with the half-bridge inverter.

4-1 Circuit Configuration

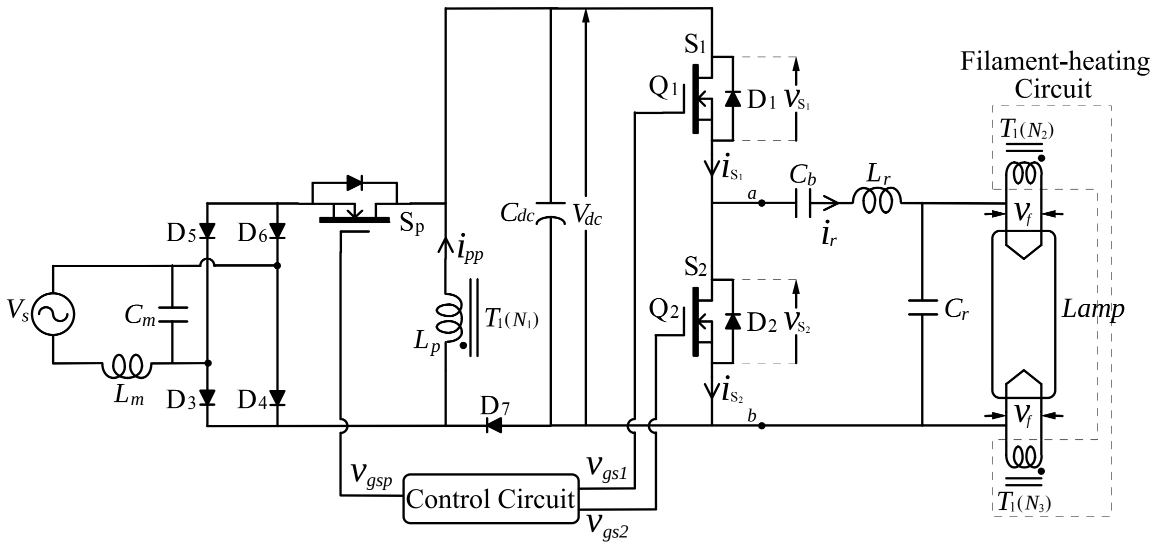

Figure 4-2 Circuit configuration of the two-stage electronic ballast

Figure 4-2 is the basic circuit of the proposed two-stage high-power-factor electronic ballast with programmed rapid-start. It mainly consists of a diode-bridge rectifier, a power factor corrector with the buck-boost converter and a quasi half-bridge series-resonant parallel-loaded inverter. Two power MOSFETs, S_1 and S_2, are adopted as the active power switches of the half-bridge inverter for high frequency switching. Each power switch is composed of an active switch and its intrinsic anti-parallel diode. The load resonant circuit of the inverter is formed by a dc-blocking capacitor, C_b, a series-resonant energy-tank, L_r and C_r, and the fluorescent lamp. The inductor of the buck-boost converter is replaced by a transformer, T_1, with two auxiliary windings, N_2 and N_3, for heating the cathode filaments. A small low-pass filter, L_m and C_m, is used to remove the high frequency current harmonics at the input line.

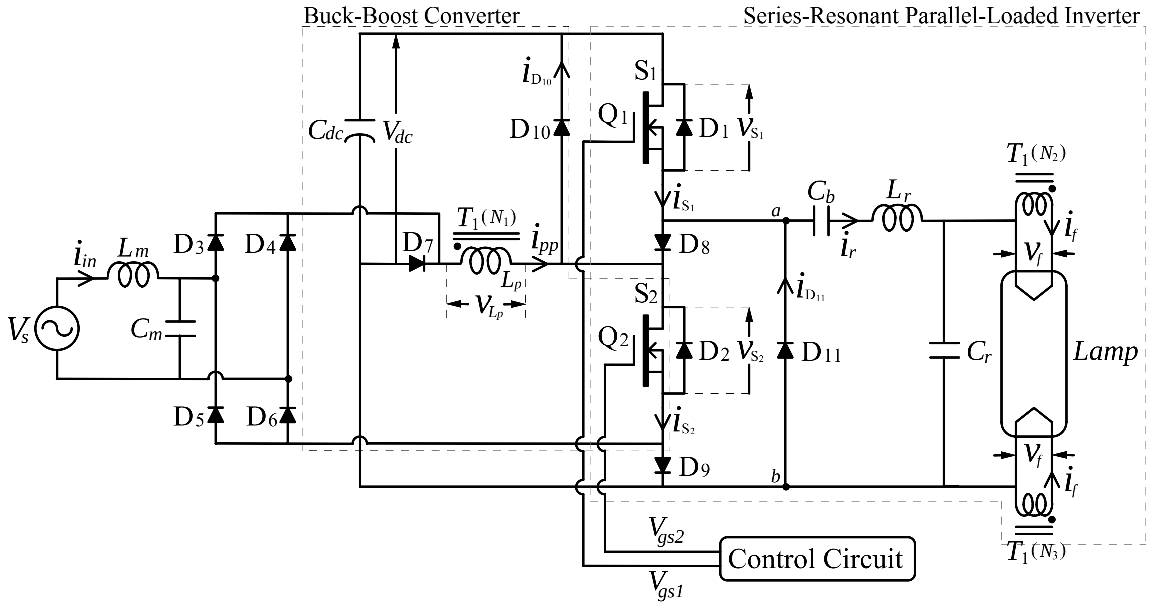

Figure 4-3 Circuit configuration of the single-stage electronic ballast

However, the two-stage topology requires two control circuits to control the buck-boost converter and the quasi half-bridge resonant inverter, respectively, and three active power switches, resulting in higher cost and lower efficiency. In order to solve this problem, the buck-boost converter can be integrated into the quasi half-bridge resonant inverter to form a single-stage high-power-factor electronic ballast, as shown in Figure 4-3. The bottom active power switch S_2 is commonly used by the buck-boost converter. To operate the buck-boost converter and the inverter independently, the freewheeling current i_{pp} in the buck-boost transformer flows through an additional D_{10} instead of the anti-parallel diode of S_1. On the other hand, the load resonant current i_r freewheels through D_{11} instead of S_2. The diode D_8 is introduced to block the primary current i_{pp} of transformer from freewheeling through D_1, and D_9 is used to prevent i_{pp} from flowing back to the input line when Q_2 is turned off. By sharing the active power switch and the control circuit, the component count can be effectively reduced.

4-2 Circuit Operation

The operation of the ballast-lamp circuit is described by three stages: preheating, ignition, and steady-state. During the preheating period, the active power switch S_2 is initiated to operate the buck-boost converter inducing voltages on the filaments for preheating. At this time, S_1 remains at “off” state and so does the resonant inverter. Therefore, there will be no voltage on the load resonant circuit and the lamp. This makes sure that no glow current will occur. After the preheating operation has been completed, S_1 is activated. Subsequently, S_1 and S_2 are alternately switched on and off with a duty-ratio of 50%. The half-bridge inverter outputs a square-wave voltage on the load resonant circuit. At the same time, the operation frequency of the resonant inverter goes toward the resonance frequency, $f_{r,ign}$, of the load resonant circuit to generate the required high ignition voltage on the lamp. Once the lamp has been ignited, the operation frequency is then regulated to produce the desired lamp power at the steady-state operation.

At the preheating stage, the operation of the electronic ballast can be subdivided into three modes within one high frequency cycle in accordance with the conducting conditions of the power switches, as shown in Figure 4-4. The input filter is omitted for simplicity. The circuit parameters are designed to operate the buck-boost converter at DCM. The circuit operation during preheating is described as follows:

Mode I ($t_0<t<t_1$):

Prior to Mode I, the primary current i_{pp} of the transformer T_1 is zero since the buck-boost converter is operated at DCM, and thus the excitation current i_e of T_1 is zero. At the beginning of Mode I, Q_2 is switched on. The rectified line voltage is imposed on the primary of T_1. i_e increases linearly from zero and its slope is proportional to the rectified line voltage. At the same time, T_1 induces a positive filament voltage for preheating the cathode filament. When Q_2 is turned off, this mode is ended.

Mode II ($t_1<t<t_2$):

At the beginning of Mode II, i_e reaches its peak and Q_2 is switched off. i_e is transferred from Q_2 to D_{10} and D_7 to charge the dc-link capacitor, C_{dc}. During this mode, i_e decreases linearly and T_1 induces a negative filament voltage for preheating the cathode filament. When i_b becomes zero, this mode ends, and then, the circuit enters Mode III.

Mode III ($t_2<t<t_3$):

During this mode, the whole ballast circuit is idle. When Q_2 is switched on, the mode ends and the operation returns to Mode I of the next cycle.

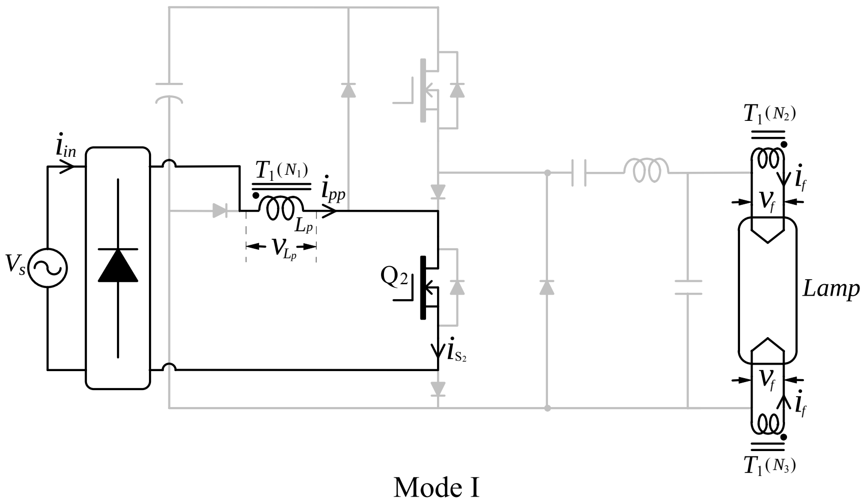

Mode I

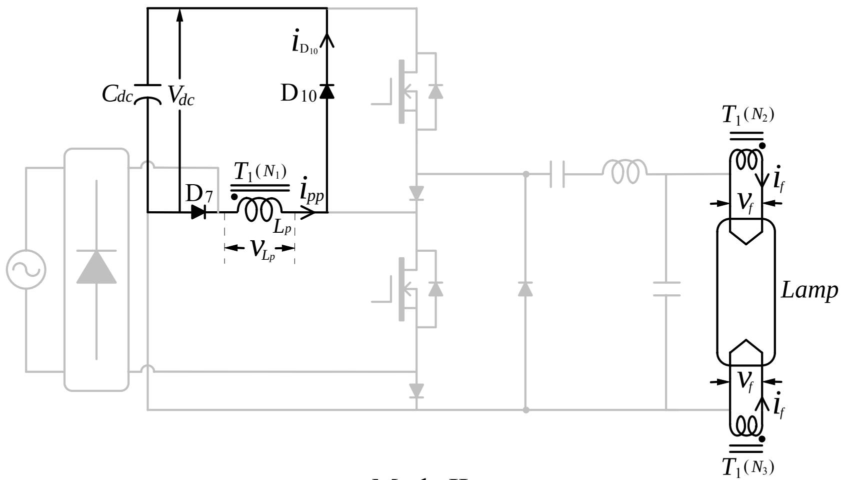

Mode II

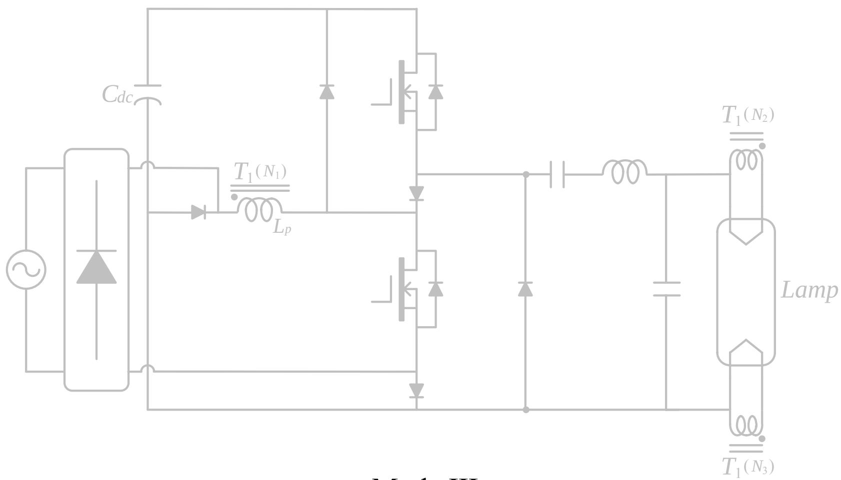

Mode III

Figure 4-4 Operation modes at the preheating stage

The operation of the electronic ballast at steady-state can be subdivided into six modes within one high frequency cycle in accordance with the conducting conditions of the power switches, as shown in Figure 4-5. Figure 4-6 illustrates the theoretical waveforms for each mode. To achieve a high power factor, the buck-boost converter is operated in DCM. The operation frequency of the inverter is greater than the resonance frequency of the load resonant circuit to ensure ZVS at the switching-on of the active switch Q_1. The circuit operation at steady-state is described as follows:

Mode I ($t_0<t<t_1$):

Prior to Mode I, a positive load resonant current i_r flows through D_{11}. At the beginning of Mode I, Q_2 is switched on. The rectified line voltage is imposed on the primary of the transformer T_1. T_1 induces a positive filament voltage for heating the cathode filament. At DCM operation, the excitation current i_e of T_1 increases linearly from zero. The slope of i_e is proportional to the rectified line voltage. When i_r resonates to zero, D_{11} turns off and Mode II is entered.

Mode II ($t_1<t<t_2$):

During this mode, Q_2 is kept at the on state and carries both the primary current of T_1 and the load resonant current. The load resonant current goes through D_8 and D_9 and the primary current flows back through the rectifier to the line source. The rectified line voltage is applied on the primary of T_1 and i_e increases continuously. In this mode, T_1 keeps inducing a positive voltage for heating the cathode filament.

Mode III ($t_2<t<t_3$):

At the beginning of Mode III, Q_2 is switched off and i_e reaches its peak. i_e is transferred from Q_2 to D_{10} and D_7 to charge C_{dc} and i_r is transferred from Q_2 to D_1 to charge C_{dc}. i_e decreases linearly and i_r resonates from negative to positive. During this mode, T_1 induces a negative filament voltage for heating the cathode filament.

Since the peak of i_e is proportional to the rectified input voltage, the duration for i_e declining to zero is not constant but varies with the rectified line voltage. Thus, there are two possible modes following Mode III, depending on which of the currents, i_e or i_r , reaches zero first.

Mode IV-a ($t_3<t<t_4$):

When the line voltage is high, i_r declines to zero before i_e does. Mode III ends at the time when i_r becomes zero, and then, the circuit enters mode IV-a. At this instant, D_1 turns off naturally and Q_1 is then turned on to carry i_r with ZVS. In this mode, i_e decreases continuously and T_1 keeps inducing a negative filament voltage for heating the cathode filament. This mode ends when i_e decreases to zero.

Mode IV-b ($t_3<t<t_4$):

At low line voltage, the peak of i_e is small and declines to zero faster. In case that i_e decreases to zero earlier than i_r does, Mode IV-b instead of Mode IV-a, follows Mode III. In this mode, i_r flows through D_1 continuously. This mode ends at the time when i_r resonates to zero. Then, Q_1 is turned on to carry i_r with ZVS.

Mode V ($t_4<t<t_5$):

During this mode, the positive i_r flows through Q_1. C_{dc} supplies energy to the load resonant circuit.

Mode VI ($t_5<t<t_6$):

Mode VI represents the short period of the dead time. At the beginning of this mode, Q_1 is switched off. At the instant, i_r is positive and freewheels through D_{11}. When Q_2 is switched on, the mode ends and the operation returns to Mode I of the next cycle.

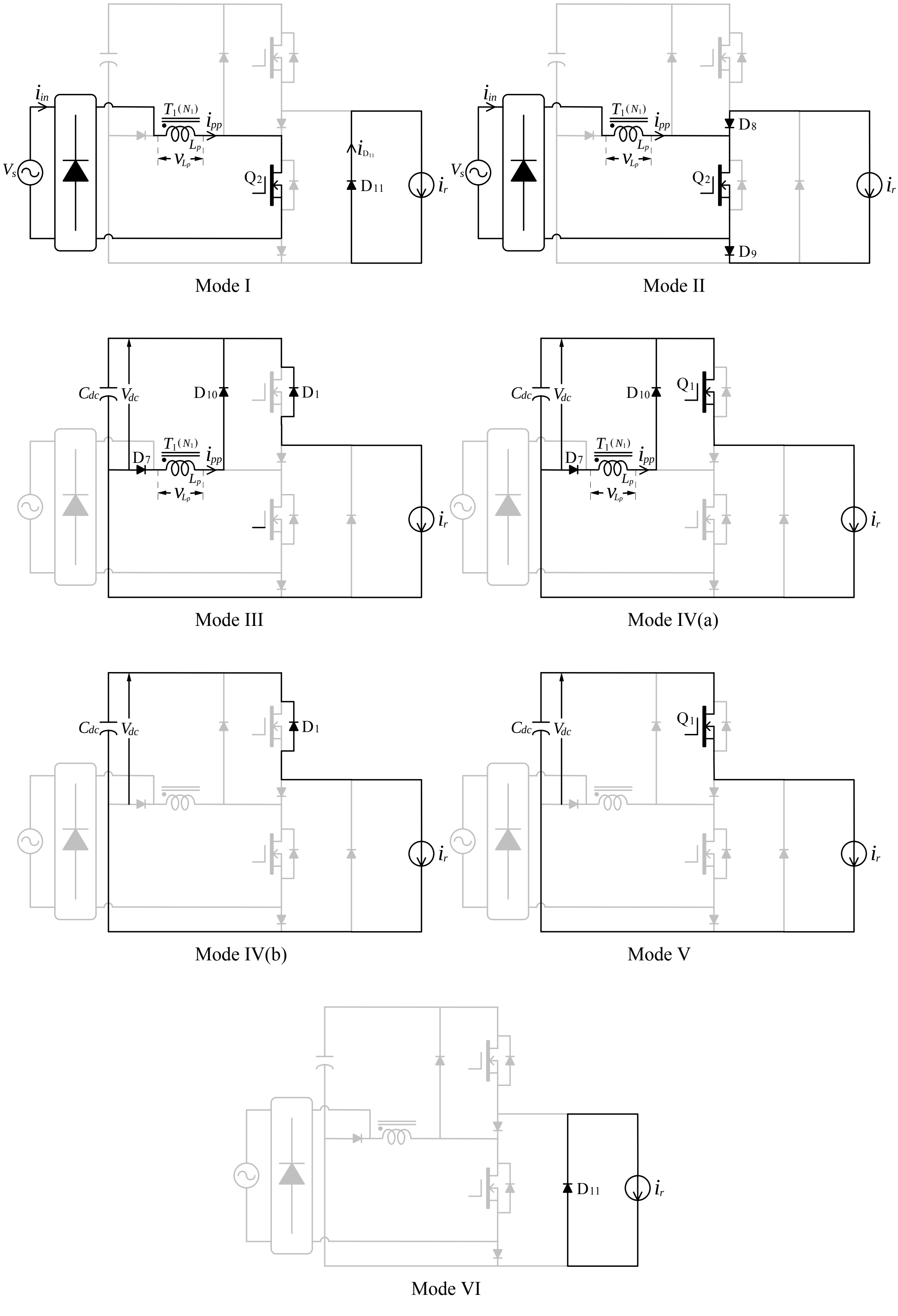

Figure 4-5 Operation modes at steady-state

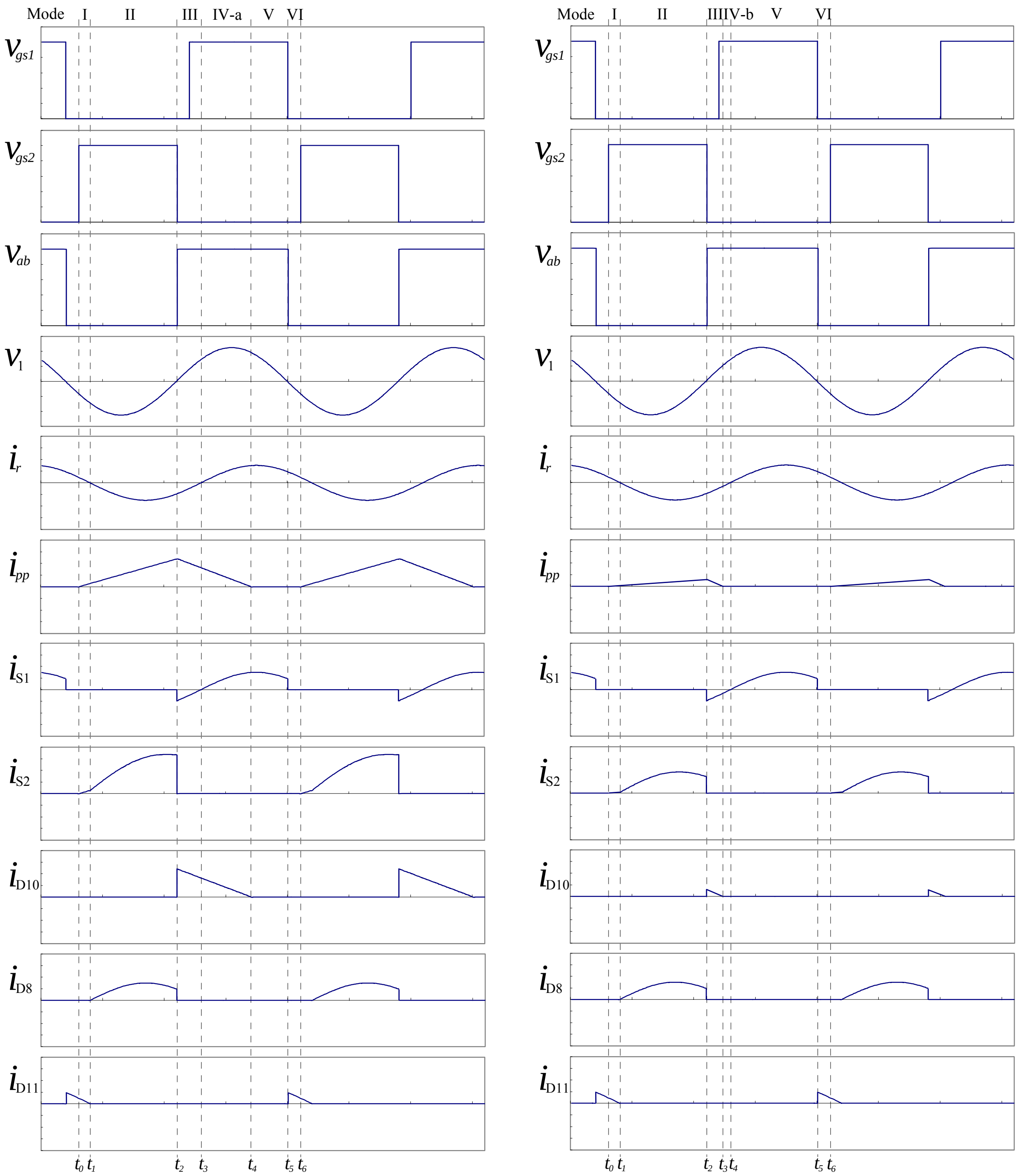

(a) Near line peak voltage (b) Near zero crossing

Figure 4-6 Theoretical waveforms at steady-state

4-3 Circuit Analysis

For simplifying the analysis, the following assumptions are made:

1) All the circuit components are ideal.
2) The load quality factor of the load resonant circuit is high enough so that the

load resonant current is sinusoidal.

3) The capacitance of C_{dc} is large enough, thus the dc-link voltage V_{dc} can be approximated as a voltage source at steady-state.
4) The capacitance of C_b in the load resonant circuit is large enough, resulting in zero reactance at the switching frequency.
5) There are no parasitical components and leakage inductance on the transformer.
6) The lamp is regarded as an open circuit before ignition, and a resistance at steady-state operation.

4-3-1 Preheating

The electronic ballast is supplied from the ac line voltage source.

$$v_s = V_m \sin(2\pi f_L t) \tag{4-1}$$

where f_L and V_m are the frequency and amplitude of the line voltage source, respectively.

During the preheating period, the ballast circuit is operated at the preheating frequency, f_p, producing a voltage, v_f, on the filament for preheating. When the active power switch S_2 is turned on, the rectified line voltage is applied on the primary of the transformer. When S_2 is turned off, the excitation current of the transformer freewheels into the dc-link capacitor, C_{dc}. At this time, the dc-link voltage V_{dc} is reversely applied on the transformer. As the freewheeling current decreases to zero, the transformer voltage drops to zero, too. Figure 4-7 shows the conceptual waveform of the filament voltage, v_f. Its amplitudes of the positive pulses in the waveform follow the envelope of the rectified line voltage and negative pulses are with amplitudes of the dc-link voltage. In practice, the preheating frequency f_p is much higher than line frequency. Therefore, both positive and negative amplitudes of filament voltage can be assumed as constants over a high frequency cycle. Then, the effective value of v_f over half line frequency cycle can be calculated as:

$$V_f = \sqrt{\frac{d}{\pi}\int_0^{\pi}\left\{\left[\frac{V_m \sin(2\pi f_L t)}{N}\right]^2 + \frac{V_{dc}(t)V_m \sin(2\pi f_L t)}{N^2}\right\} d(2\pi f_L t)}$$
$$= \frac{\sqrt{d}}{N}\cdot\sqrt{\frac{V_m^2}{2}+\frac{2V_{dc}(t)V_m}{\pi}} \tag{4-2}$$

where d is the duty-ratio of S_2 and N is the turn-ratio of the primary winding of T_1 to its auxiliary windings. The preheating voltage can be as high as possible to start the lamp rapidly, but should be limited by the rated filament voltage.

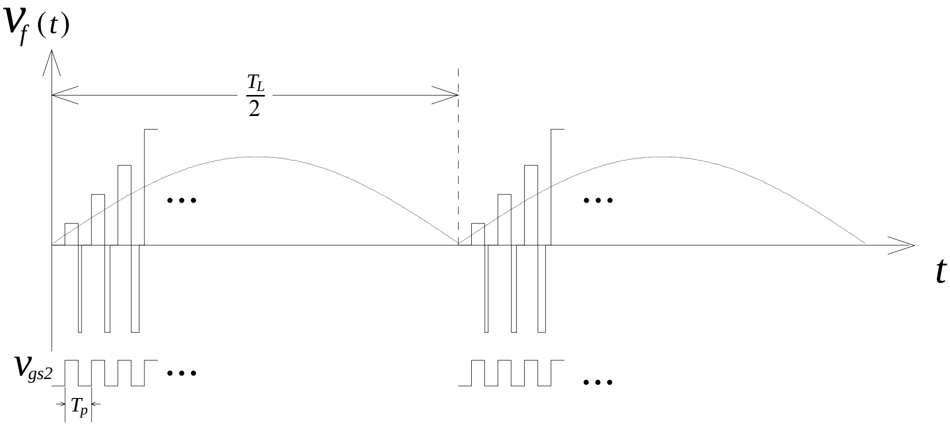

Figure 4-7 Conceptual waveform of v_f

When S_2 is turned on, the buck-boost converter draws a power P_{in} continually from the input line source.

$$P_{in} = \frac{d^2V_m^2}{4L_p f_p} + \frac{dV_m^2}{r_f N^2} \tag{4-3}$$

where L_p is the inductance of the primary winding of the transformer and r_f is the resistance on each cathode filament. The first term in (4-3) is the power stored in the transformer while the second term dissipates to filaments. The stored power in turn is partly delivered to the cathode filaments and is partly transferred to C_{dc}. As a result, the dc-link voltage V_{dc} varies in accordance with the power consumption on the filament. Since only a small amount of filament power is consumed, V_{dc} may rises rapidly to an impracticably high level at the preheating stage. The increasing energy in C_{dc} during the preheating interval can be expressed as:

$$\frac{1}{2}C_{dc}\left\{\left[V_{dc}(t+\Delta t)\right]^2-\left[V_{dc}(t)\right]^2\right\}=\left[\eta P_{in}-\frac{2V_f^2}{r_f}\right]\cdot\Delta t$$
$$=\left[\frac{\eta d^2V_m^2}{4L_p f_p}-\frac{4dV_mV_{dc}(t)}{\pi r_f N^2}\right]\cdot\Delta t \tag{4-4}$$

where η is the conversion efficiency of the buck-boost converter. This equation indicates that the variation of V_{dc} during the preheating interval depends on the operation frequency of the ballast circuit. By increasing the operation frequency, the input power can be reduced leading to lower V_{dc} and hence the component stresses. For this reason, the preheating frequency, f_p, is set much higher than the steady-state frequency, f_s.

4-3-2 Ignition and Steady-state

After the cathode filaments have been preheated to an appropriate emission temperature, the active power switch S_1 is activated. The half-bridge inverter begins to output a square-wave voltage, v_{ab}. The square-wave voltage can be represented by the Fourier series:

$$v_{ab}=\frac{V_{dc}}{2}+\sum_n\left[\frac{2V_{dc}}{n\pi}\sin(2n\pi f_o t)\right] \qquad n=1,3,5\cdots \tag{4-5}$$

where f_o is the operation frequency of the inverter. With a high load quality factor of the load resonant circuit, almost all the harmonic contents, as well as the dc term, will be filtered out by the load resonant circuit. Only the fundamental current at the switching frequency will be present in the load resonant inverter. Therefore, the ballast-circuit can be analyzed using the fundamental component approximation. The rms value of the fundamental component of v_{ab} is:

$$V_1=\frac{\sqrt{2}V_{dc}}{\pi} \tag{4-6}$$

- *Ignition*

Before ignition, the fluorescent lamp is regarded as an open circuit. The equivalent circuit of the half-bridge series-resonant parallel-loaded inverter is shown in Figure 4-8. Neglecting C_b, the resonance frequency of the circuit is equal to the resonance frequency of the series-resonant energy-tank.

$$f_{r,ign} = \frac{1}{2\pi\sqrt{L_r C_r}} \tag{4-7}$$

Operating the inverter at a frequency f_o, the rms value of the lamp voltage for ignition can be expressed as:

$$V_{ign} = \frac{V_1}{\left|1-\left(\frac{f_o}{f_{r,ign}}\right)^2\right|} \tag{4-8}$$

This equation indicates that the open circuit voltage on the lamp for ignition can be extremely high if the inverter is operated at the resonance frequency of the load resonant circuit. For conventional control, the resonance frequency of the series-resonant energy-tank is designed to lie between the preheating frequency and the steady-state frequency. This ensures that the inverter frequency will pass through the resonance frequency to generate a high ignition voltage when it is adjusted from the preheating frequency to the steady-state frequency.

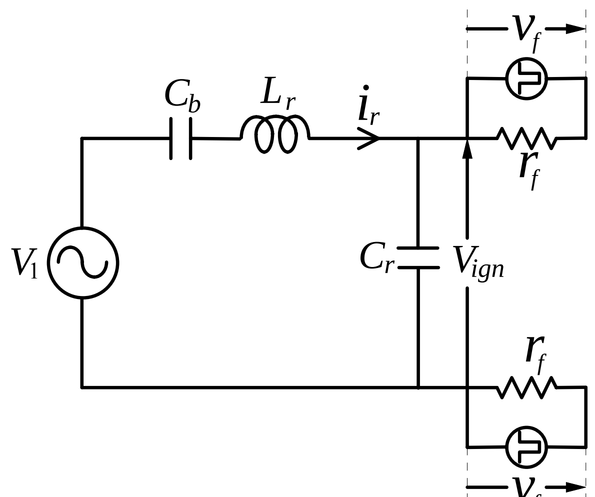

Figure 4-8 Equivalent circuit of the resonant inverter at the ignition stage

● *Steady-state*

At steady-state, the ballast circuit is operated at a frequency of f_s to output the required lamp power. The equivalent circuit of the load resonant inverter is shown in Figure 4-9, in which the fluorescent lamp is represented by a power-dependent resistance model. In practice, the filament resistances are very small as compared with the equivalent resistance of the lamp arc and the impedance of the load resonant circuit at the steady-state frequency. Neglecting the filament resistance and C_b, the resonance frequency of the load resonant circuit can be expressed as:

$$f_{r,std} = f_{r,ign}\sqrt{1-\frac{1}{Q_L^2}} \quad \text{for} \quad Q_L \geq 1 \tag{4-9}$$

where Q_L is the loaded quality factor at undamped natural frequency.

$$Q_L = 2\pi f_{r,ign} C_r R_{lamp} = \frac{R_{lamp}}{\sqrt{\dfrac{L_r}{C_r}}} \tag{4-10}$$

The total impedance of the resonant circuit can be calculated as:

$$\overrightarrow{Z_{in}} = j2\pi f_s L_r + \frac{\dfrac{R_{lamp}}{j2\pi f_s C_r}}{R_{lamp} + \dfrac{1}{j2\pi f_s C_r}} = \frac{R_{lamp}\left[1-\left(\dfrac{f_s}{f_{r,ign}}\right)^2 + j\dfrac{f_s}{Q_L f_{r,ign}}\right]}{1+jQ_L\dfrac{f_s}{f_{r,ign}}} \tag{4-11}$$

Being operated at a frequency higher than the resonance frequency, the load resonant circuit will present inductive load and Q_1 can be switched under ZVS. The lamp current and voltage can be calculated by (4-12) and (4-13), respectively.

$$I_{lamp} = \left|\frac{\overrightarrow{V_1}}{\overrightarrow{Z_{in}}}\frac{\dfrac{1}{j2\pi f_s C_r}}{R_{lamp}+\dfrac{1}{j2\pi f_s C_r}}\right| = \frac{V_1}{R_{lamp}\sqrt{\left[1-\left(\dfrac{f_s}{f_{r,ign}}\right)^2\right]^2 + \left(\dfrac{f_s}{Q_L f_{r,ign}}\right)^2}} \tag{4-12}$$

$$V_{lamp} = \frac{V_1}{\sqrt{\left[1-\left(\frac{f_s}{f_{r,ign}}\right)^2\right]^2+\left(\frac{f_s}{Q_L f_{r,ign}}\right)^2}} \tag{4-13}$$

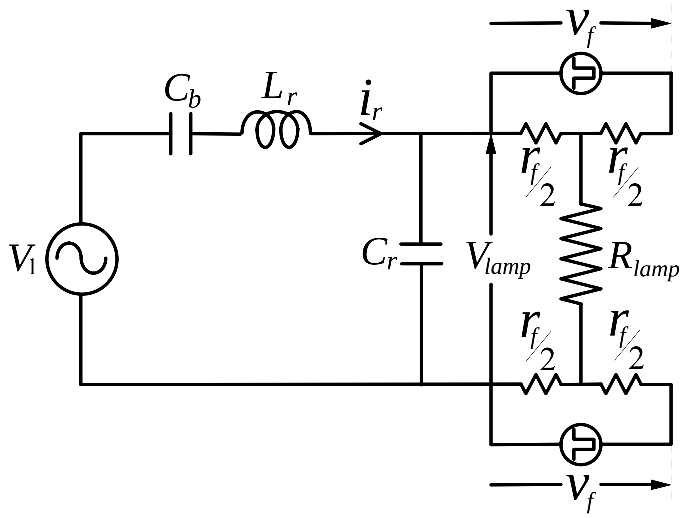

Figure 4-9 Equivalent circuit of the resonant inverter at steady-state

4-3-3 DCM Operation

The dc-link voltage can be calculated from (4-6) and (4-13).

$$V_{dc} = \frac{\pi V_{lamp}}{\sqrt{2}}\sqrt{\left[1-\left(\frac{f_s}{f_{r,ign}}\right)^2\right]^2+\left(\frac{f_s}{Q_L f_{r,ign}}\right)^2} \tag{4-14}$$

In order to operate the buck-boost power factor corrector at DCM, the dc-link voltage V_{dc} should be high enough so that the excitation current i_e always declines to zero in every high frequency cycle. To meet this requirement, the following equation should be satisfied.

$$V_{dc} \geq \frac{d}{1-d}V_m \tag{4-15}$$

With a duty cycle of 50%, V_{dc} should be always greater than the peak of the input line voltage.

4-4 Design Example

Table 4-1 Circuit specifications (Osram T8-36W)

Input voltage, V_s		110V, 60Hz
Rated lamp power, P_{lamp}	Arc power, P_{arc}	33W
	Filament power, P_f	3W
Rated lamp voltage, V_{lamp}		94.5V
Rated lamp current, I_{lamp}		0.35A
Equivalent lamp resistance, R_{lamp}		270Ω
Filament resistance (25°C), r_f		2.5Ω
Preheating frequency, f_p		100kHz
Steady-state operation frequency, f_s		20kHz
Duty-ratio, d		0.5

An electronic ballast for an Osram T8-36W rapid-start fluorescent lamp is illustrated as a design example. The circuit specifications are listed in Table 4-1. The rated lamp power, P_{lamp}, is 36W consisting of an arc power of 33W and a filament power of 3W. The circuit parameters are designed to operate the buck-boost converter at DCM and to turn on the active switch Q_1 with ZVS so that a high power factor and high circuit efficiency can be achieved. The design procedure is outlined as follows.

Step 1. Determine L_p

L_p can be obtained from the following equation:

$$L_p = \frac{\eta d^2 V_m^2}{4 P_{arc} f_s} \tag{4-16}$$

Assuming a circuit efficiency of 85% at steady-state, L_p is then calculated to be 2.0mH.

Step 2. Choose Q_L and $f_{r,ign}$ for DCM and ZVS operation

Figure 4-10 illustrates the variation of the dc-link voltage at steady-state. The dashed line stands for the boundary between DCM and continuous conduction mode (CCM). As indicated in this figure, a smaller Q_L can ensure DCM in the steady-state operation frequency range. However, it leads to a higher dc-link voltage at steady-state, resulting in higher voltage stress on circuit components. In addition, a lower Q_L requires a larger inductor for the resonant circuit. In this design, Q_L and $f_{r,ign}$ are chosen to be 1.4 and 20.8kHz, respectively, to have V_{dc} and $f_{r,std}$ equal to 1.05 times the input peak voltage and 14.6kHz, respectively.

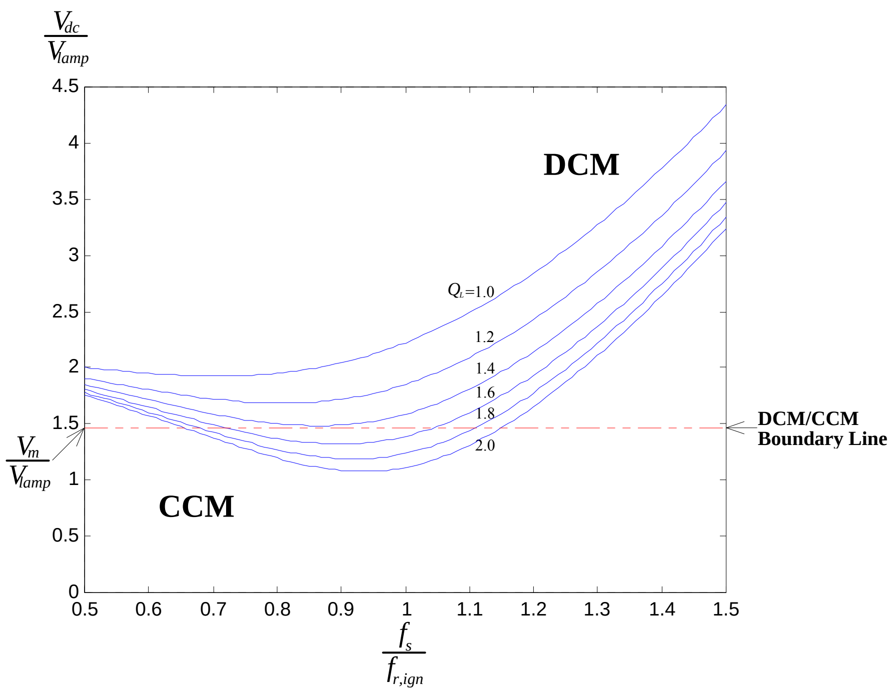

Figure 4-10 Operation condition for DCM

Step 3. Determine L_r and C_r

From (4-7) and (4-10), L_r and C_r can be obtained.

$$L_r = \frac{R_{lamp}}{2\pi f_{r,ign} Q_L} \tag{4-17}$$

$$C_r = \frac{Q_L}{2\pi f_{r,ign} R_{lamp}} \tag{4-18}$$

$L_r = 1.48$mH and $C_r = 40.0$nF.

Step 4. Determine C_{dc}

The magnitude of the dc-link voltage ripple will influence dominantly the lamp current CF. In order to remain a long lamp life. Therefore, the ripple of the dc-link voltage should be as small as possible to keep the lamp current CF be much smaller than 1.7. However, a smaller ripple of the dc-link voltage requires a larger dc-link capacitance C_{dc}, resulting in higher cost. In this design, the ripple factor r_{vo} of the dc-link voltage at steady-state is set to be below 3%. Then, C_{dc} can be obtained from the following equation.

$$C_{dc} \geq \frac{P_{in}}{2\pi f_L V_{dc}^2 r_{vo}} \tag{4-19}$$

$C_{dc} \geq 117$ μF.

In this design example, C_{dc} is chosen as 120μF.

Step 5. Determine turn-ratio N

By using the filament model derived in chapter 2, the variation of the dc-link voltage during preheating for some N can be depicted in Figure 4-11. The dashed line of t_{pp} represents the proper preheating time. At this time, the appropriate hot filament resistance approximately 4.5 times the cold filament resistance. The dashed lines of t_{min} and t_{max} are the acceptable minimum and maximum preheating time for rapid-start operation, respectively. As shown in this figure, a smaller N will reduce the dc-link voltage during preheating and hence the voltage stress on circuit components will be reduced. In addition, a smaller N leads to a larger preheating voltage, resulting in a shorter preheating time to heat up the cathode filament to a proper emission temperature. However, it requires more power to been consumed on the cathode filaments at the steady-state operation. In this example, N is chosen to be 22 to keep the dc-link voltage during preheating be lower than 350V and the preheating time is about 1 second.

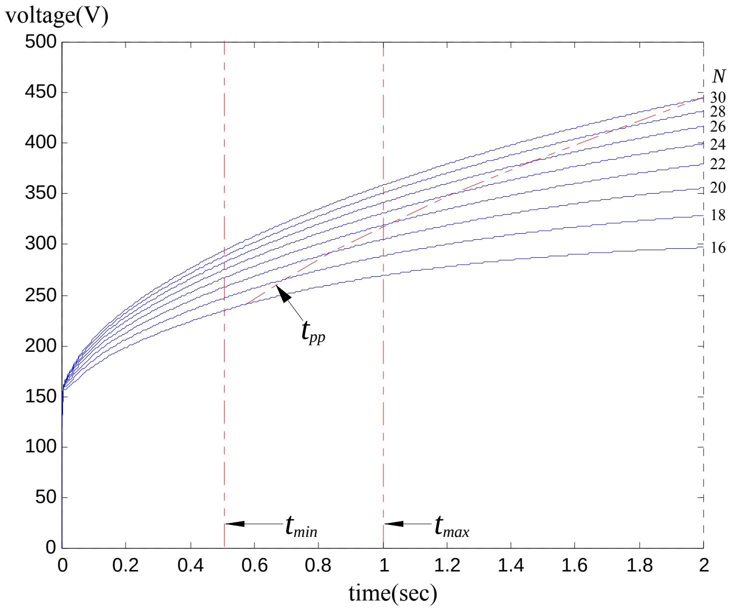

Figure 4-11 Variation of the dc-link voltage during preheating

4-5 Simulation Results

According to the circuit parameters calculated in the previous section, an IsSpice model of the proposed electronic ballast is built to simulate. Figure 4-12 shows the simulation waveforms of the primary voltage v_p of the transformer and the filament voltage and current during the preheating interval. Due to the non-ideal property of the active power switches and diodes, the simulation waveforms near zero crossing of the line voltage are slightly different with the theoretical predictions. Figure 4-13 shows the waveforms of the input voltage and current and the primary current i_{pp} of the transformer. Figure 4-14 shows the main voltage and current waveforms of the ballast circuit at steady-state operation. These simulation results are identical with the theoretical predictions.

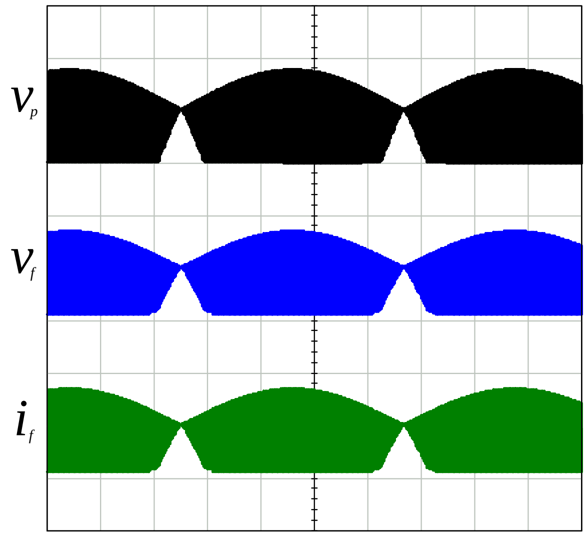

v_p:200V/div; v_f:10V/div; i_f:2A/div; time:2ms/div

Figure 4-12 Waveforms of v_p, v_f and i_f during preheating

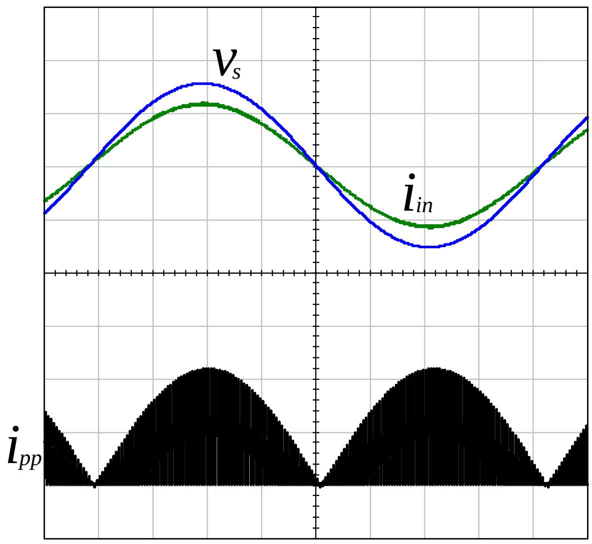

v_s:100V/div; i_{in}:0.5A/div; i_{pp}:1A/div; time:2ms/div

Figure 4-13 Waveforms of v_s, i_{in} and i_{pp} at steady-state

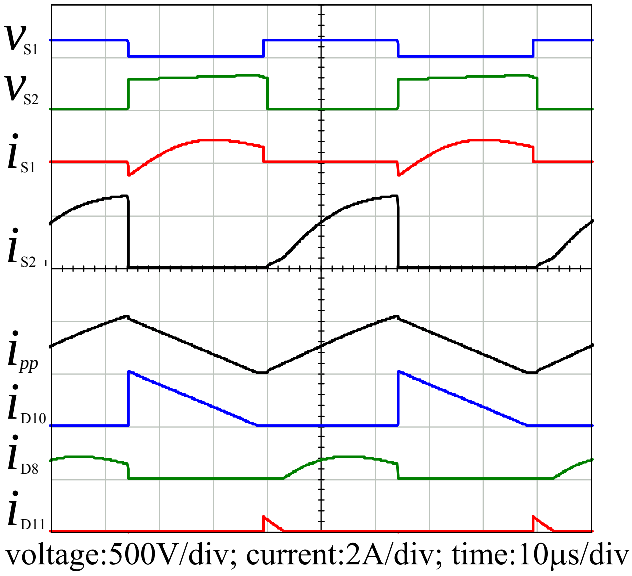

(a) Near line peak voltage

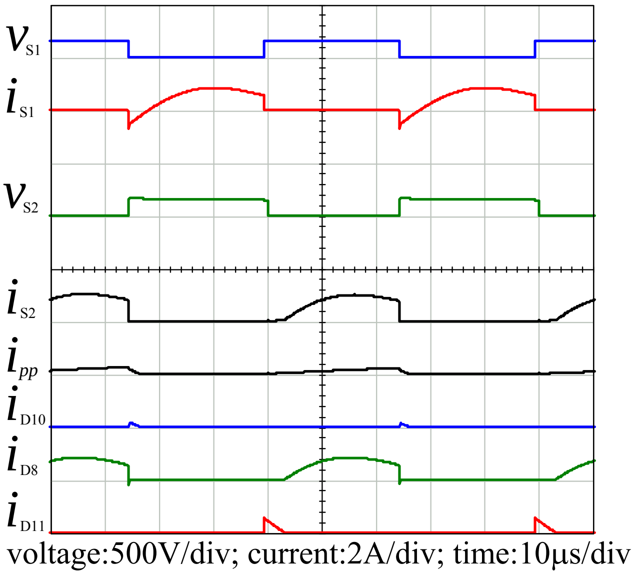

(b) Near zero crossing

Figure 4-14 Waveforms of v_{S1}, v_{S2}, i_{S1}, i_{S2}, i_{pp}, i_{D10}, i_{D8} and i_{D11} at steady-state

4-6 Experimental Results

An electronic ballast designed for a rapid-start fluorescent lamp of Osram T8-36W is built and tested to verify the theoretical analyses. Table 4-2 lists the circuit parameters. The resonance frequency of the series-resonant energy-tank is designed at 20.8kHz. At steady-state, the resonance frequency of the load resonant circuit becomes 14.6kHz when the lamp takes part in the load resonant circuit. The preheating frequency is set at 100kHz and the steady-state operation frequency for the rated lamp power is 20kHz. Such a design ensures that the resonant inverter is able to generate a sufficiently high ignition voltage when the operation frequency is adjusted from the preheating frequency to the steady-state frequency. Figure 4-15 illustrates the variations of the operation frequency of the electronic ballast, lamp voltage and resonance frequency of the load resonant circuit.

Table 4-2 Circuit parameters

Steady-state operation frequency, f_s	20kHz
Preheating frequency, f_p	100kHz
Resonance frequency of resonant circuit, $f_{r,ign}$	20.8kHz
Inductance of the primary winding, L_p	2.0mH
Dc-link capacitance, C_{dc}	120μF
Resonant inductance, L_r	1.48mH
Resonant capacitance, C_r	40.0nF
Dc-blocking capacitance, C_b	2.2μF
Turn-ratio, N	22
Filtering inductance, L_m	2.0mH
Filtering capacitance, C_m	330nF

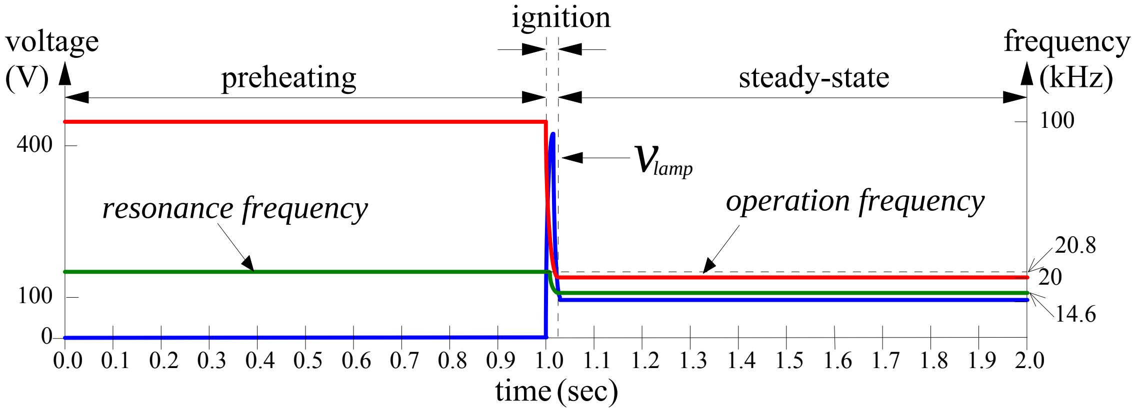

Figure 4-15 Variations of the operation frequency, lamp voltage and resonance frequency

Figure 4.16 shows the interested waveforms during starting transient. When switched on, the electronic ballast begins to extract power from the ac line source for preheating. The preheating interval lasts for 1 second. During this interval, only a small amount of the power dissipates to cathode filaments as well as circuit components. At the beginning, the dc-link voltage is low and buck-boost converter is operated with a continuous transformer current drawing a large power. As the dc-link voltage is built up, transformer current becomes discontinuous drawing less power. The dc-link voltage rises first rapidly and then gradually increases up to 320V. The negative part of the filament voltage increases accordingly. On the other hand, the positive filament voltage remains unchanged while the positive peaks of the preheating current decline from 2.9A at the beginning to 0.65A at the end of the preheating interval. This indicates that the ratio of the hot filament resistance to the cold resistance has reached about 4.5 at this point. Since the half-bridge series-resonant parallel-loaded inverter is not active, neither a lamp voltage nor a glow current is found during preheating time. The active power switch S_1 is activated when the cathode filaments have reached the appropriate emission temperature and the operation frequency is adjusted from 100kHz to 20kHz. At this time, the lamp voltage rises up immediately for ignition. After being ignited, a lamp arc current flows and eventually reaches the thermal equilibrium.

Figure 4-17 shows the waveforms of the filament voltage v_f and filament current i_f during the preheating interval. The waveforms agree with the theoretical calculations except for those near zero crossing of the line voltage. The negative pulses decrease at these areas. This is caused by the leakage inductance on the transformer and the non-ideal property of the power switches. Figure 4-18 shows the waveforms of the input voltage and current and the primary current i_{pp} of the transformer. The input current is sinusoidal and in phase with the input voltage. The buck-boost power factor corrector is operated at DCM over the entire cycle of the line voltage source leading to a high power factor greater than 0.99 and a low THD less than 8%. Figure 4-19 shows the voltage and current waveforms of the active power switches at the steady-state operation. These waveforms indicate that the ZVS operation for the active switch Q_1 of the ballast circuit can be always retained. Figure 4-20 shows the measured lamp voltage and current waveforms at the steady-state operation. The lamp current is nearly sinusoidal with a crest factor below 1.55. The circuit efficiency is 85% when the lamp is operated at the rated power.

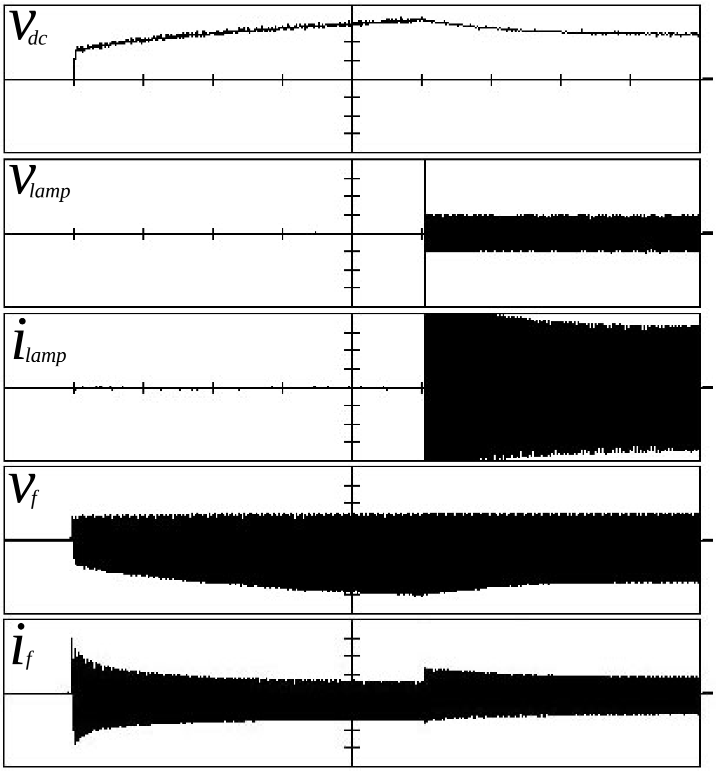

v_{dc}, v_{lamp}:100V/div; i_{lamp}:0.2A/div; v_f:5V/div; i_f:1A/div; time:0.2s/div

Figure 4-16 Starting transition waveforms

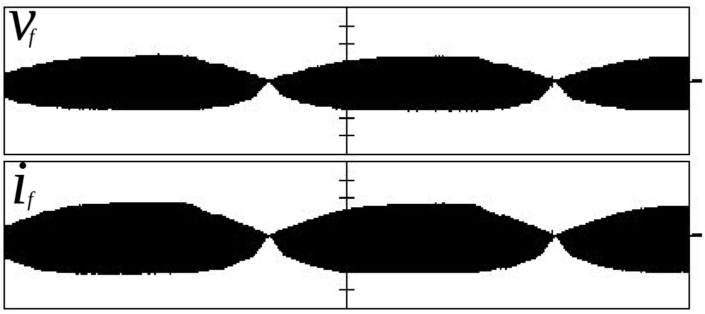

voltage:5V/div; current:1A/div; time:2ms/div

Figure 4-17 Filament voltage and current waveforms during preheating

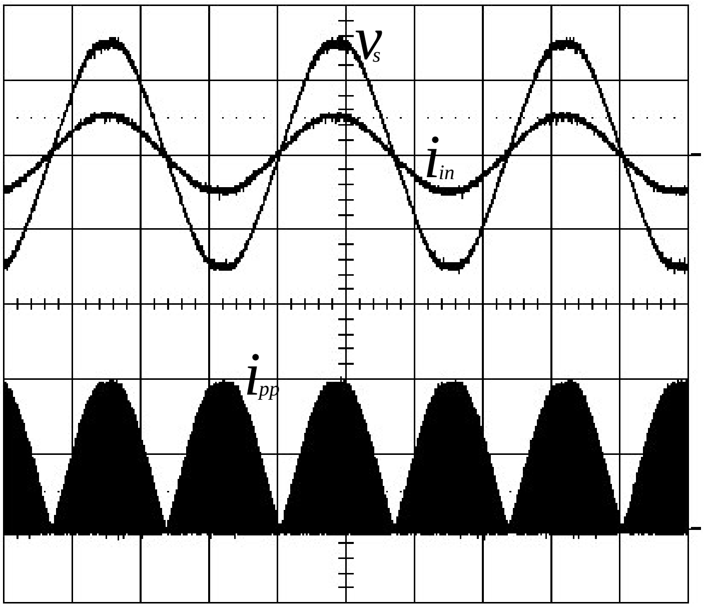

voltage:100V/div; current:1A/div; time:5ms/div

Figure 4-18 Waveforms of v_s, i_{in} and i_{pp}

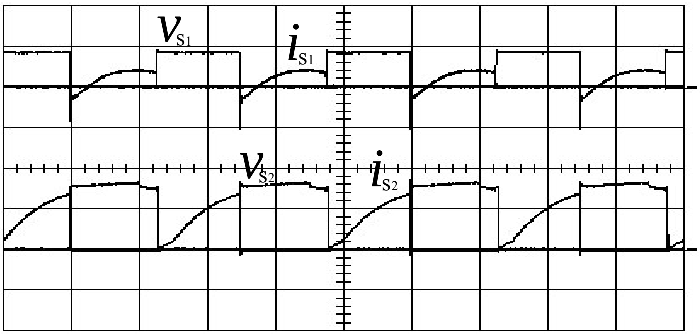

voltage:200V/div; current:2A/div; time:10μs/div

(a) Near line peak voltage

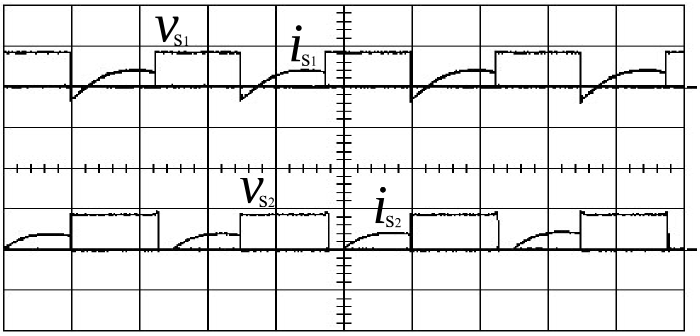

voltage:200V/div; current:2A/div; time:10μs/div

(b) Near zero crossing

Figure 4-19 Switching voltage and current waveforms at steady-state

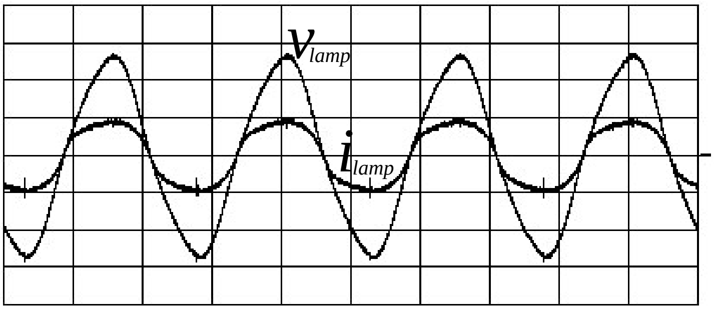

voltage:50V/div; current:0.5A/div; time:20μs/div

Figure 4-20 Lamp voltage and current waveforms at steady-state

Chapter 5 Programmed Rapid-Start Electronic Ballast with A Series-Resonant Energy-Tank

As described in chapter 3, by adding an ac switch on the load resonant circuit in parallel with the lamp to provide a short-circuited path, the lamp voltage can be kept at a very low level during the preheating interval, resulting in zero glow current. However, a short-circuited path can also be provided by a series-resonant energy-tank, since the series-resonant energy-tank looks like short-circuited as operating at its resonance frequency. By replacing the ac switch with a series-resonant energy-tank, a programmed frequency control scheme is proposed in this chapter. In the proposed control scheme, the series-resonant energy-tank is introduced as the starting-aid circuit for preheating and starting the lamp. With the starting-aid circuit, the lamp can be started in a sophisticated manner. During the preheating stage, the lamp voltage can be greatly reduced to a very low level by deliberately operating the inverter at the resonance frequency of the starting-aid circuit. After the cathode filaments have been preheated to an appropriate emission temperature, the inverter frequency is adjusted to generate the required high ignition voltage. Once the lamp has been started up, the frequency is regulated to produce the required lamp power.

5-1 Circuit Configuration and Operation

Figure 5-1 shows the conventional electronic ballast with the series-resonant parallel-loaded inverter. The input PFC stage providing the pre-regulated dc-link voltage may be of any standard type and is not explicitly shown. The half-bridge inverter consists of two active power switches, S_1 and S_2, which are complementary switched on and off at a 50% duty-ratio to convert the dc voltage to a resultant square-wave voltage, v_{ab}, on the load resonant circuit. The load resonant circuit is composed of a dc-blocking capacitor, C_b, a series-resonant energy-tank, L_r and C_r, and the fluorescent lamp. The fluorescent lamp is connected in parallel with the capacitor C_r of the resonant energy-tank. The capacitor C_b is used for blocking any dc voltage that may be introduced from the discrepancy between the used components.

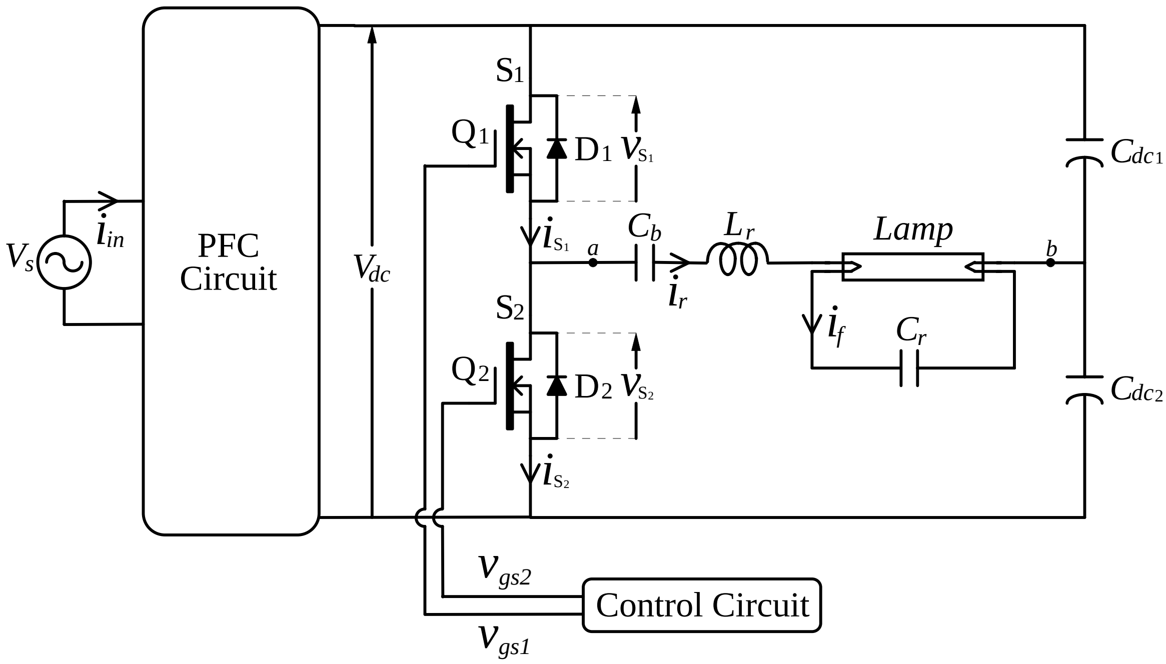

Figure 5-1 Conventional series-resonant electronic ballast

The circuit configuration of the proposed electronic ballast with programmed rapid-start is shown in Figure 5-2. This proposed circuit is to add a starting-aid circuit on the conventional series-resonant electronic ballast topology. Although a quasi half-bridge inverter is most frequently used in the ballast circuit of commercial products, the standard half-bridge inverter is adopted to avoid introducing any dc voltage upon the lamp before ignition. In the load resonant circuit, the shunted capacitor, C_r, is replaced by a series-resonant energy-tank formed by L_f and C_f serving as the starting-aid circuit. The resonant capacitor C_r is moved to the other side of the lamp. With such a rearrangement, the filament current flows through the starting-aid circuit but not through C_r.

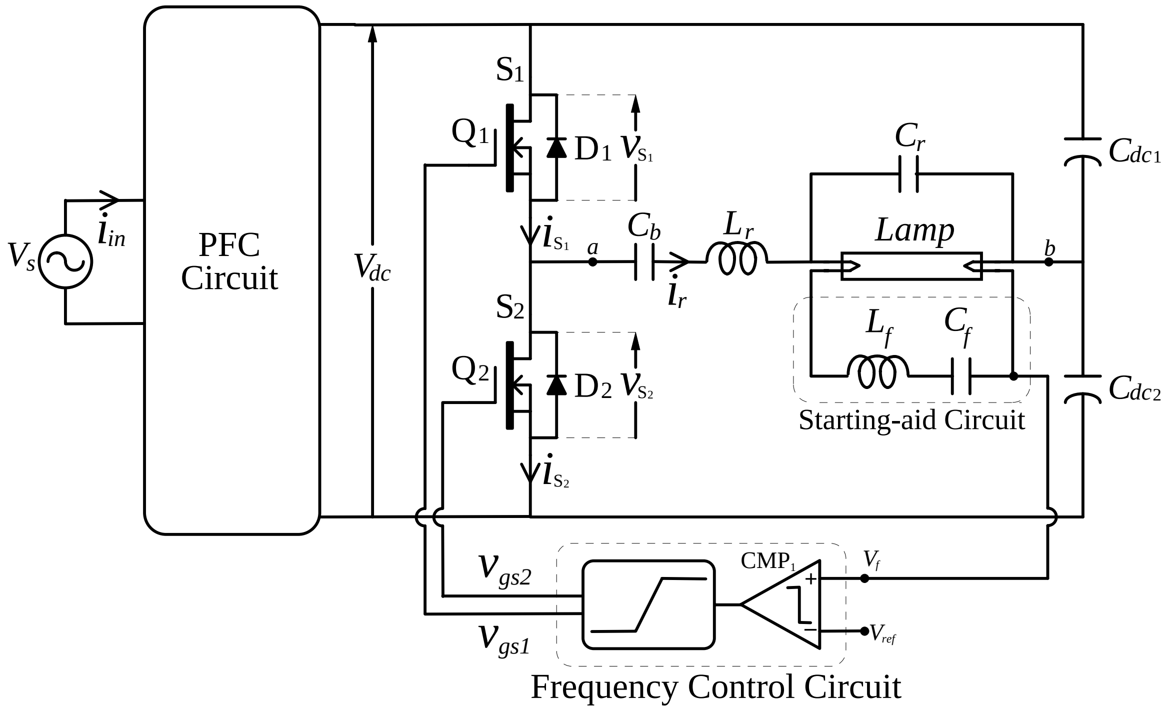

Figure 5-2 Circuit configuration of the proposed electronic ballast

To fulfill the requirements for both starting and steady-state operations, the switching frequency of the inverter is adjusted by a frequency control circuit. By controlling the inverter frequency, the ballast can provide an appropriate preheating current during the preheating interval and a compensated filament current to maintain the emission temperature at the steady-state operation. In addition, it can generate a sufficiently high voltage to ignite the lamp by operating the load resonant circuit at a frequency close to the resonance frequency.

The operation of the ballast-lamp circuit is described by three stages: preheating, ignition, and steady-state. During the preheating stage, the inverter is operated at the resonance frequency of the starting-aid circuit, f_p. Being operated at this frequency, the fundamental voltage on the starting-aid circuit and thus the lamp voltage can be reduced to zero. However, the harmonic voltages may present on the lamp. Fortunately, these harmonic voltages can be effectively attenuated by the shunted capacitor C_r.

Before ignition, the cathode filaments of the fluorescent lamp should be preheated up to a proper emission temperature (about 1000K). In practical implementations, the filament temperature can be estimated by photocell technique or by measuring the variation of the filament resistance [74]. Since the preheating current remains almost constant, the filament temperature can be estimated by measuring the variation of the filament voltage. The filament voltage, v_f, is compared with a preset voltage, V_{ref}, which stands for the emission temperature. When the filament voltage rises to the preset voltage, the inverter frequency is changed from the preheating frequency toward the resonance frequency, $f_{r,ign}$, of the load resonant circuit. At this frequency, a very high lamp voltage can be generated to ensure that the lamp can be successfully ignited at any condition. As a stable lamp arc has been built, the inverter frequency is then adjusted to the steady-state frequency, f_s, to have the required lamp power.

5-2 Circuit Analysis

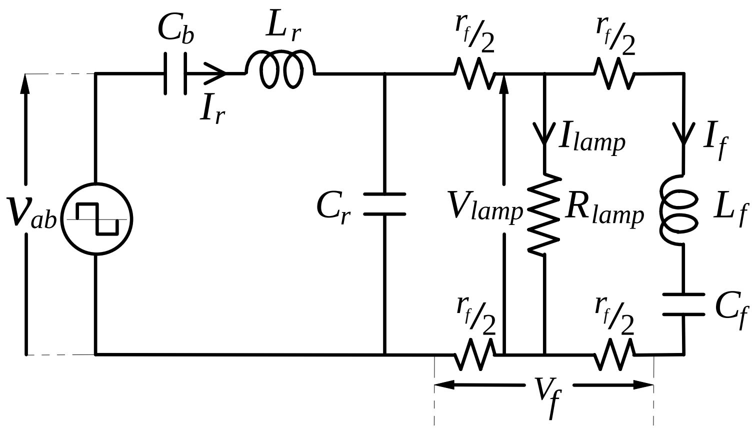

Figure 5-3 Equivalent circuit of the proposed electronic ballast

The equivalent circuit of the ballast-lamp circuit is shown in Figure 5-3 in which the fluorescent lamp is represented by a power-dependent resistance model. The square-wave voltage, v_{ab}, at the inverter output can be represented by the sum of its n-th order harmonic components, v_n.

$$v_{ab}(t) = \sum_{n=1}^{\infty} v_n(t) = \sum_{n=1,3,5}^{\infty} \sqrt{2} V_n \sin(2\pi n f_o t) \tag{5-1}$$

where f_o is the operation frequency of the inverter. The rms value of v_n can be obtained from Fourier series analysis.

$$V_n = \frac{\sqrt{2}}{n\pi} V_{dc} \qquad n = 1,3,5\cdots \tag{5-2}$$

where V_{dc} is the dc-link voltage.

5-2-1 Preheating

During the preheating interval, the inverter is deliberately operated at the resonance frequency of the starting-aid circuit, f_p.

$$f_p = \frac{1}{2\pi\sqrt{L_f C_f}} \tag{5-3}$$

The fluorescent lamp is regarded as an open circuit in this period. Since the capacitance of C_b in the load resonant circuit is large enough, the reactance is very small as compared with the impedance of the load resonant circuit at the preheating frequency. Neglecting C_b, the n-th harmonic of the filament current for preheating can be expressed as:

$$\overrightarrow{I_{pn}} = n\omega_p C_f \overrightarrow{V_n} \Big/ \Big\{ 2r_f n\omega_p C_f \left(1 - n^2\omega_p^2 L_r C_r\right) - j\left[n^4\omega_p^4 L_r L_f C_r C_f - n^2\omega_p^2\left(L_r C_r + L_r C_f + L_f C_f\right) + 1\right] \Big\} \tag{5-4}$$

where r_f is the resistance on each cathode filament and $\omega_p = 2\pi f_p$. In practice, only the fundamental component will be present in the preheating current while the harmonics are filtered by the load resonant circuit. To start the lamp rapidly, the preheating current may be as high as possible but should be limited by the rated filament current.

Before ignition, the fluorescent lamp is regarded as an open circuit. Therefore, the equivalent circuit in Figure 5-3 can be further simplified as shown in Figure 5-4 before a significant lamp current is built. As stated above, the reactance of C_b can be neglected and the series impedance Z_{sn} at n-th harmonic frequency can be expressed as:

$$\overrightarrow{Z_{sn}} = \frac{1}{jn\omega_o C_b} + jn\omega_o L_r \cong jn\omega_o L_r \tag{5-5}$$

where $\omega_o = 2\pi f_o$.

On the other hand, the parallel impedance Z_{pn} can be expressed as:

$$\overrightarrow{Z_{pn}} = \frac{1}{\left(2r_f n^2\omega_o^2 C_r C_f\right)^2 + \left[n^3\omega_o^3 L_f C_r C_f - n\omega_o\left(C_r + C_f\right)\right]^2} \cdot \left\{ 2r_f n^2\omega_o^2 C_f^2 - j\left[n^5\omega_o^5 L_f^2 C_r C_f^2 + n\omega_o\left(C_r + C_f\right) + n^3\omega_o^3\left(4r_f^2 C_r C_f^2 - 2L_f C_r C_f - L_f C_f^2\right)\right] \right\} \tag{5-6}$$

Then, the n-th harmonic of the lamp voltage can be calculated as:

$$\overrightarrow{V_{lampn}} = \frac{\overrightarrow{Z_{pn}}}{\overrightarrow{Z_{sn}} + \overrightarrow{Z_{pn}}} \overrightarrow{V_n} \tag{5-7}$$

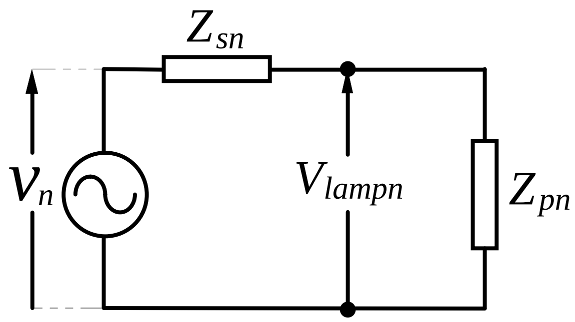

Figure 5-4 Simplified equivalent circuit

When operated at the preheating frequency, the impedance at the fundamental frequency of the starting-aid circuit is zero, and hence is the fundamental voltage on the lamp. However, the impedance is not zero but presents inductive at harmonic frequencies. This introduces harmonic voltages on the lamp. Fortunately, the harmonic components of the square-wave voltage are relatively low as compared with the fundamental component. Moreover, the harmonic voltages can be effectively attenuated by the capacitor C_r. This ensures that no glow current will occur during preheating.

5-2-2 Ignition

Assuming an open circuit for the lamp and neglecting the small harmonics, the rms value of the lamp voltage for ignition can be obtained from (5-7).

$$V_{ign} = \left| \frac{\overrightarrow{Z_{p1}}}{\overrightarrow{Z_{s1}} + \overrightarrow{Z_{p1}}} \right| \cdot V_1 \tag{5-8}$$

where V_1 is the fundamental voltage of the inverter output. This equation indicates that the lamp voltage is nearly zero at f_p and becomes extremely high at the resonance frequency, $f_{r,ign}$, of the resonant circuit, as shown in Figure 5-5. Neglecting the filament resistance and C_b, $f_{r,ign}$ can be calculated as:

$$f_{r,ign} = \left[\frac{\left(L_r C_r + L_r C_f + L_f C_f\right) \pm \sqrt{\left(L_r C_r + L_r C_f + L_f C_f\right)^2 - 4 L_r L_f C_r C_f}}{4\pi^2 L_r L_f C_r C_f} \right]^{\frac{1}{2}} \tag{5-9}$$

There are two resonance frequencies, $f_{r,ign+}$ and $f_{r,ign-}$, in this resonant circuit. For convenient control, one of the resonance frequencies is designed to lie between the preheating frequency and the steady-state frequency. This ensures that the operation will pass through the ignition stage when the inverter frequency is adjusted from the preheating frequency to the steady-state frequency. Consequently, a sufficiently high ignition voltage can be obtained.

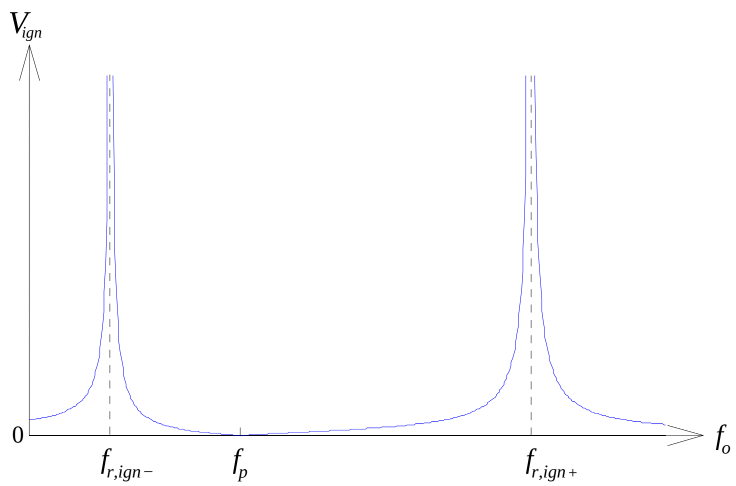

Figure 5-5 Ignition voltage during starting

5-2-3 Steady-State

At steady-state, the inverter is operated at the frequency, f_s, to output the required lamp power. At this frequency, the impedance of the starting-aid circuit, Z_{fs}, is no longer zero.

$$Z_{fs} = \omega_s L_f - \frac{1}{\omega_s C_f} \tag{5-10}$$

where $\omega_s = 2\pi f_s$. Then, the filament current flowing through the starting-aid circuit can be calculated as:

$$I_f = \frac{V_{lamp}}{\left(r_f^2 + Z_{fs}^2\right)^{1/2}} \tag{5-11}$$

Based on the equivalent circuit in Figure 5-3, the relationship between lamp voltage, V_{lamp}, and fundamental voltage, V_1, can be obtained as:

$$V_{lamp} = \left[\left(1 - \omega_s^2 L_r C_r + \frac{\omega_s L_r}{Z_{fs}}\right)^2 + \left(\frac{\omega_s L_r}{R_{lamp}}\right)^2\right]^{-1/2} \cdot V_1 \tag{5-12}$$

The filament resistances are neglected in the equation since they are very small as compared with the equivalent resistance of the lamp arc and the impedance of the load resonant circuit at the steady-state frequency.

5-2-4 Design Equations

From (5-3) and (5-10), the component values in the starting-aid circuit can be determined.

$$L_f = \frac{\omega_s Z_{fs}}{\omega_s^2 - \omega_p^2} \tag{5-13}$$

$$C_f = \frac{\omega_s^2 - \omega_p^2}{\omega_s \omega_p^2 Z_{fs}} \tag{5-14}$$

Neglecting the small harmonics in (5-4), L_r can be written as:

$$L_r = \frac{4r_f^2\omega_p C_r \pm \sqrt{\left(4r_f^2\omega_p^2 C_r^2 + 1\right)\frac{V_1^2}{I_p^2} - 4r_f^2}}{\omega_p\left(4r_f^2\omega_p^2 C_r^2 + 1\right)} \tag{5-15}$$

On the other hand, L_r can be obtained from (5-12) and can be expressed as a function of C_r.

$$L_r = \frac{R_{lamp}Z_{fs}}{\omega_s\left[R_{lamp}^2\left(Z_{fs}\omega_s C_r - 1\right)^2 + Z_{fs}^2\right]}\left\{ R_{lamp}\left(Z_{fs}\omega_s C_r - 1\right) \pm \sqrt{R_{lamp}^2\left(Z_{fs}\omega_s C_r - 1\right)^2\left(\frac{V_1}{V_{lamp}}\right)^2 + Z_{fs}^2\left[\left(\frac{V_1}{V_{lamp}}\right)^2 - 1\right]}\right\} \tag{5-16}$$

Theoretically, one can find two solutions of L_r for a given C_r in both (5-15) and (5-16). With the smaller ones, however, the load resonant circuit of the inverter will present capacitive. In order to reduce the switching-on losses of the active power switches, the load resonant circuit is preferred to be inductive for both preheating and steady-state operations. Excluding the undesired solutions, only one combination of L_r and C_r can be adopted.

5-3 Design Example

An electronic ballast for a Philip T8-36W rapid-start fluorescent lamp is illustrated as a design example. The ballast is supplied by the 110V, 60 Hz voltage source from ac mains. Table 5-1 lists the specifications and the rated values of the used lamp. It should be noted that the lamp power, P_{lamp}, is rated at 36W consisting of an arc power of 33.5W and a filament power of 2.5W. A power-factor-correction circuit is used in front of the inverter to provide a dc-link voltage of 200V.

Table 5-1 Lamp specifications (Philip T8-36W)

Rated lamp power, P_{lamp}	Arc power, P_{arc}	33.5W
	Filament power, P_f	2.5W
Rated lamp voltage, V_{lamp}		101.5V
Rated lamp current, I_{lamp}		0.33A
Equivalent lamp resistance, R_{lamp}		307.6Ω
Filament resistance (25°C), r_f		2Ω
Filament current at steady-state, I_f		0.25A

Step 1. Preheating Current I_p

In order to retain a long lamp life, the cathode filament should be preheated to a proper emission temperature before ignition. According to the calculated results, the cathode filament will be preheated up to a proper emission temperature (about 1000K) when the hot filament resistance becomes around 4.5 times the cold filament resistance. Figure 5-6 shows the variation of the filament resistance of the rapid-start fluorescent lamp at different preheating currents. The dashed line of r_{f_p} represents the appropriate hot filament resistance approximately 4.5 times the cold filament resistance. The dashed lines of t_{min} and t_{max} are the acceptable minimum and maximum preheating time for rapid-start operation, respectively. As indicated in this figure, the cathode filament can be heated up to the proper emission temperature at the acceptable preheating time when the preheating current is between 0.75A and 0.95A. The higher the preheating current is, the less the required preheating time is. However, a higher preheating current will result in higher current stress on the circuit components. In this design, the preheating current is chosen to be 0.75A.

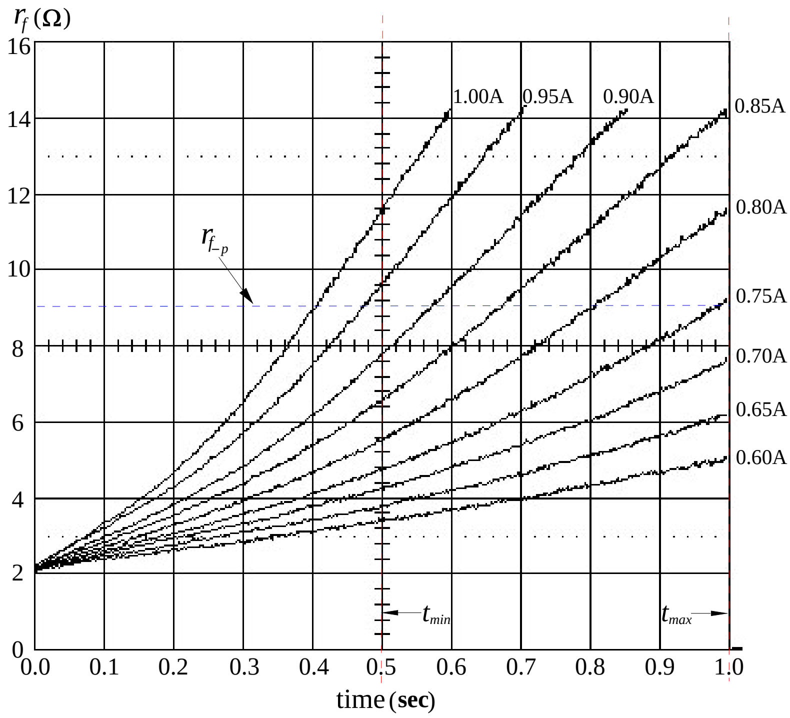

Figure 5-6 Variation of the filament resistance

Step 2. Determine preheating and steady-state frequencies, f_p and f_s

In order to ensure that one of the resonance frequencies of the resonant circuit will fall between the preheating frequency and the steady-state frequency and the lamp can be stably operated, the preheating frequency f_p and steady-state frequency f_s must be carefully chosen.

● *Resonance Frequency*

Figure 5-7 shows the variations of the resonance frequencies of the load resonant circuit with the ratio of f_p to f_s. The dashed lines of f_p/f_s and f_s/f_s represent the preheating frequency and the steady-state frequency, respectively. From this figure, it can be found that neither of the resonance frequencies of the resonant circuit will lie between the preheating frequency and the steady-state frequency when the ratio of f_p to f_s is higher than 1. Once no resonance frequency falls between the preheating frequency and the steady-state operation frequency, a more complicated control circuit will be required. Since the operation of the ballast circuit may not pass through the ignition stage when the inverter frequency is adjusted from the preheating frequency to the steady-state frequency. At this condition, the inverter frequency must first be adjusted from the preheating frequency toward the resonance frequency which does not lie between the preheating frequency and the steady-state frequency to generate a sufficiently high lamp voltage for ignition. After the lamp is successfully ignited, the inverter frequency is then adjusted to the steady-state frequency. Therefore, in order to ensure that one of the resonance frequencies will be in the range between the preheating frequency and the steady-state frequency, the ratio of f_p to f_s should be chosen to be lower than 1.

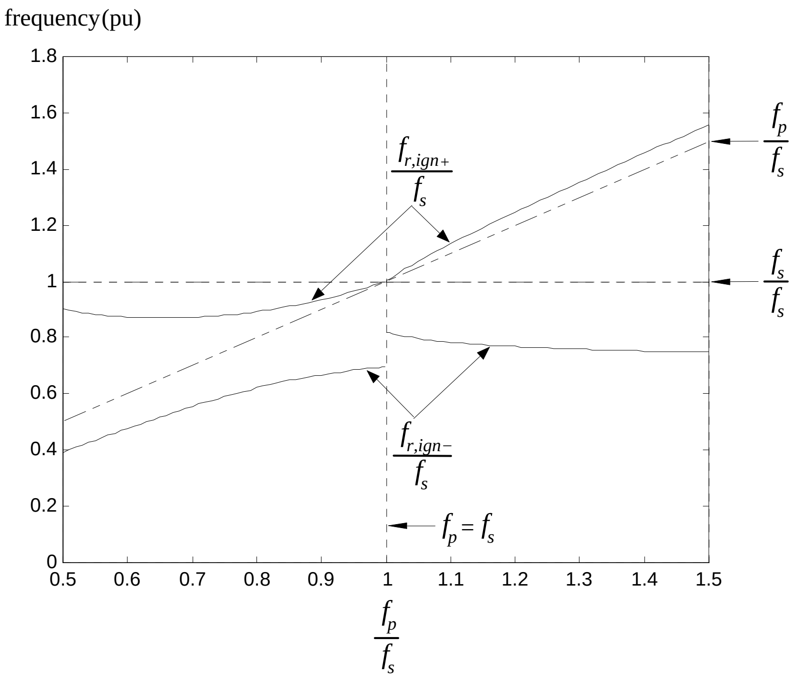

Figure 5-7 Variations of the resonance frequencies

● *Stability*

In order to ensure that the lamp can be stably operated, the following requirement must be satisfied [75].

$$Z_{eq} \geq R_{lamp} \tag{5-17}$$

where

$$Z_{eq} = \left| \frac{\overrightarrow{Z_{s1}} \cdot \overrightarrow{Z_{p1}}}{\overrightarrow{Z_{s1}} + \overrightarrow{Z_{p1}}} \right| \tag{5-18}$$

Figure 5-8 illustrates the variation of Z_{eq} with the ratio of f_p to f_s. The dashed line stands for the boundary between stable operation and unstable operation. As indicated in this figure, the lamp can be stably operated when the ratio of f_p to f_s is lower than 0.62. To avoid the non-ideal property of the used components resulting in unstable operation, the ratio of f_p to f_s is chosen to be 0.6.

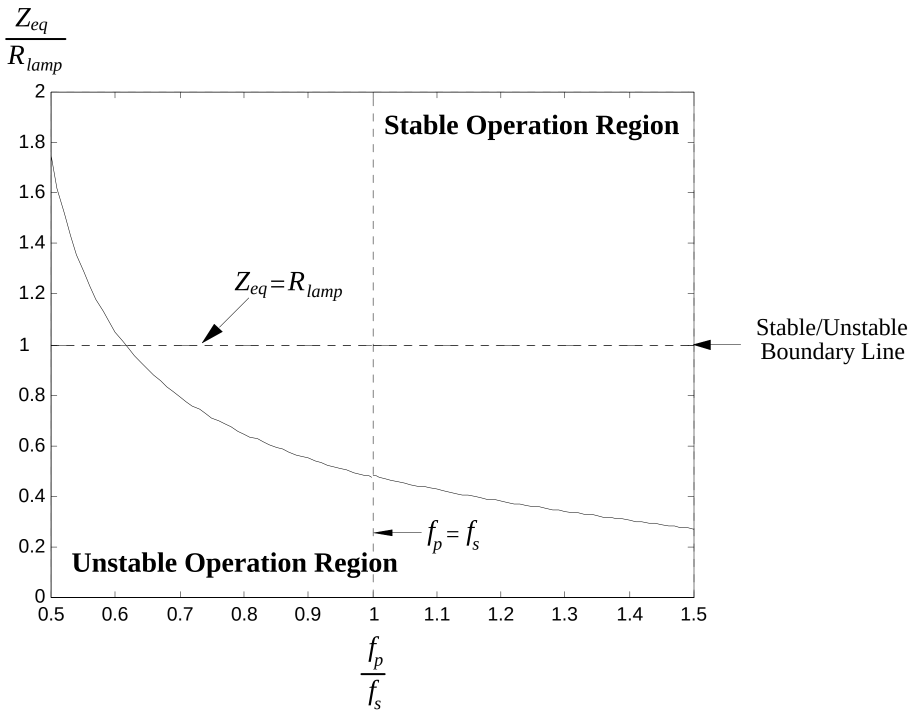

Figure 5-8 Variation of Z_{eq}

After the ratio of f_p to f_s is chosen, f_p and f_s can be determined. Theoretically, one can find infinite combinations of f_p and f_s for the chosen ratio of f_p to f_s. It is preferable to operate the ballast at a frequency higher than the acoustic frequency. Operation at a higher frequency is advantageous of using smaller magnetic components. However, a higher operation frequency may cause more switching losses in active power switches, resulting in a lower efficiency. In this design, the steady-state frequency f_s is chosen to be 40kHz and then the preheating frequency f_p can be obtained to be 24kHz.

Step 3. Determine L_r, C_r, L_f and C_f

Once the preheating current, the preheating frequency and the steady-state frequency are determined, L_r, C_r, L_f and C_f can be calculated in accordance with the above design equations. The calculated results are shown as follows:

L_r = 0.80mH, C_r = 41.3nF, L_f = 2.58mH and C_f = 17.0nF.

5-4 Simulation Results

The circuit parameters obtained from the above section are applied in an IsSpice model of the proposed electronic ballast to simulate the operation of the circuit. Figure 5-9 shows the simulation waveforms of the voltage and current of the active power switches and the lamp during the preheating interval. Figure 5-10 shows the waveforms of the voltage and current of the active power switches and the lamp at the steady-state operation. The simulation results are the same as the theoretical predictions.

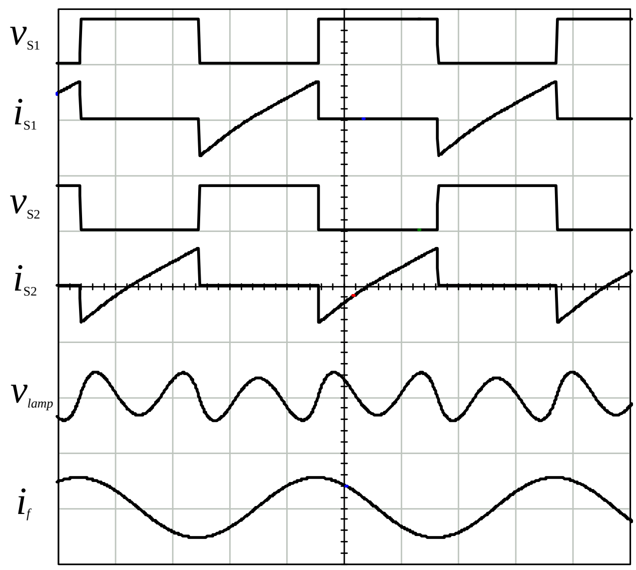

v_{S1}, v_{S2}:250V/div; i_{S1}, i_{S2}:2A/div; v_{lamp}:20V/div; i_f:2A/div; time:10μs/div

Figure 5-9 Waveforms of v_{S1}, i_{S1}, v_{S2}, i_{S2}, v_{lamp} and i_f during preheating

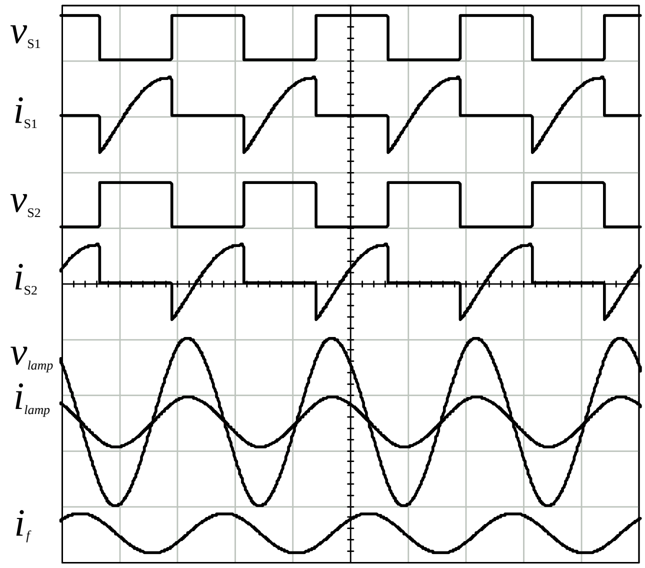

v_{S1}, v_{S2}:250V/div; i_{S1}, i_{S2}:2A/div; v_{lamp}:100V/div; i_{lamp}, i_f:1A/div; time:10μs/div

Figure 5-10 Waveforms of v_{S1}, i_{S1}, v_{S2}, i_{S2}, v_{lamp}, i_{lamp} and i_f at steady-state

5-5 Experimental Results

Table 5-2 Designed circuit parameters

Steady-state operation frequency, f_s	40kHz
Preheating frequency, f_p	24kHz
Resonance frequency of load resonant circuit, $f_{r,ign}$	35kHz
Dc-blocking capacitance, C_b	2.2μF
Resonant inductance, L_r	0.80mH
Resonant capacitance, C_r	41.3nF
Inductance in starting-aid circuit, L_f	2.58mH
Capacitance in starting-aid circuit, C_f	17.0nF

An electronic ballast was built to operate a rapid-start fluorescent lamp of Philip T8-36W in order to test and verify the theoretical predictions. The circuit parameters are listed in Table 5-2. The resonance frequency of the starting-aid circuit is set at 24kHz and the steady-state frequency for the rated lamp power is 40kHz. One of the resonance frequencies of the resonant circuit is designed to be 35kHz, which lies between the preheating frequency and the steady-state frequency.

At steady-state, the resonance frequency of the load resonant circuit with the lamp becomes 21.2kHz. The variations of the operation frequency of the electronic ballast, the lamp voltage and the resonance frequency of the load resonant circuit are illustrated in Figure 5-11. As the ballast is started, the operation frequency begins from the preheating frequency and then goes through the ignition frequency, and finally operates at the steady-state frequency.

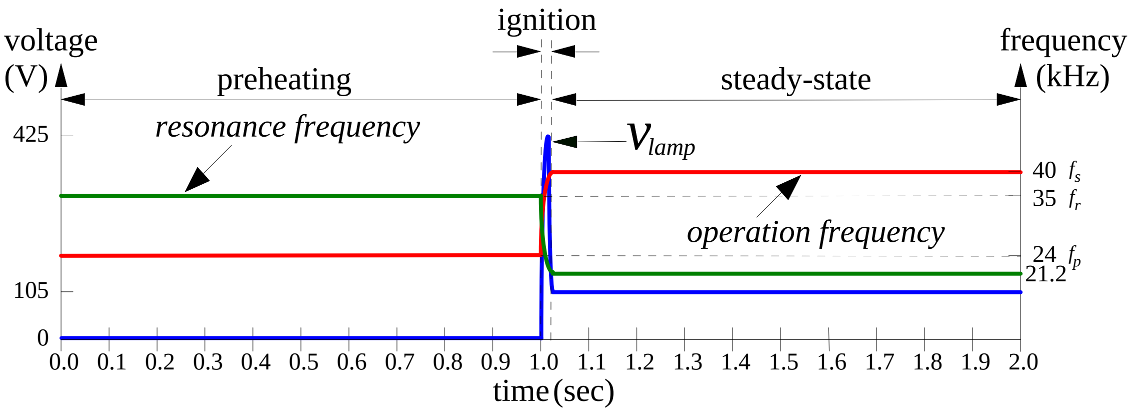

Figure 5-11 Variations of the operation frequency, lamp voltage and resonance frequency

Figure 5-12 shows the starting transient waveforms. After switched on, the filament current increases rapidly up to a constant value of about 0.75A. With this preheating current, the filament voltage increases gradually up to a peak value of 9V. This means that the ratio of the hot resistance of the filaments to their cold resistance has reached about 4.5. The preheating interval lasts for 1 second. Once the cathode filaments have reached the appropriate emission temperature, the operation frequency is increased rapidly to the rated frequency. As the operation frequency increasing, the lamp voltage is increased up for ignition. The lamp is successfully ignited at about 425V. Then, a stable lamp arc current flows. The filament current decreases to about 0.25A to maintain the cathode filaments at the proper emission temperature.

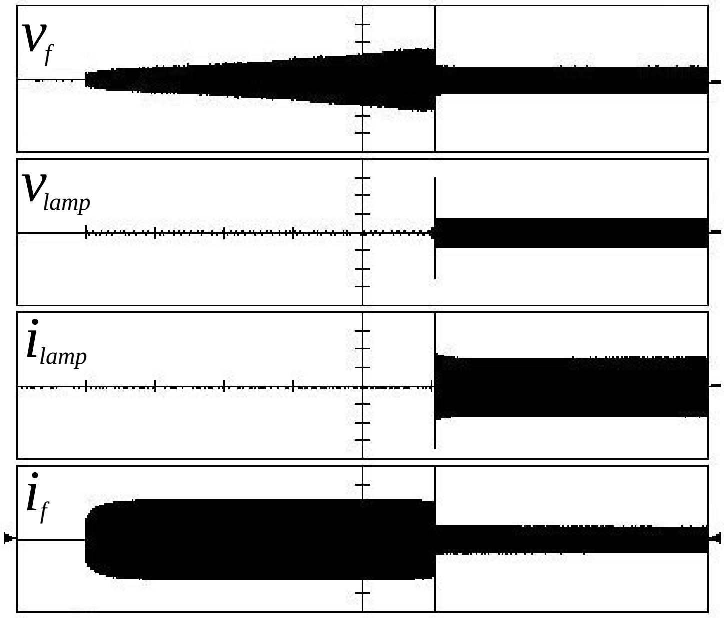

v_f:5V/div; v_{lamp}:200V/div; i_{lamp}:0.2A/div; i_f:0.5A/div; time:0.2s/div

Figure 5-12 Starting transient waveforms

During the preheating interval, only a very small voltage is found on the lamp, which consists dominantly of the third harmonic. The peak value of this small voltage is less than 12V. Such a small voltage results in no glow current as shown in Figure 5-13. Figure 5-14 shows the measured lamp voltage and current waveforms at the steady-state operation. The lamp current is nearly sinusoidal with a crest factor below 1.55. Figure 5-15 shows the input voltage and current waveforms of the PFC circuit. The input current is sinusoidal and in phase with the input voltage. The power factor is 0.99 and the THD is 8%. Figures 5-16 and 5-17 show the voltage and current waveforms of the active power switches during the preheating interval and at the steady-state operation. These waveforms indicate that the ZVS operation for the active power switches of the inverter can be always retained. The total circuit efficiency including the PFC circuit and the resonant inverter is 81% when the lamp is operated at the rated power.

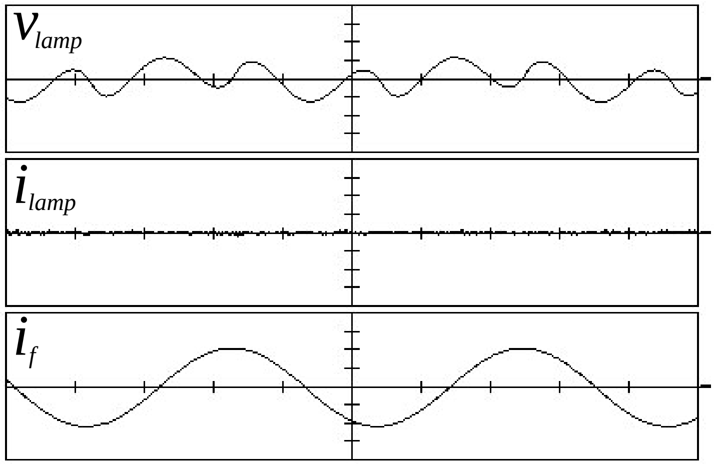

v_{lamp}:10V/div; i_{lamp}:20mA/div; i_f:0.5A/div; time:10μs/div

Figure 5-13 Lamp voltage and current waveforms during preheating

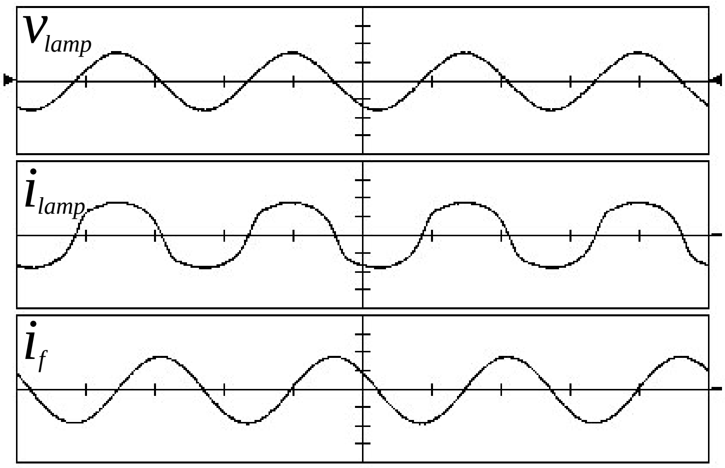

voltage:100V/div; current:0.2A/div; time:10μs/div

Figure 5-14 Lamp voltage and current waveforms at steady-state

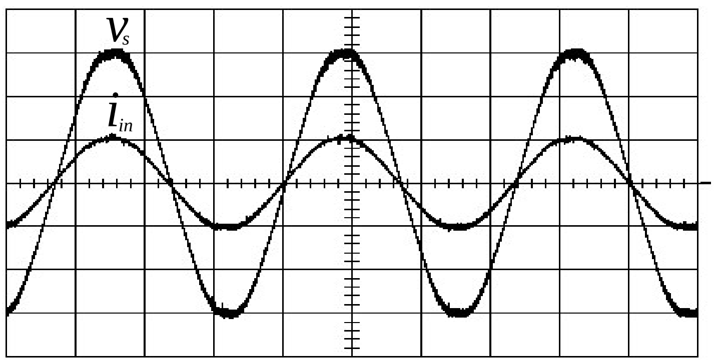

voltage:50V/div; current:0.5A/div; time:5ms/div

Figure 5-15 Input voltage and current waveforms

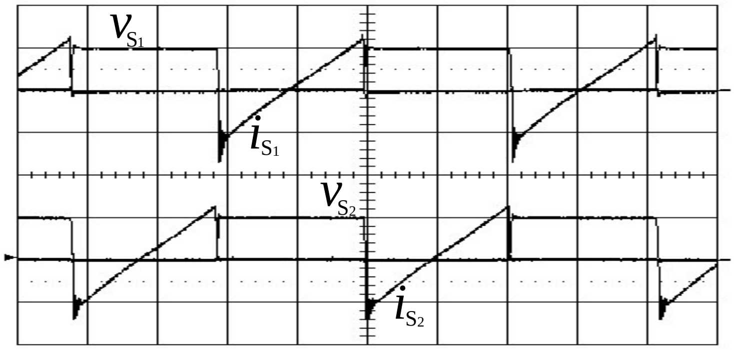

voltage:200V/div; current:1A/div; time:10μs/div

Figure 5-16 Switching voltage and current waveforms during preheating

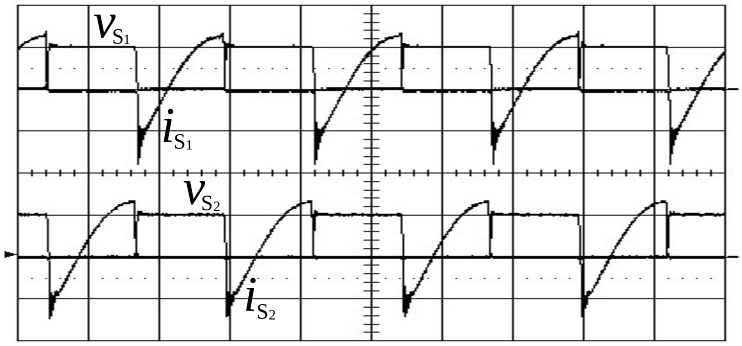

voltage:200V/div; current:1A/div; time:10μs/div

Figure 5-17 Switching voltage and current waveforms at steady-state

Chapter 6 Conclusions and Discussions

In this dissertation, three programmed rapid-start control schemes have been proposed for the electronic ballast with a half-bridge series-resonant inverter. With the proposed programmed rapid-start control schemes, the glow current in the rapid-start fluorescent lamp during preheating can be completely eliminated and the lamp can be ignited under an adequate filament temperature, resulting in minimum damage to the cathode filaments during starting. This would greatly increase the possible number of switching cycle without adverse effects on the service life of the fluorescent lamp. The laboratory circuits are fabricated for the T8-36W rapid-start fluorescent lamps. Satisfied performances have been demonstrated by the experimental results.

As compared with the conventional circuit configurations, the extra expenses of the proposed programmed rapid-start control schemes are small. That is, for the programmed rapid-start control scheme with an ac switch, a solid-state ac switch with its simple control circuit is added; for the programmed rapid-start control scheme with inductively coupled filament-heating circuits, only two auxiliary windings and few diodes are needed; while for the programmed frequency control scheme with a series-resonant energy-tank, only few small reactive components are attached. Thus, these proposed ballast circuits are simpler and more cost-effective than the other solutions. Additionally, for these proposed schemes, the operation principles of the inverter under steady-state are exactly inherited from those of the conventional ones. Therefore, the power factor correction circuit can be easily interposed into the circuit just as in the conventional circuits. Besides, the ZVS operation on the active power switches can be retained by carefully designing the circuit parameters and therefore high power efficiency can be achieved.

For all those proposed schemes, the filament current or voltage under starting and steady-state can be explicitly specified. For the proposed programmed rapid-start electronic ballast with an ac switch, the filament current for both preheating and steady-state operations can be designated by properly choosing the component values of the inverter and the corresponding operation frequencies and duty-ratios. For the programmed rapid-start electronic ballast with inductively coupled filament-heating circuits, the filament voltage for both preheating and steady-state operations can be designated by properly choosing the turn-ratio of the transformer of the buck-boost converter and the corresponding duty-ratios. By properly choosing the components values of the inverter and the corresponding operation frequencies, the filament current of the programmed rapid-start electronic ballast with a series-resonant energy-tank for both preheating and steady-state operations can be designated.

Among these proposed programmed rapid-start control schemes, the control schemes proposed in chapters 3 and 5 can be used in both single-stage or two-stage high-power-factor electronic ballast and electronic ballast without the active PFC circuit. However, the circuit parameters and operation frequencies of the programmed rapid-start electronic ballast with a series-resonant energy-tank must be chosen carefully. Otherwise, the high harmonic voltages may be introduced on the lamp during the preheating interval, resulting in glow discharging. As compared with the control scheme with a series-resonant energy-tank, the control schemes proposed in chapters 3 and 4 can maintain the lamp voltage at zero during the preheating stage. However, the control scheme with an ac switch requires an additional control circuit for driving the solid-state ac switch. The programmed rapid-start control scheme with inductively coupled filament-heating circuits is not possible to be used in the electronic ballast without the active PFC circuit, since it requires two auxiliary windings added on the inductor of the active PFC circuit for providing a filament-heating voltage. In addition, this control scheme may also be unsuitable for the two-stage high-power-factor electronic ballast, where the dc-link voltage is regulated by adjusting the duty-ratio of the active power switch of the front-stage PFC circuit. The PFC circuit of the two-stage high-power-factor electronic ballast is responsible for the function of pre-regulating the dc-link voltage. Since the dc-link voltage is regulated by adjusting the duty-ratio of the active power switch of the PFC circuit, the duty-ratio of the PFC circuit during the preheating interval might be much smaller than that at the steady-state operation. That is because the power consumed by the lamp during preheating is much smaller than that at steady-state. This will cause the preheating voltage provided from the auxiliary windings which are coupled to the PFC circuit becomes very low and thus the lamp filaments may not be heated up to the proper emission temperature before ignition. Finally, the characteristics of the above three programmed rapid-start control schemes are summarized in Table 6-1.

Table 6-1 Comparison of three control schemes

	First Control Scheme	Second Control Scheme	Third Control Scheme
Additional Components	A solid-state ac switch with its control circuit	Two auxiliary windings and few diodes	A small inductor and a small capacitor
Lamp Voltage during Preheating	Zero	Zero	Small harmonic voltages
Glow current during Preheating	Zero	Zero	Zero
Requirement of Active PFC Circuit	Not essential	Essential	Not essential
Cost	High	Low	Medium
Stability	Good	Good	Good

The programmed rapid-start control schemes proposed in this dissertation can provide the adequate filament preheating before ignition and efficaciously eliminate the glow current during preheating. However, the treatment presented in this dissertation is by no means exhaustive; there are some issues left should be further investigated in detail.

1). The investigation of this dissertation only focuses on the electronic ballast with constant power operation. However, the proposed control schemes can also be used in the electronic ballast with dimming operation. For the programmed rapid-start electronic ballasts proposed in chapter 3 and 5, the dimming operation can be achieved by simply adjusting the operation frequency or duty-ratio. For the programmed rapid-start electronic ballast with inductively coupled filament-heating circuits, it is recommended to use the method of adjusting the operation frequency to fulfill the dimming operation.

2). In this dissertation, the circuit parameters of the ballast circuit are designed in accordance with a specific filament voltage or current at steady-state. However, the magnitude of the filament voltage or current at steady-state would affect the operation life of the fluorescent lamp. The optimal filament voltage or current at steady-state is left to be determined through further lamp life test.

References

[1] Lighting Handbook, Reference and Application, Illuminating Engineering Society of North America, 1993.

[2] American Nation Standards for Fluorescent Lamp-Rapid-Start Types-Dimensional and Electrical Characteristics, American National Standards Institute, Inc.

[3] E. E. Hammer, "Fluorescent Lamp Starting Voltage Relationships at 60Hz and High Frequency," Journal of the Illuminating Engineering Society, October 1983, pp. 36-46.

[4] E. E. Hammer, "High Frequency Characteristics of Fluorescent Lamps up to 500 kHz," Journal of the Illuminating Engineering Society, Winter 1987, pp. 52-61.

[5] E. E. Hammer and T. K. McGowan, "Characteristics of Various F40 Fluorescent Systems at 60 Hz and High Frequency," IEEE Transactions on Industry Applications, Vol. 21, No. 1, January/February 1985, pp. 11-16.

[6] E. Deng and S. Ćuk, "Negative Incremental Impedance and Stability of Fluorescent Lamps," IEEE Applied Power Electronics Conference APEC 1997, February 1997, pp. 23-27.

[7] C. Blanco, M. Alonso, E. Lopez, A. Calleja, and M. Rico, "A Single Stage Fluorescent Lamp Ballast with High Power Factor," IEEE Applied Power Electronics Conference APEC 1996, March 1996, pp. 616-621.

[8] R. O. Brioschi and J. F. Vieira, "High-Power-Factor Electronic Ballast with Constant Dc-Link Voltage," IEEE Transactions on Power Electronics, Vol. 13, No. 6, November 1998, pp. 1030-1037.

[9] W. R. Alling, "Important Design Parameters for Solid-State Ballast," IEEE Transactions on Industry Applications, Vol. 25, No. 2, March/April 1989, pp. 203-207.

[10] A. Heidemann, S. Hien, E. Panofski, and U. Roll, "Compact Fluorescent Lamps," IEE Proceedings-Science, Measurement and Technology, Vol. 140, No. 6, November 1993, pp. 429-434.

[11] R. Verderber, "Electronic Ballast Improves Efficiency," Electronic Consultant, Vol. 60, November/December 1980, pp. 22-26.

[12] E. C. Nho, K. H. Jee, and G. H. Cho, "New Soft-Switching Inverter for High

Efficiency Electronic Ballast with Simple Structure," Int. J. Electronic, Vol. 71, No. 3, 1991, pp. 529-542.

[13] D. M. Vasiljevic, "The Design of a Battery-Operated Fluorescent Lamp," IEEE Transactions on Industrial Electronics, Vol. 36, No. 4, November 1989, pp 499-503.

[14] W. R. Alling, "Preserving Lamp Life Using A Low Cost Electronic Ballast with Compact Fluorescent Lamps, A New Approach," IEEE Industry Application Society 1993 IAS Annual Meeting, October 1993, pp. 2247-2253.

[15] T. Leyh and S. Fancher, "Fluorescent Lamp High Frequency Evaluation," IEEE Industry Application Society 1997 IAS Annual Meeting, October 1997, pp. 2346-2352.

[16] E. E. Hammer, "Cathode Fall Voltage Relationship with Fluorescent Lamps," Journal of the Illuminating Engineering Society, Winter 1995, pp. 116-122.

[17] K. Misono, "Cathode Fall Voltage of Low-Current Fluorescent Lamps," Journal of the Illuminating Engineering Society, Summer 1991, pp. 108-115.

[18] S. T. Lee, H. S. Chung, and S. Y. Hui, "An Electrode Power Control Scheme for Dimmable Electronic Ballasts," IEEE Transactions on Industrial Electronics, Vol. 50, No. 6, December 2003, pp. 1335-1337.

[19] E. E. Hammer, "Comparative Starting-Operating Characteristics of Typical F40 Systems," Journal of the Illuminating Engineering Society, Winter 1989, pp. 63-69.

[20] A. Heidemann, W. Denz, and W. Roche, "Specifications for the Operation of Preheated Cathode Fluorescent Lamps on Electronic Ballasts," Journal of the Illuminating Engineering Society, Winter 1994, pp. 115-121.

[21] G. W. Mortimer, "Real-Time Measurement of Dynamic Filament Resistance," Journal of the Illuminating Engineering Society, Winter 1998, pp. 22-28.

[22] S. T. Lee, H. S. Chung, and S. Y. Hui, "A Novel Electrode Power Profiler for Dimmable Ballasts Using DC Link Voltage and Switching Frequency Controls," IEEE Power Electronics Specialists Conference PESC 2002, June 2002, pp. 23-27.

[23] E. E. Hammer and L. Nerone, "Performance Characteristics of An Integrally Ballasted 20-W Fluorescent Quad Lamp," Journal of the Illuminating Engineering Society, Summer 1993, pp. 183-190.

[24] T. F. Wu, C. C. Chen, and J. N. Wu, "An Electronic Ballast with Inductively

Coupled Preheating Circuits," IEEE Industry Applications Society 2001 IAS Annual Meeting, October 2001, pp. 517-523.

[25] E. W. M. Chui, R. Davis, C. O'Rourke, and Y. Ji, "Compatibility Testing of Fluorescent Lamp and Ballast Systems," IEEE Transactions on Industry Applications, Vol. 35, No. 6, November/December 1999, pp. 1271-1276.

[26] E. E. Hammer, "Fluorescent System Interactions with Electronic Ballasts," Journal of the Illuminating Engineering Society, Winter 1991, pp. 56-63.

[27] D. Klien, "A New Heating Concept for Fluorescent Lamp Ballasts," IEEE Industry Applications Society 2000 IAS Annual Meeting, October 2000, pp. 3428-3433.

[28] Y. Ji and R. Davis, "Starting Performance of High-Frequency Electronic Ballast for 4-Foot Fluorescent Lamps," IEEE Industry Applications Society 1995 IAS Annual Meeting, October 1995, pp. 2083-2089.

[29] B. L. Hesterman and T. M. Poehlman, "A Novel Parallel-Resonant Programmed Start Electronic Ballast," IEEE Industry Application Society 1999 IAS Annual Meeting, October 1999, pp. 249-255.

[30] T. F. Wu and Y. J. Wu, "Improved Start-Up Scenario for Single-Stage Electronic Ballast," IEEE Transactions on Power Electronics, Vol. 15, No 3, May 2000, pp. 471-478.

[31] T. J. Ribarich and J. J. Ribarich, "A New Procedure for High-Frequency Electronic Ballast Design," IEEE Transactions on Industry Applications, Vol. 37, No. 1, January/February 2001, pp.262-267.

[32] T. J. Ribarich, "A New Power Factor Correction and Ballast Control IC," IEEE Industry Application Society 2001 IAS Annual Meeting, October 2001, pp. 504-509.

[33] J. H. G. OP het Veld, "HF-TL Ballast with UBA2021 for TLD58W Lamp," Philips Semiconductors, Application Note, No. AN98099, 1999.

[34] E. Derckx, "CFL 13W Demo PCB with UBA2021 for Integrated Lamp-Ballast Designs," Philips Semiconductors, Application Note, No. AN99066, 2000.

[35] S. Zudrell-Koch, "Mixed Signal ASIC for Closed Loop Fluorescent Lamp Management Using Novel Digital Frequency Control Strategies," IEEE Industry Application Society 2000 IAS Annual Meeting, October 2000, pp. 3434-3440.

[36] T. F. Wu, C. Y. Lee, Y. J. Wu, and J. Y. Su, “Improvement on Component Stresses of Single-Stage Electronic Ballasts,” IEEE Industry Application Society 1999 IAS Annual Meeting, October 1999, pp. 285-292.

[37] S. Ben-Yaakov, M. Shvartsas, and G. Ivensky, “HF Multiresonant Electronic Ballast for Fluorescent Lamps with Constant Filament Preheating Voltage,” IEEE Applied Power Electronics Conference APEC 2002, March 2002, pp. 911-917.

[38] C. S. Moo, T. F. Lin, H. L. Cheng, and M. J. Soong, “ Electronic Ballast for Programmed Rapid-Start Fluorescent Lamps,” IEEE International Conference on Power Electronics and Drive Systems PEDS 2001, November 2001, pp. 538-542.

[39] Chin S. Moo and Wei M. Chen, “Starting Control for Series-Resonant Electronic Ballast with Rapid-Start Fluorescent Lamp”, IEE Electronic Letters, Vol. 38, No. 5, February 2002, pp. 212-214.

[40] Chin S. Moo, Wei M. Chen, and Hau C. Yen, “A Series-Resonant Electronic Ballast for Rapid-Start Fluorescent Lamps with Programmable Starting,” IEEE/JIEE Joint-IAS Power Conversion Conference PCC 2002, April 2002, pp. 36-41.

[41] Chin S. Moo, Wei M. Chen, Hau C. Yen, and Mu E. Lee, “Electronic Ballast with Programmable Starting for Rapid-Start Fluorescent Lamps,” IEEE Power Electronics Specialists Conference PESC 2004, June 2004, pp. 2639-2644.

[42] M. K. Kazimierczuk and W. Szaraniev, “Electronic Ballast for Fluorescent Lamps,” IEEE Transactions on Power Electronics, Vol. 8, No. 4, October 1993, pp. 386-395.

[43] M. K. Kazimierczuk, “Class D Voltage-Switching MOSFET Power Amplifier,” IEE Proceedings-Electric Power Applications, Vol. 138, No. 6, November 1991, pp. 285-296.

[44] M. C. Cosby, Jr. and R. M. Nelms, “A Resonant Inverter for Electronic Ballast Applications,” IEEE Transactions on Industrial Electronics, Vol. 41, No. 4, August 1994, pp. 418-425.

[45] M. A. Co, D. S. L. Simonetti, and J. L. F. Vieira, “High-Power-Factor Electronic Ballast Based on A Single Power Processing Stage,” IEEE Transactions on Industrial Electronics, Vol. 47, No. 4, August 2000, pp. 809-820.

[46] S. Y. R. Hui, L. M. Lee, H. S. Chung, and Y. K. Ho, “ An Electronic Ballast

with Wide Dimming Range, High PF, and Low EMI," IEEE Transactions on Power Electronics, Vol. 16, No. 4, July 2001, pp. 465-472.

[47] L. Laskai and M. Ilic, "An Approach for Selecting Switching Devices for CFL Ballasts," IEEE Transactions on Industry Applications, Vol. 37, No. 1, January/February 2001, pp. 268-275.

[48] Y. R. Yang and C. L. Chen, " Steady-State Analysis and Simulation of A BJT Self-Oscillating ZVS-CV Ballast Driven by A Saturable Transformer," IEEE Transactions on Industrial Electronics, Vol. 46, No. 2, April 1999, pp. 249-260.

[49] T. F. Wu, Y. C. Liu, and Y. J. Wu, "High-Efficiency Low-Stress Electronic Dimming Ballast for Multiple Fluorescent Lamps," IEEE Transactions on Power Electronics, Vol. 14, No. 1, January 1999, pp. 160-166.

[50] C. S. Moo, Y. C. Chuang, and C. R. Lee, "A New Power-Factor-Correction Circuit for Electronic Ballasts with Series-Load Resonant Inverter," IEEE Transactions on Power Electronics, Vol. 13, No. 2, March 1998, pp. 273-278.

[51] C. S. Moo, H. L. Cheng, H. N. Chen, and H. C. Yen, "Designing Dimmable Electronic Ballast with Frequency Control," IEEE Applied Power Electronics Conference APEC 1999, March 1999, pp. 727-733.

[52] J. Adams, T. J. Ribarich, and J. Ribarich, "A New Control IC for Dimmable High-Frequency Electronic Ballasts," IEEE Applied Power Electronics Conference APEC 1999, March 1999, pp. 713-719.

[53] M. Radecker and F. Dawson, "Ballast-On-A-Chip Realistic Expectation or Technical Delusion?," IEEE Industry Applications Magazine, Vol. 10, No. 1, January/February 2004, pp. 48-58.

[54] G. Marent and S. Zudrell-Koch, "Novel Electronic Ballast with Integrated Digital Power Factor Controller," IEEE Industry Application Society 2003 IAS Annual Meeting, October 2003, pp. 791-798.

[55] P. J. Baxandall, "Transistor Sine-Wave LC Oscillators, Some General Considerations and New Developments," Proc. IEE, Vol. 106, Pt. B, suppl. 16, May 1959, pp. 748-758.

[56] M. R. Osborne, "Design of Tuned Transistor Power Inverters," Electron. Eng., Vol. 40, No. 486, 1968, pp. 436-443.

[57] W. J. Chudobiak and D. F. Page, "Frequency and Power Limitations of Class-D Transistor Inverter," IEEE J. Solid-State Circuits, Vol. Sc-4, February 1969, pp. 25-37.

[58] M. Kazimierczuk and J. S. Modzelewski, “Drive-Transformerless Class-D Voltage Switching Tuned Power Inverter,” Proc. IEEE, Vol. 68, June 1980, pp. 740-741.

[59] H. L. Krauss, C. W. Bostian, and F. H. Raab, Solod State Radio Engineering, New York: John Wiley & Sons, Ch. 14.1-2, 1980, pp. 432-448.

[60] F. H. Raab, “Class-D Power Inverter Load Impedance for Maximum Efficiency,” RF Technology Expo’85 Conference, Anaheim, CA, January 1985, pp. 287-295.

[61] M. K. Kazimierczuk and W. Szaraniec, “Class D Voltage-Switching Inverter with Only One Shunt Capacitor,” IEE Proceedings-Electric Power Applications, Vol. 139, September 1992, pp. 449-456.

[62] R. Severns, “Topologies for Three-Element Resonant Converter,” IEEE Transactions on Power Electronics, Vol. 7, No. 1, January 1992, pp. 89-98.

[63] R. L. Steigerwald, “A Comparison of Half-Bridge Resonant Converter Topologies,” IEEE Transactions on Power Electronics, Vol. 8, No. 4, October 1993, pp. 386-395.

[64] A. K. S. Bhat and C. Wei-qun, “Analysis, Selection, and Design of Resonant Inverters for Electronic Ballasts,” IEEE Power Electronics Specialists Conference PESC 1994, June 1994, pp. 796-804.

[65] M. K. Kazimierczuk and D. Czarkowski, Resonant Power Converters, New York: Wiley, 1995.

[66] C. S. Moo, Y. C. Chuang, Y. H. Huang, and H. N. Chen, “Modeling of Fluorescent Lamps for Dimmable Electronic Ballasts,” IEEE Industry Applications Society 1996 IAS Annual Meeting, October 1996, pp. 2231-2236.

[67] C. S. Moo, Y. C. Hsieh, H. C. Yen, and C. R. Lee, “Fluorescent Lamp Model with Power and Temperature Dependence for High-Frequency Electronic Ballasts,” IEEE Transactions on Industry Applications, Vol. 39, No. 1, January/February 2003, pp. 121-127.

[68] C. S. Moo, H. L. Cheng, T. F. Lin, and H. C. Yen, “Designing Dimmable Electronic Ballast with Voltage Control for Fluorescent Lamp,” IEEE International Symposium on Industrial Electronics ISIE 1999, July 1999, pp. 786-791.

[69] Y. K. Ho, S. T. Lee, H. S. Chung, and S. Y. Hui, “A Comparative Study on Dimming Control Methods for Electronic Ballasts, ” IEEE Transactions on

Power Electronics, Vol. 16, No. 6, November 2001, pp. 828-836.

[70] T. F. Wu and T. H. Yu, “Analysis and Design of A High Power Factor, Single-Stage Electronic Dimming Ballast,” IEEE Transactions on Industry Applications, Vol. 34, No. 3, May/June 1998, pp. 606-615.

[71] J. M. Alonso, A. J. Calleja, E. Lopez, J. Ribas, and M. Rico-Secades, “A Novel Single-Stage Constant-Wattage High-Power-Factor Electronic Ballast,” IEEE Transactions on Industrial Electronics, Vol. 46, No. 6, December 1999, pp. 1148-1158.

[72] E. Deng and S. Ćuk, “Single Switch, Unity Power Factor, Lamp Ballasts,” IEEE Applied Power Electronics Conference APEC 1995, March 1995, pp. 670-676.

[73] C. S. Moo, H. L. Cheng, and Y. H. Chang, “Single-Stage High-Power-Factor Dimmable Electronic Ballast With Asymmetrical Pulse-Width-Modulation for Fluorescent Lamps,” IEE Proceedings-Electric Power Applications, Vol. 148, No. 2, March 2001, pp. 125-132.

[74] E. E. Hammer, “Photocell Enhanced Technique for Measuring Starting Electrode Temperature of Fluorescent Lamps,” IEEE Industry Application Society 1997 IAS Annual Meeting, October 1997, pp. 2313-2333.

[75] J. Ribas, J. M. Alonso, E. L. Corominas, A. J. Calleja, and M. Rico-Secades, “Design Considerations for Optimum Ignition and Dimming of Fluorescent Lamps Using A Resonant Inverter Operating Open Loop,” IEEE Industry Application Society 1998 IAS Annual Meeting, October 1991, pp. 2068-2075.